Reactions of Manganese Hydrides with Amine-Boranes and Fluoroalkenes

Bakr Barnawi

Thesis submitted to the

University of Ottawa

in partial fulfillment of the requirements for the

for the degree of Master of Science, Chemistry

Department of Chemistry and Biomolecular Sciences

Faculty of Science

University of Ottawa

© Bakr Barnawi, Ottawa, Canada, 2021

Abstract

Organofluorine compounds find various applications ranging from pharmaceuticals to refrigerants, insecticides, high-value fluoropolymers and reagents in catalysis. However, the synthesis of organofluorine compounds depends on toxic chemicals such as hydrogen fluoride, chlorinated hydrocarbons, reactive F_2 gas and environmentally persistent long-chain fluorosurfactants. Recently more sustainable, energy-efficient syntheses have been developed using base metal-catalyzed transformations of fluoroalkenes and the formation and functionalization of d^{6-8} fluorometallacycles. In this thesis, we use manganese complex precursors to prepare the first examples of d^4 fluorometallacycles.

Work in **Chapter 2** describes the synthesis and one-electron reduction of manganese bis(diphosphine)- and tetrakis(phosphite) dibromide complexes, $MnBr_2(P\text{-}P)_2$ and $MnBr_2[P(O\text{-}i\text{-}Pr)_3]_4$ and reactions of the corresponding reduced Mn(I)Br complexes with tetrafluoroethylene (TFE). Products proposed to be d^4 perfluorometallacycles, $MnBr[\text{-}CF_2(CF_2)_2CF_2\text{-}](P\text{-}P)$ proved to be unstable, reforming TFE upon application of vacuum. In **Chapter 3** we show that photolysis of ligated manganese(I) carbonyl bromide complexes, $MnBrL_n(CO)_{5-n}$, in the presence of TFE, chlorotrifluoroethylene (CTFE) or perfluoro(methyl vinyl ether) (PMVE) in tetrahydrofuran affords the Mn-H insertion products, $Mn(CF_2CFXH)(L_2)(CO)_3$ (X = F, Cl, OCF_3) only for L_2 = DPPE [1,2-bis(diphenylphosphino)ethane] as well as a solid by-product proposed to be $MnBr_2L_n$. These reactions are accompanied by THF fluoroalkylation products, $O[\text{-}(CH_2)_3CH(CF_2CFHX)\text{-}]$. By switching to methyl *t*-butyl ether solvent, we showed that exhaustive photolysis of $MnBr(CO)_5$ + 3 equiv. of DPPE gave a new product proposed to be the first stable d^4 fluorometallacycle, $MnBr[\text{-}(CF_2)_4\text{-}](CO)(DPPE)$. Reactions of the fluoroalkenes with zerovalent $Mn_2(CO)_{10}$ also contributed to our understanding of potential reaction pathways to form these Mn-H-derived products.

Previous work in the Baker group compared $FeH_2(dmpe)_2$ and $[FeH(H_2)(dmpe)_2]^+$ as catalysts for the dehydrogenation of amine-boranes [dmpe = 1,2-bis(dimethylphosphino)ethane]. In **Chapter 4** the catalytic reactivity and selectivity of $MnH(H_2)(dmpe)_2$ are compared with those observed using the Fe analogs and the catalyst resting state, $Mn(\eta^2\text{-}BH_4)(dmpe)_2$, is identified.

Finally, in **Chapter 5** we summarize the findings of this thesis and suggests future directions based on this work.

Acknowledgments

First, I must thank Allah, god the almighty, for providing me with the strength and perseverance to complete this thesis, overcome obstacles, and bless me with a great support system, both in my education and personal life.

My most sincere gratitude extends to my parents Khadijah and Hassan, my brother Mustafa, my sisters Marwah and Safa and my uncle Soliman. Thanks to my friends, who are almost certainly better described as brothers from another mother: Owais, Baraa, and Yahya. They have all supported me in their own way as I threw myself into my studies. Thank you very much for your endless love, encouragement, and support.

I would also like to thank Prof. Tom Baker as a supervisor who has no alternative. Baker is one of the most optimistic men I have ever met, who always encourages thoughtful experiments and new ideas. He is the one who has never grown tired of the thrill of discovery even after a lifetime of science. Baker has been an invaluable source of optimism, the genesis of ideas, intelligence, and friendship. I am honoured to have been given the opportunity to work with him. I have learned so much knowledge during these past two years and really appreciated Baker for his guidance, comments, support, and engagement throughout this learning process.

I must take a moment to thank the Baker lab, old and new, for their constant assistance, moral guidance, and friendship. All of them have contributed to make my grad school days (and nights) such an exciting experience. Thank you to my lab mates for their insightful comments and encouragement; their support throughout this journey is genuinely appreciated. I also want to thank Alex Daniels, an ocean of knowledge on organometallics, for tutoring me to teach me scientific background, helping me to make a better and stronger foundation in my studies.

Thank you also to the staff, technicians, and administration at the University, especially Jeff Ovens, Annette Campeau, NMR Geniuses – Glen Facey and Peter Pallister, and an army of others dedicated to their students.

Finally, many thanks are extended to the Ministry of Education in Saudi Arabia, represented by the Saudi Arabian Cultural Bureau in Canada, for financial support.

Table of Contents

List of Figures

List of Schemes

List of Tables

List of Appendices

List of Permission Figures

List of Compounds

1-1	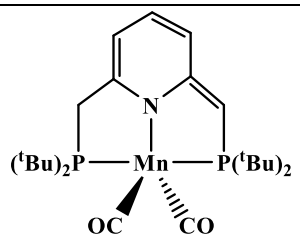	1-2	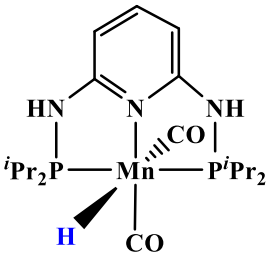	1-3	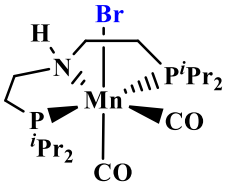
1-4	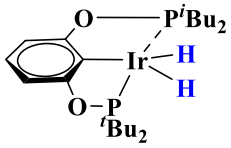	1-5	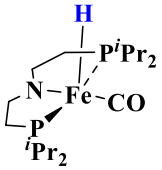	1-6	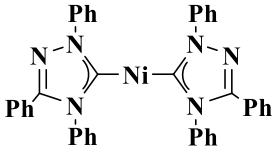
1-7	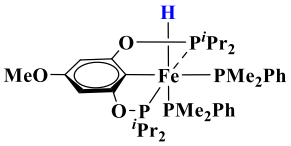	2-1A	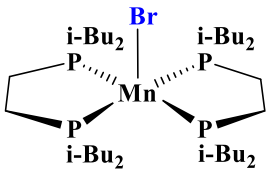	2-1B	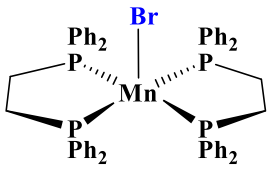
2-1C	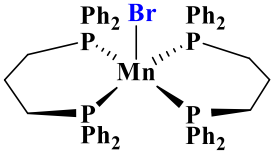	2-1D	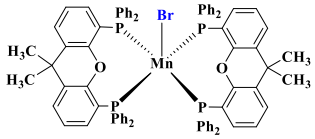	2-1E	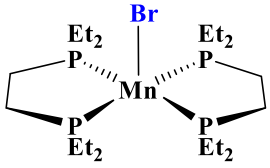
2-1F	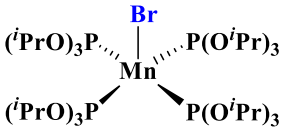	2-2A	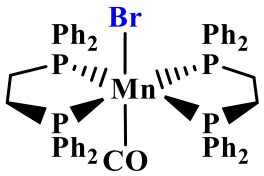	2-2B	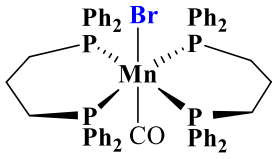
2-3	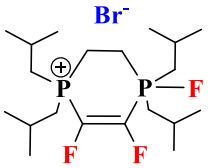	2-4	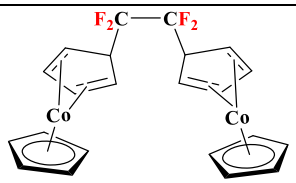	2-5	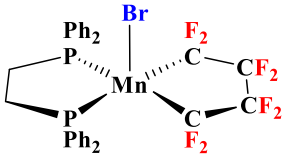
2-6	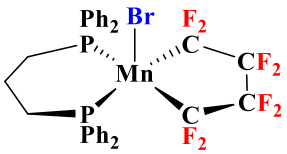	2-7	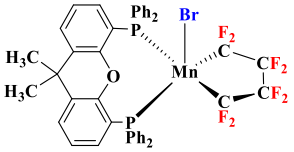	2-8	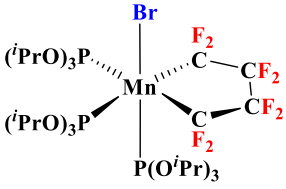

3-1	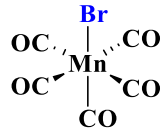	3-2	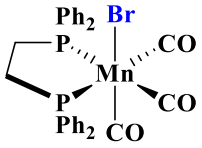	3-3	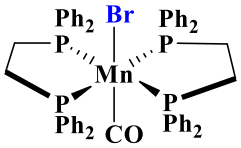
3-4	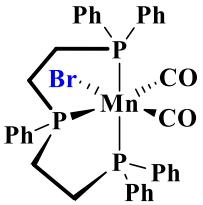	3-5	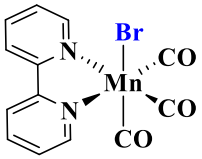	3-6	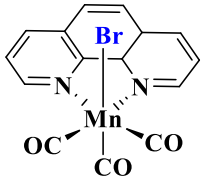
3-7	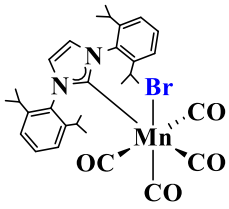	3-8	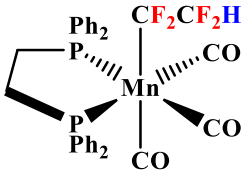	3-9	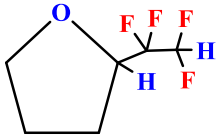
3-10	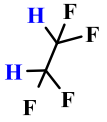	3-11 3-12	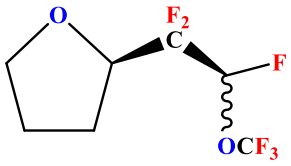	3-13	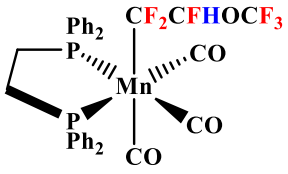
3-14 3-15	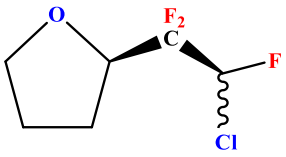	3-16	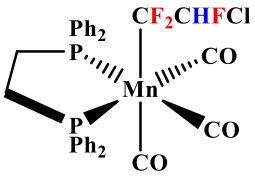	3-17	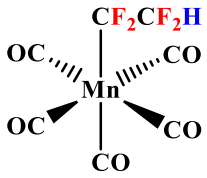
3-18	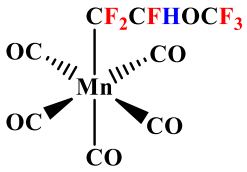	3-19	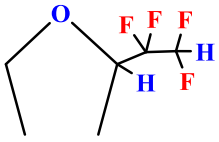	3-20	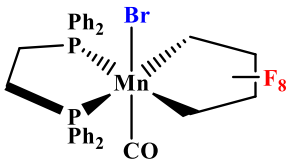
3-21	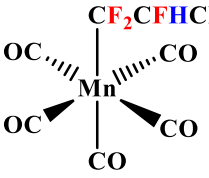	4-1	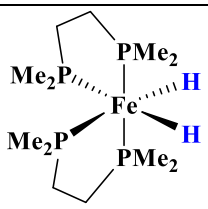	4-2	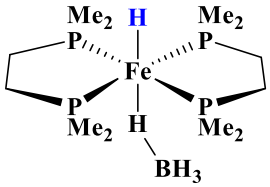

4-3	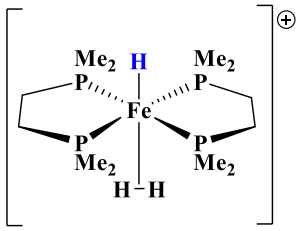	**4-4**	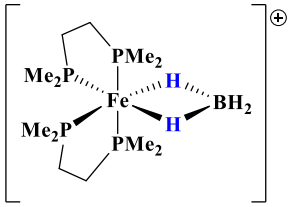	**4-5**	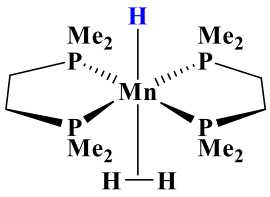
4-6	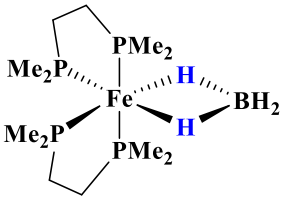				

List of Abbreviations and Symbols

BDE	Bond dissociation energy
Bu	Butyl
Bipy	2,2′-Bipyridine
ca.	Approximately
Cp	Cyclopentadienyl
CFC	Chlorofluorocarbon
CTFE	Chlorotrifluoroethylene
Cod	1,5-Cyclooctadiene
d	Days
DEPE	1,2-Bis(diethylphosphino)ethane
DiBPE	1,3-Bis(diisobutylphosphino)ethane
DME	1,2-Dimethoxyethane
DMPE	1,2-Bis(dimethylphosphino)ethane
DPPE	1,2-Bis(diphenylphosphino)ethane
DPPF	1,1′-Ferrocenediyl-bis(diphenylphosphine)
DPPP	1,3-Bis(diphenylphosphino)propane
Et	Ethyl
FT-IR	Fourier Transform Infrared Spectroscopy
h	Hour
HCFC	Hydrochlorofluorocarbon
HCFO	Hydrochlorofluoroolefin
HFCB	Hexafluorocyclobutene
HFC	Hydrofluorocarbon
HF	Hydrofluoric acid
HFO	Hydrofluoroolefin
HFP	Hexafluoropropene
Hz	Hertz
IPr	1,3-Bis(2,6-diisopropylphenyl)imidazol-2-ylidene
IMes	1,3-Bis(2,4,6-trimethylphenyl)imidazol-2-ylidene
kcal	Kilocalorie

L	Ligand
M	Metal
Me	Methyl
NHC	*N*-Heterocyclic carbene
OTf	Triflate, $-OSO_2CF_3$
NMR	Nuclear magnetic resonance
PCy_3	Tricyclohexylphosphine
Phen	1,10-phenanthroline
PMVE	Perfluoro(methyl vinyl ether)
Psig	Pounds per square inch gauge
Py	Pyridine
R^F	Fluoroalkyl group
RT	Room temperature
THF	Tetrahydrofuran
TFE	Tetrafluoroethylene
TMNO	Trimethylamine N-oxide
TMS	Trimethylsilyl
UV-vis	Ultraviolet–visible spectroscopy
VDF	1,1-Difluoroethylene
Xantphos	4,5-Bis(diphenylphosphino)-9,9-dimethylxanthene

List of Contributions

Presentations:

(1) **B. Barnawi** and R. T. Baker (**2019**), "Reactions of MnBr Bis(phosphine) Complexes with Tetrafluoroethylene," 52nd annual Inorganic Discussion Weekend (IDW). (poster presentation)

(2) **B. Barnawi,** J. S. Ovens and R. T. Baker (**2020**), "Taming a Paramagnetic Personality: Synthesis and Reactivity of d^4 Mn(III) Perfluorometallacycles," 102nd Canadian Chemistry Conference and Exhibition (CCCE). (poster presentation)

(3) **B. Barnawi,** J. S. Ovens and R. T. Baker (**2020**), "Synthesis and Characterization of Mn Fluoroalkyl Complexes," Ottawa-Carleton Chemistry Institute virtual symposium (OCCI Day). (oral presentation)

(4) **B. Barnawi,** J. S. Ovens and R. T. Baker (**2021**), "Taming a Paramagnetic Personality: Synthesis and Reactivity of d^4 Mn(III) Perfluorometallacycles," American Chemical Society (ACS) Spring National Meeting. (oral presentation)

Publications:

(5) **B. Barnawi**, J. S. Ovens and R. T. Baker, "Synthesis and Reactivity of d^4 Mn(III) Fluorometallacyclopentanes," Communication to be submitted **2021**, manuscript in preparation.

(6) A. Cingolani, **B. Barnawi**, I. Rittaco, I. Korobkov, R. Mazzoni, E. Sicilia and R. T. Baker, "Mechanistic studies of amine-borane dehydrogenation using bis(phosphine) Fe- and Mn-hydride catalysts," full paper to be submitted **2021**, manuscript in preparation.

Chapter 1: Introduction

1.1 First Row Transition Metal Complex Catalysts

In the first decades of its development and applications, molecular homogeneous catalysts have been typically based on complexes of the noble metals (Ru, Os, Rh, Ir, Pd, Pt, Au).[1] Over the last three decades, however, there has been a drive to supplement noble-metal catalysts with analogs from the first row (Mn, Fe, Co, Ni, Cu) that are less toxic, more economical, and earth-abundant.[2] In addition, first-row transition metal complexes can show various coordination geometries and multiple spin states which can be used to manipulate their electronic structure, orbital overlap, and bonding character. Moreover, first-row metal complexes often exhibit increased substitutional lability in comparison to their heavier analogs. Recent examples of efficient base-metal catalysis include C-C coupling,[3] polymerization,[4] (de)hydrogenation,[5] E-H bond addition to unsaturated organics (E = B, Si),[6] and C−H borylation.[7]

1.1.1 Manganese complex catalysts

The last decade has seen an explosion in the applications of molecular manganese catalysts in organic synthesis including C–H bond activation, late-stage fluorination, hydrosilylation and cross-coupling.[8] Most relevant to this thesis are catalyzed dehydrogenative coupling reactions that have been applied to a number of tandem reaction schemes.[9,10] In 2016 Milstein and co-workers reported a highly active manganese catalyst (**1-1**) for dehydrogenative coupling of amines and alcohols (**Scheme 1.1**).[11] Diverse aliphatic and benzylic alcohols were efficiently transformed to imines with broad functional group tolerance. The Kirchner group used a PN^3P manganese complex (**1-2**) as a useful catalyst for the same reaction.[12]

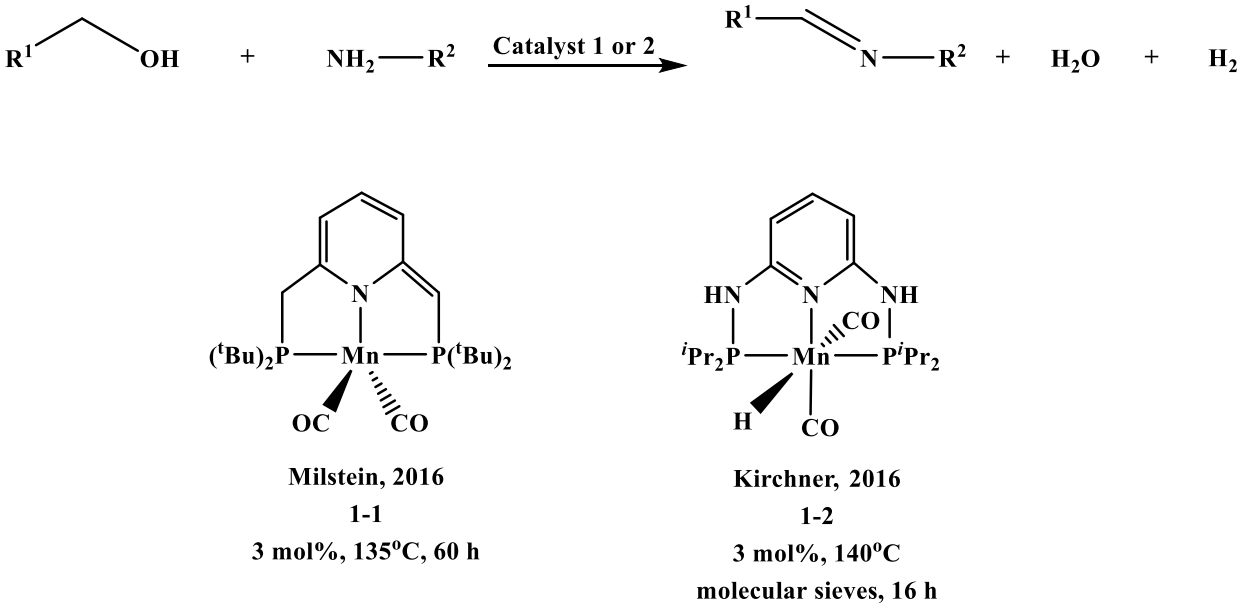

Scheme 1.1. Catalytic synthesis of imines by dehydrogenative coupling.[11, 12]

Liu *et al.* used a well-defined manganese pincer complex (**1-3**) as a catalyst for conversion of ethanol to *n*-butanol (Guerbet reaction; **Scheme 1.2**). This tandem reaction involves ethanol dehydrogenation followed by base-catalyzed aldol coupling and then hydrogenation of the resulting α,β,-unsaturated aldehyde. Although the reaction required high temperatures for the initial alcohol dehydrogenation, the catalyst is quite stable as *n*-butanol was produced with high selectivity and turnover number.[13]

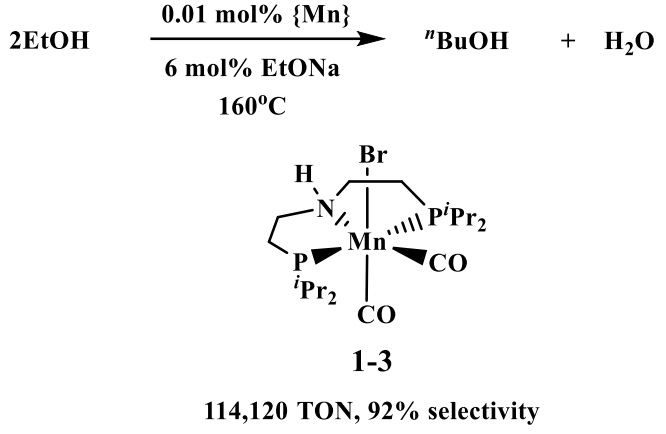

Scheme 1.2. Manganese-catalyzed Guerbet reaction.[13]

1.2 **Amine-Borane Dehydrogenation Catalysis by Transition Metal Hydrides**

Dehydrogenation of amine-boranes has been studied intensively over the last 15 years both as hydrogen storage materials and sources of inorganic B-N polymers.[14] The advantage of amine-boranes vs. cyclic hydrocarbons as hydrogen sources stem from their hydridic B-H and protic N-H bonds that facilitate hydrogen release at low temperatures. Investigators have developed both homogeneous and heterogeneous catalysts to release H_2 from ABs under mild conditions.[15] However, the dehydrogenation mechanisms and product selectivity vary widely with different experimental conditions and catalyst choice.[16]

1.2.1 Selectivity of catalyzed amine-borane dehydrogenation

In their investigations of homogeneous transition metal catalysts for dehydrogenation of ammonia-borane (AB), Baker, Paul and co-workers identified two types of catalyst based on their product selectivity.[17a-c] Type I catalysts rapidly generate a single equivalent of H_2 and aminoborane, NH_2BH_2, which is subsequently polymerized to insoluble poly(aminoborane) (**Scheme 1.3**). Typical Type I catalysts include Ir- and Fe pincer complexes **1-4** and **1-5** (**Figure 1.1**).[18,19] In contrast, Type II catalysts allow for the cyclo-oligomerization of aminoborane, with initial formation of the branched cyclic tetramer, *B*-cyclodiborazanylamine-borane (BCTB), followed by iminoborane cyclic trimer, borazine, and two equiv of H_2. Further B-N dehydrocoupling of borazine can generate additional H_2 along with polyborazylene precursors to BN-graphene.[20] Typical type II catalysts include Ni bis(*N*-heterocyclic carbene) complex **1-6** and Fe pincer complex **1-7**.[21,22]

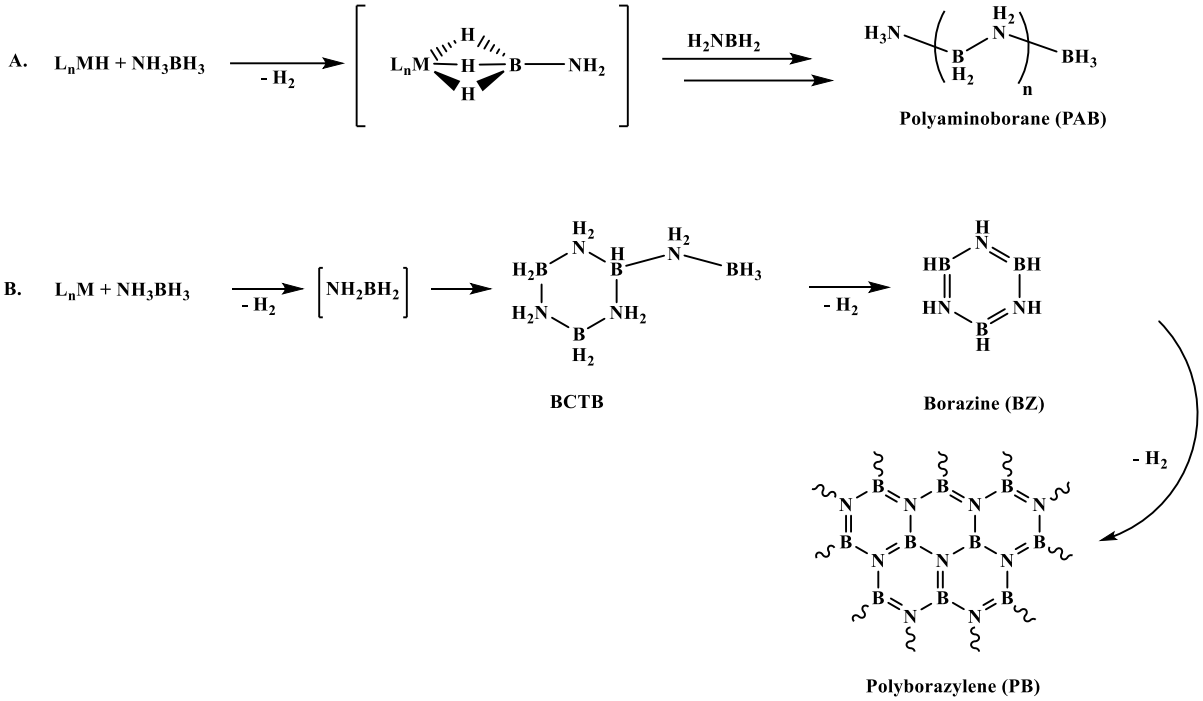

Scheme 1.3. General scheme for AB dehydrogenation using Type I (A) or Type II catalysts (B).[17a-c]

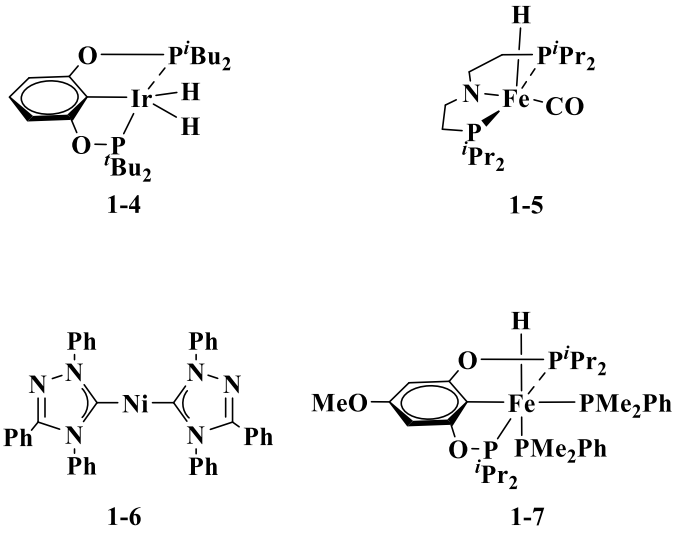

Figure 1.1. Typical Type I (**1-4** and **1-5**) and Type II (**1-6** and **1-7**) AB dehydrogenation catalysts.[18,19,21,22]

1.2.2 Mechanisms for amine-borane dehydrogenation reactions

Paul and co-workers first identified the novel mechanism employed by Type I catalysts (**Scheme 1.4**).[17c] These catalysts contain electron-rich metal hydrides that are readily protonated by the amine-borane, followed by β-hydride elimination to rapidly generate aminoborane, in which

the Lewis acidity of B and basicity of N are modulated by formation of the B=N π-bond. Insertion of aminoborane into M-H generates a 4-coordinate B that yields in turn a basic terminal amido site that reacts with a second aminoborane, generating another basic amido site, growing the polymer chain remote from the metal center. Although the chain termination step has not been determined, higher poly(aminoborane) molecular weights are obtained from alkylamine-boranes (ca. 20,000 from $NMeH_2$-BH_3)[23] vs. AB as unsubstituted poly(aminoborane) is thought to contain only about 20 monomers when it precipitates from solution.

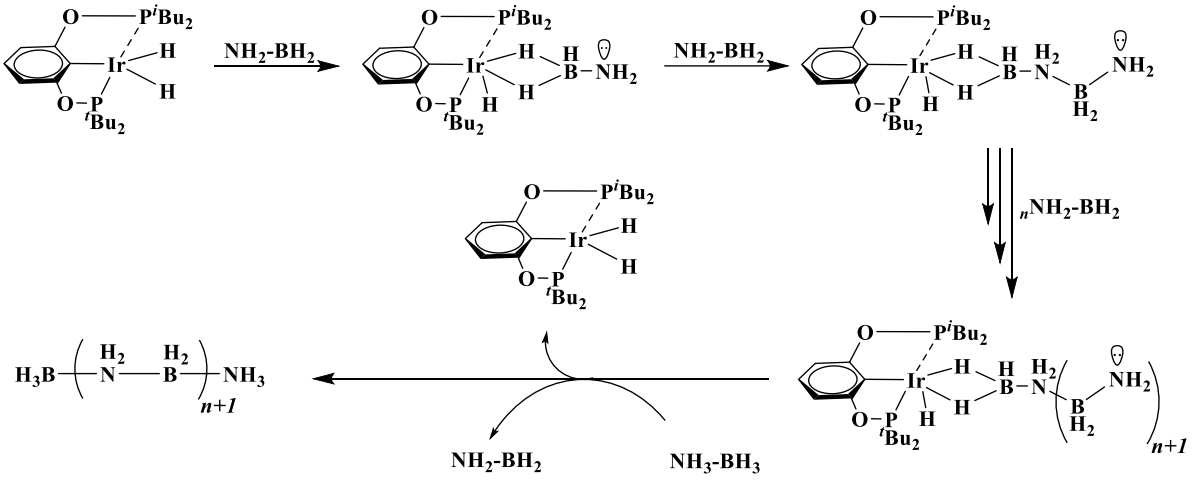

Scheme 1.4. Proposed catalytic cycle for AB dehydrogenation using Type I catalysts.[17c]

For Type II catalysts, the B-H and N-H bonds of the amine-borane are often cleaved in a concerted step, allowing escape of the aminoborane from the metal where it undergoes cyclization. Guan et al. investigated the catalytic cycle using iron bis(phosphinite) pincer complex and ammonia-borane that affords > 2 equiv of H_2 at 60°C (**Scheme 1.5**).[22] After initial dissociation of PMe_2Ph, binding of AB through the B-H bond is followed by protonation of the ligand's ipso carbon as hydride is transferred to the Fe center. Finally, loss of dihydrogen regenerates the catalyst. Dixon, Baker et al. showed that dimerization of aminoborane proceeds through the

reactive $H_3BNH_2BHNH_2$ intermediate[17a] and that conversion of BCTB to borazine is also metal-catalyzed.[20]

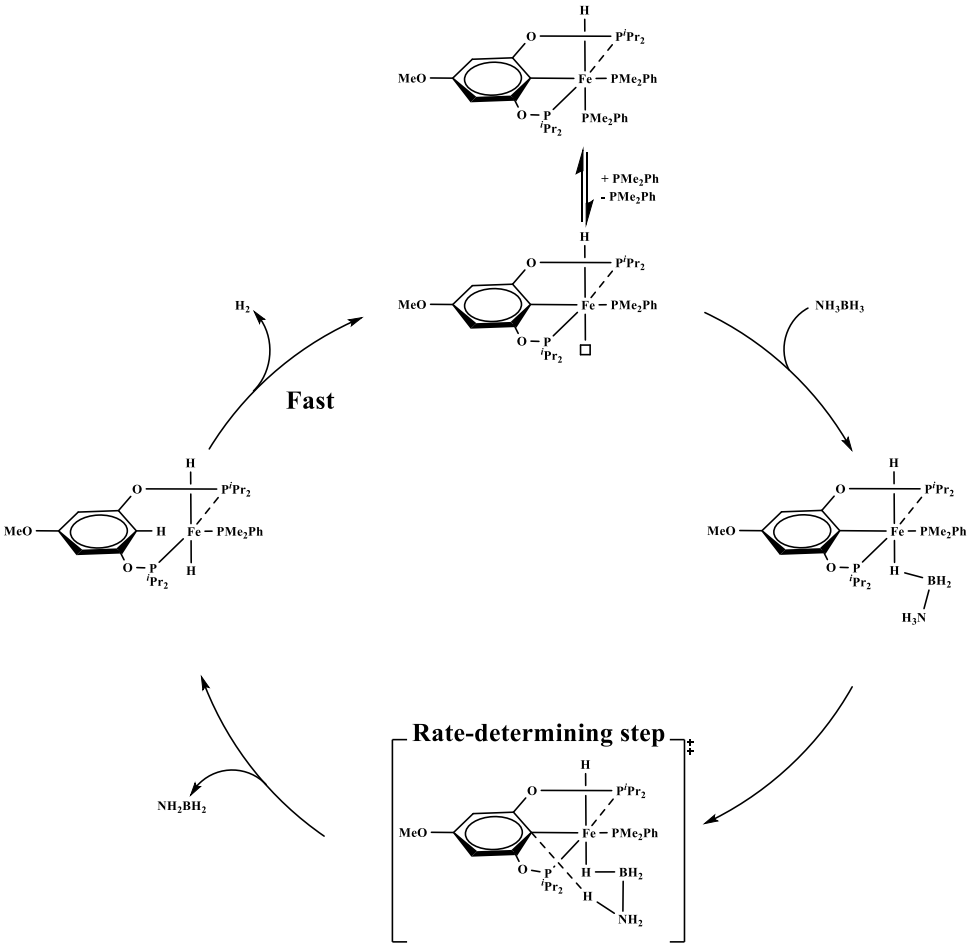

Scheme 1.5. Proposed cycle for Fe-catalyzed dehydrogenation of AB.[22]

Dehydrogenation pathways of methylamine-borane (MeAB) are less studied with a variety of catalysts[24] and in some cases Type I catalysts that yield polymer with AB give only cyclic products *N*-trimethylcyclotriborazane and *N*-trimethylborazine with MeAB, although competing B-N bond cleavage often yields additional products such as $HB(NMeH)_2$. In contrast, dimethylamine-borane (DMAB) is most widely studied and competing reaction pathways leading to the cyclic aminoborane dimer *vs.* linear $H_3BNMe_2BH_2NMe_2H$ are well understood.[25]

1.3 **Metal Organofluorine Chemistry**

Fluorine forms the strongest single bond to carbon with a bond dissociation energy (BDE) of 115 kcal/mol *vs* 104.9 kcal/mol for CH_3-H because the high electronegativity of fluorine makes the bond more polar.[26] As a result, fluorinated molecules can be used as versatile materials that can display thermal stability and chemical inertness, making them useful in various applications ranging from pharmaceuticals and insecticides to refrigerants, foam-blowing agents, and reagents in catalysis.[27] The synthesis of fluorinated molecules has benefited greatly from the development of metal organofluorine chemistry by pioneers such as Stone[28] and Hughes.[29]

1.3.1 Fluoroalkenes – 4th generation of greener refrigerants and foam-blowing agents

Owing to their stability and physical properties, chlorofluorocarbons (CFCs) were developed in the 1950s as foam-blowing agents, solvents, propellants, and refrigerants.[30] However, their development on an industrial level was followed by atmospheric release that negatively impacted the earth's ozone layer. Following the Montreal Protocol, hydrochlorofluorocarbons (HCFCs) soon replaced the CFCs, followed by hydrofluorocarbons (HFCs) that could not serve as a source of atmospheric chlorine.[31,32a] Although HFCs have a marginal effect on the ozone layer, IR-absorbing C-F bonds make them good greenhouse gases. In contrast, the double bond of recently developed 4th generation refrigerants, HCFOs and HFOs, is easily oxidized, reducing their capacity to serve as greenhouse gases (**Figure 1.2**).

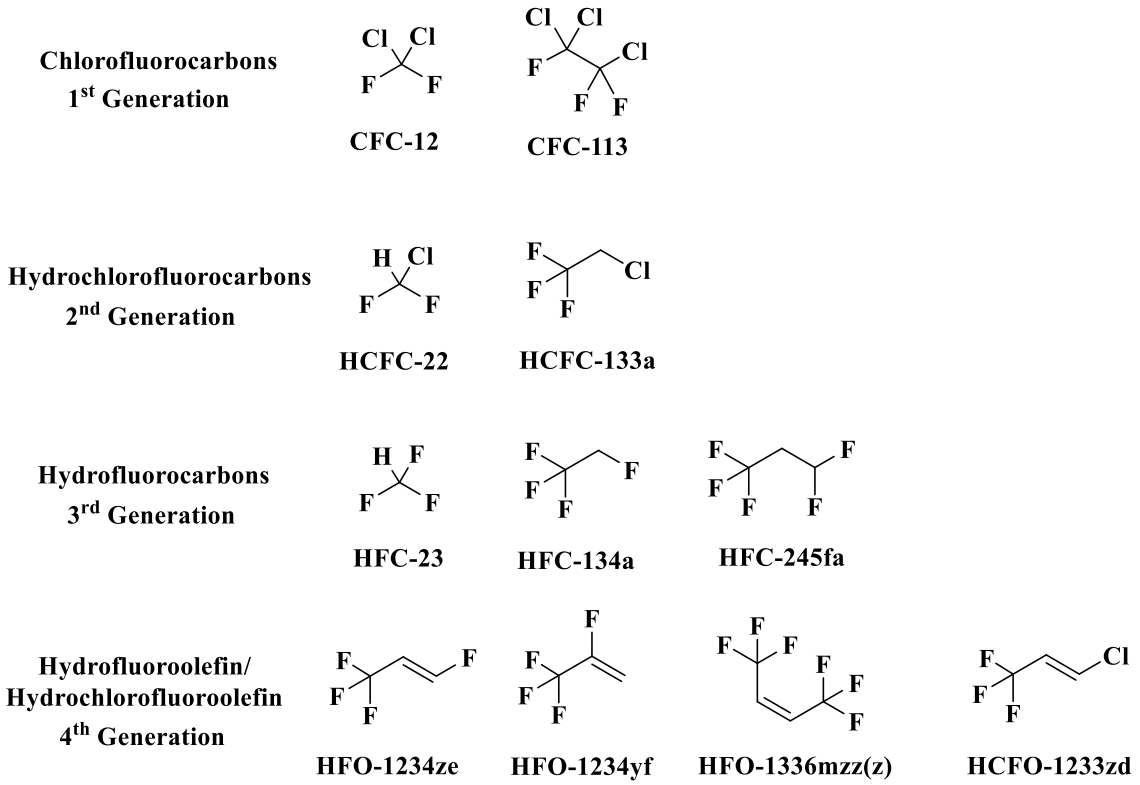

Figure 1.2. Selection of important CFCs, HCFCs, HFCs, HFOs and HCFOs.[31, 32a, 33, 34]

Regarding nomenclature, many marketing materials and patents for small fluorinated molecules employ the refrigerant naming system developed by the American Society of Heating, Refrigerating, and Air-Conditioning Engineers (ASHRAE).[32b] These naming conventions vary according to the type of refrigerant. Refrigerants are assigned a four-digit R number including d, c, h and f. The first digit represents the number of double bonds in the compound, the second the number of carbon atoms less one, the third the number of hydrogen atoms plus one and the fourth the number of fluorine atoms. For example, trifluoromethane CHF_3 has no double bonds (d = 0), one carbon atom less one (c = 0), one hydrogen atom plus one (h = 2) and three fluorine atoms (f = 3). Thus the R number 23 refers to a hydrofluorocarbon (HFC-23). Moreover, the R numbering systems has undergone two evolutions: for two-carbon refrigerants, the letters a, b, or c can be

added at the end of the R-number, as the structure becomes less symmetrical (*cf.* $CFCl_2CF_2Cl$ is CFC-113 and CF_3CCl_3 is CFC-113a). For fluoroalkenes, *Z* or *E* are added at the end of the R-number to denote *cis* or *trans* and the structures are more fully delineated by additional letters representing the halocarbon fragment (**Table 1.1**).[32b]

Fragment	Designation		Fragment	Designation
CCl_2	A		$CHCl_2$	N
CClF	B		CH_2Cl	O
CF_2	C		CHF_2	P
CHCl	D		CH_2F	Q
CHF	E		CHClF	R
CH_2	F		CH_3	S
CCl_3	J		C	T
CCl_2F	K		CCl	X
$CClF_2$	L		CF	Y
CF_3	m		CH	Z

Table 1.1. Halocarbon molecular fragments and corresponding letter designations.[32b]

One of the most promising HFC substitutes, 2,3,3,3-Tetrafluoropropene (HFO-1234yf), can be prepared by hydrogenation of $CF_3CF{=}CHF$ (HFP) using Pd/C catalyst, followed by defluorination over γ-alumina.[33] Another common HFO, 1,3,3,3-tetrafluoropropene (HFO-1234ze), is manufactured from 3-chloro-1,1,1,3-tetrafluoropropane (HCFC-244fa) or 1,1,1,3,3 pentafluoropropane (HFC-245fa). However, the processes for HCFC and HFC synthesis are lengthy and additional purification steps are needed as multiple products are formed in both these processes.[34] To sum up, fluoroalkene synthesis as CFC substitutes requires toxic compounds[35]and energy-intensive processes.

1.3.2 Reactions of metal complexes with fluoroalkenes

Fluorine's high electronegativity has a depletive effect on the electron density in the π-bond of olefin. As a result, it will affect the ability to donate σ electrons leading to reaction only

with low-valent metals because of the latter's ability for strong π-backbonding. Retro-dative metal bonding is thus highly essential for fluoroolefins and will depend on ancillary ligands and the metal's oxidation state (**Figure 1.3**).[36]The bond between metal and fluoroolefin is like the normal π-bond in metal-olefin complexes in which a filled metal d-orbital participates in back-bonding with the π-antibonding orbital of the olefin. As this back-bonding becomes especially strong, a more consistent bonding picture is the bis(σ-bonded) three-membered ring. Besides, intermediate situations are likely where the mode of bonding is not exclusively metallacyclopropane or olefin-like.[37]

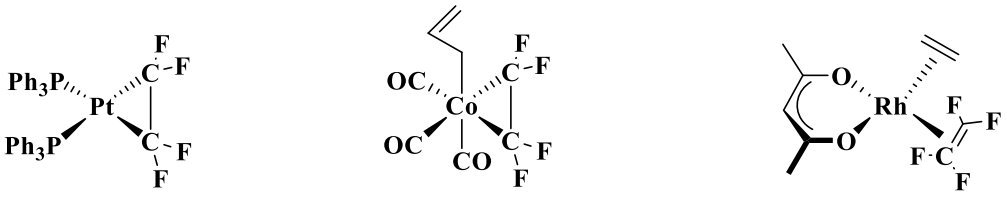

Figure 1.3. Example of important fluoroolefin complexes.[36]

1.3.3 Fluoroalkene insertion into M-H, M-C and M-M bonds

Because of their electrophilic nature, fluoroolefins are sensitive to nucleophilic attack, thus allowing for their insertion into a reactive metal hydride link. Stone first identified this reaction in 1961 with a complex of tetrafluoroethylene (TFE) and manganese pentacarbonyl hydride (**Scheme 1.6**),[38] followed by other cases involving rhenium pentacarbonyl hydride[39], tungsten tricarbonyl hydride and π-cyclopentadienyl molybdenum.[40]

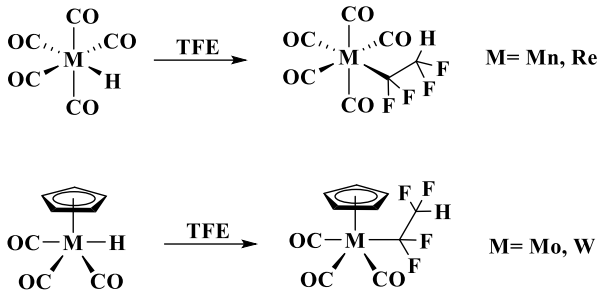

Scheme 1.6. Insertion of TFE into metal hydride to form M-fluoroalkyl.[38,39,40]

While non-fluorinated olefins can undergo polymerization by inserting into M-C bonds, fluoroalkenes such as TFE generally do not insert into M-C^F bonds, as Roper has shown for iridium complexes (**Scheme 1.7**).[41] Heating $IrH(CO)(PPh_3)_3$ under TFE pressure gives $IrH(C_2F_4)(CO)(PPh_3)_2$ upon heating. As the latter was processed under even more vigorous conditions with more TFE, fluoroolefin was inserted into the metal-hydride bond and a second TFE equivalent was coordinated without insertion into the fluoroalkyl Ir-C or carbonyl Ir-C bond. In contrast, work by Wilford and Stone demonstrated insertion of TFE into the M-C^{Me} bond of $M(CH_3)(CO)_5$ (M = Mn, Re), although further insertion of TFE into the M-C bond of M-$CF_2CF_2CH_3$ was not observed.[42]

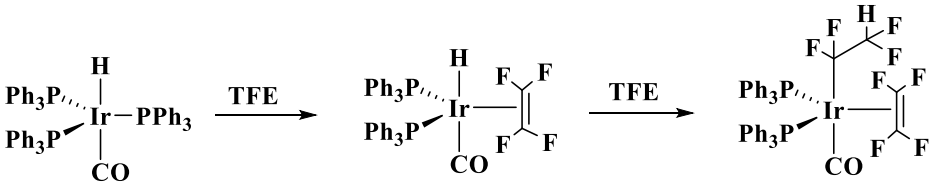

Scheme 1.7. Insertion of TFE into Ir-H bond and coordination of a second TFE.[41]

Fluoroalkenes can also insert into M-M bonds. Zerovalent dicobalt octacarbonyl reacts with TFE to produce the Co(I) tetrafluoroethanediyl-bridged complex, $(CO)_4CoCF_2CF_2Co(CO)_4$.[43] Similar reactivity of TFE was observed with tin–manganese[44] and germanium–manganese[45] bonds.

1.3.4 Fluoroalkene coupling to fluorometallacycles

Oxidative coupling of two olefins at the metal centre (**Scheme 1.8**) causes the cyclization reaction to form a metallacyclopentane, which results in an increase in the formal oxidation state of the metal by two units. While alkynes easily undergo this reaction in comparison to alkenes, ring-strain or electron-withdrawing substituents can activate the latter. TFE readily undergoes this reaction as it decreases the repulsion between the π-bond of C=C and lone pairs of fluorine due to transformation of sp^2 C–F bonds to sp^3 C-F bonds to a less electronegative carbon.[46] Olefin complex vs. five-membered ring metallacycle formation is determined by many factors.[47] For example, both steric and π-acceptor vs σ-donor ancillary ligands can affect the type of complex formed.

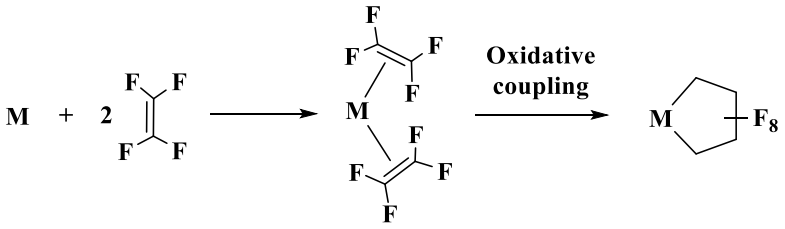

Scheme 1.8. Oxidative coupling to form a perfluorometallacyclopentane.[46]

In 1961, Stone showed that photolysis of $Fe(CO)_5$ and TFE in octane gave $Fe(CO)_4(1,4\text{-}C_4F_8)$, the first perfluorometallacyle (**Figure 1.4**).[48a] The same complex had been synthesized previously by Nobel prize-winner Geoff Wilkinson but it was misassigned as the bis (olefin) complex.[48b] An isoelectronic d^6 cobaltacyclopentane (prepared from TFE and cyclopentadienylcobalt dicarbonyl)[49] was identified shortly afterwards by Stone et al. who then expanded this class extensively using nickel.[50] They and others showed, for example, that zerovalent Ni phosphine complexes react readily with fluoroalkenes to yield d^8 nickelacyclopentanes, whereas Pd and Pt analogs typically yield olefin complexes.[51,52]

Furthermore, the dibridged complex, (cod)Pt(μ-C_2F_2)$_2$Pt(cod), was obtained from Pt(cod)$_2$ and TFE.

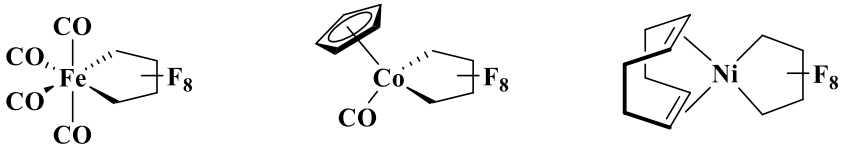

Figure 1.4. First reported perfluorometallacyles.[48a-b, 49, 50]

A report by Ogoshi et al.[53] confirmed that ligand steric effects dictate the observed metallacycle size in Ni reactions (**Scheme 1.9**).

L_2 = 2 Et_3P
2 Ph_2PMe
2 $Bu^n{}_3P$
$Ph_2P(CH_2)_2PPh_2$
2 $(MeO)_3P$
2,2'-bipyridyl
2 Ph_3P
2 4-picoline

L_2 = 2 PCy_3
2 $^iPr_3$
$Cy_2P(CH_2)_2PCy_2$
$Cy_2P(CH_2)_4PCy_2$

Scheme 1.9. Ligand effects on perfluoronickelacycle formation.[53]

Several d^6 ruthenium metallacycles have also been synthesized. For instance, TFE and Ru(CO)$_2$(PPh$_3$)$_3$ afford Ru(CO)$_2$(PPh$_3$)$_2$(1,4-C_4F_8)[54] and reduction of RuCl$_2$(PPh$_3$)$_4$ using NaH in MeCN in the presence of TFE gave the (tetrakis)phosphine analog (**Figure 1.5**).[55]

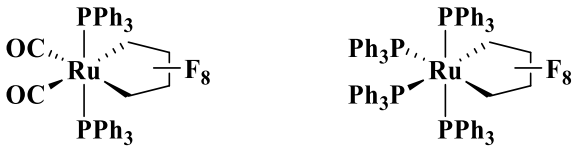

Figure 1.5. Ruthenium metallacyclopentane complexes.[54,55]

Recently, Vicic and co-workers reported an alternate route to perfluorometallacycles using dinuclear fluoroalkylzinc reagents $[(MeCN)_2Zn[(CF_2)_n]_2Zn(MeCN)_2]$[56] such as that derived from 1,4-diiodooctafluorobutane and diethylzinc (**Scheme 1.10**). By adding co-ligand, L, the zinc complex can rapidly transmetalate nickel to produce the mononuclear d^8 perfluoronickelacycle

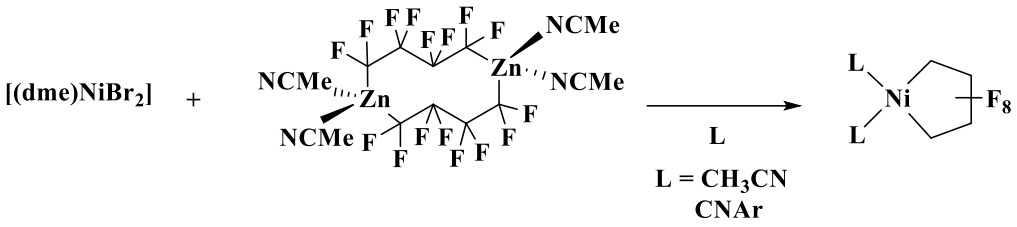

Scheme 1.10. Synthesis of perfluoronickelacycles via a transmetallation reaction.[56]

In a recent review of transition metal complexes of fluorinated dienes,[57] Kühnel and Lentz summarize examples of fluorometallacyclopentenes (**Scheme 1.11**). In a Mn example of relevance

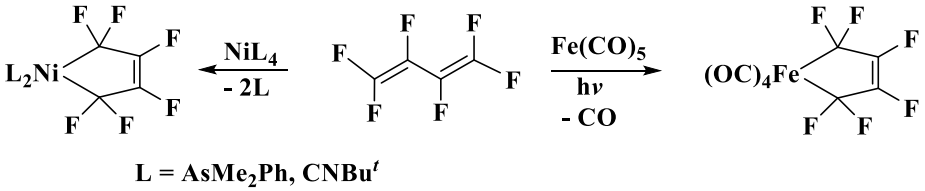

Scheme 1.11. Formation of fluorometallacyclopentenes from perfluorobutadiene.[57]

to this Thesis, both η^4-diene and η^1,η^1-metallacyclopentene coordination modes are accessed in formation of the novel d^3 oxo-bridged dimanganese oxidation product (**Scheme 1.12**).[58]

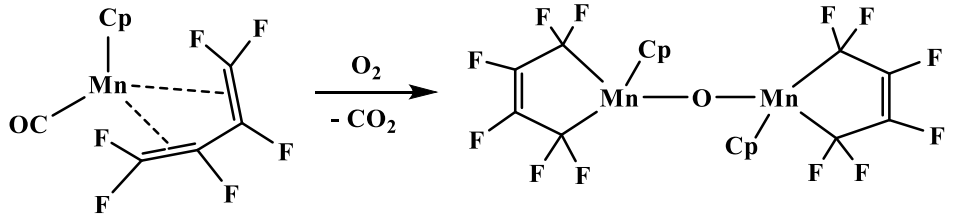

Scheme 1.12. Oxidation of d^6 Mn diene complex to d^3 fluorometallacyclopentene.[58]

1.3.5 Reactivity of fluorometallacycles

In 1961, Stone showed that the d^6 fluorometallacycle $Fe(C_4F_8)(CO)_4$ is extremely stable, requiring heating at 160 °C for 12 d for conversion to perfluorocyclobutene and FeF_2. Heating with bromine afforded the reductive elimination product, perfluorocyclobutane.[48a] Much later in 1994, Baker et al. showed that this same metallacycle undergoes slow Fe–C^F bond hydrogenolysis complex under harsh conditions to form both $H(CF_2)_4H$ (338pcc) and related hydrodefluorinated products such as $H(CF_2)_3CFH_2$ (347pcc).[59] The proposed mechanism for this reaction involves initial CO loss and formation of a dihydrogen complex that can then follow competing paths (**Scheme 1.13**). One of the α-carbons may be protonated by the dihydrogen intermediate, resulting in the iron alkyl hydride complex that undergoes reductive elimination to 338pcc. In the other pathway, the Cα-F is protonated, affording the iron metallacyle carbene hydride. Further addition of H_2 and subsequent hydrogenolysis then affords HFC-347pcc. Indeed, more recently Ghostine and Baker demonstrated that photolysis of Fe(CO)(triphos)(1,4-C_4F_8) induces Cα-F bond activation with formation of FeF(=$CFCF_2CF_2CF_2$-)(triphos) (triphos = bis(diphenyl-phosphinoethyl)phenylphosphine).[60]

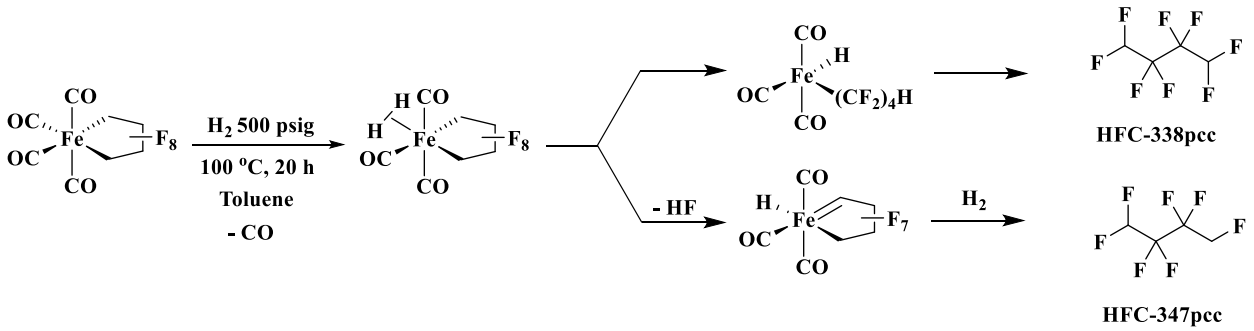

Scheme 1.13. Proposed reaction pathways for hydrogenolysis of $Fe(CO)_4(1,4\text{-}C_4F_8)$.[59]

Burch and coworkers reported Cα−F bond activation of $Ni(PEt_3)_2(1,4\text{-}C_4F_8)$ using the Lewis acid BF_3 (**Scheme 1.14**).[61] Subsequent phosphine migration to Cα produced the phosphonium-functionalized metallacycle. Moreover, adding a second equiv of BF_3 activated the other Cα−F bond and the resulting dicationic product was stabilized with a bis(phosphine) ligand.

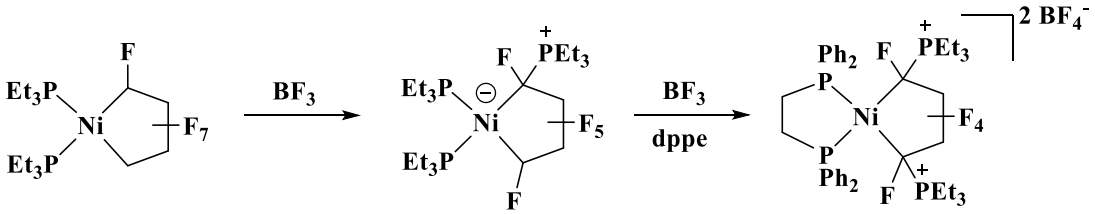

Scheme 1.14. Cα-F abstraction from a bis(phosphine) nickel perfluorocyclopentane.[61]

Recently, the Baker group demonstrated selective ligand migration to Cα in the [P,S^{iPr}]-ligated nickel perfluorocyclopentane (**Scheme 1.15**).[62] Treatment of the phosphonium zwitterion with isonitrile ligands gave Ni-C bond cleavage and, more remarkably, hydrolysis afforded a single C_4 HFO isomer via hydrodefluorodimerization of TFE (**Scheme 1.16**).

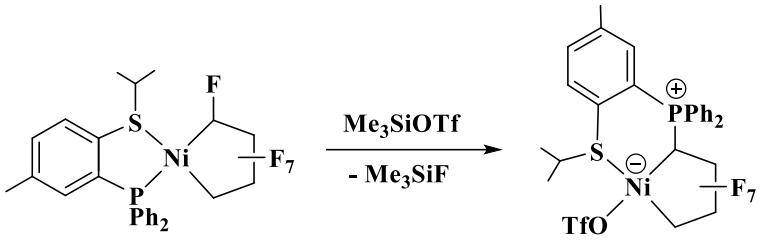

Scheme 1.15. Cα-F abstraction from a [P,S^{iPr}]-ligated metal perfluorocyclopentane by TMS-OTf.[62]

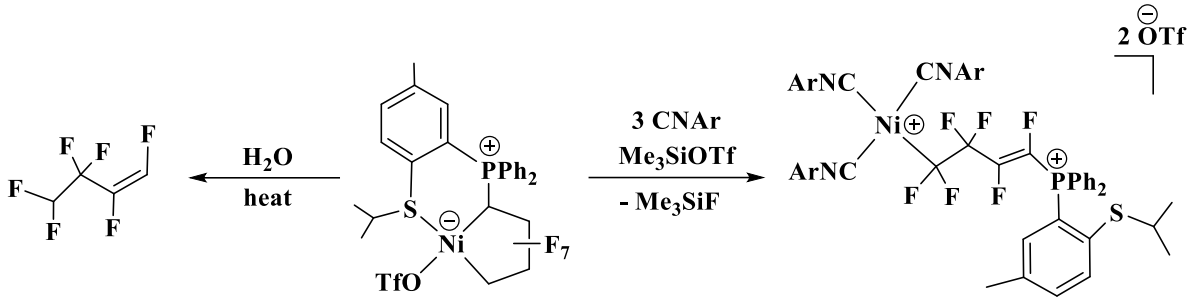

Scheme 1.16. Reactivity of phosphonium-functionalized nickelacyclopentane.[62]

On the other hand, C_α–F bond activation in pseudo-three-coordinate NHC-perfluoronickelacyclopentane using Me_3SiOTf resulted in C-C bond formation, forming the perfluorocyclobutyl ring, without migration of the NHC ligand[63] (**Scheme 1.17**). Thermolysis of this product affords perfluorocyclobutene likely through β-fluoride elimination although the expected Ni-F co-product was not characterized.

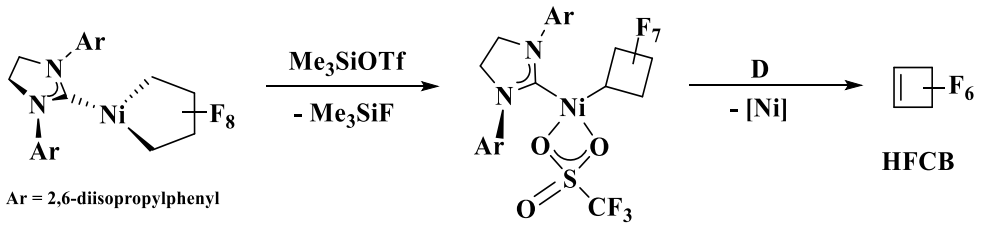

Scheme 1.17. Cα-F fluoride abstraction from a low-coordinate NHC perfluoronickelacycle.[63]

In other reactions of this low-coordinate nickelacyclopentane, trifluoroacetic acid produced trifluoroacetate-substituted metallacycle and HF. However, use of bulkier and less acidic

trimethylbenzoic acid cleaved the Ni–C^F bond, forming a very stable Ni fluoroalkyl complex (**Scheme 1.18**).[63] Remarkably, no β-F elimination was observed even after 12 h at 80 °C.

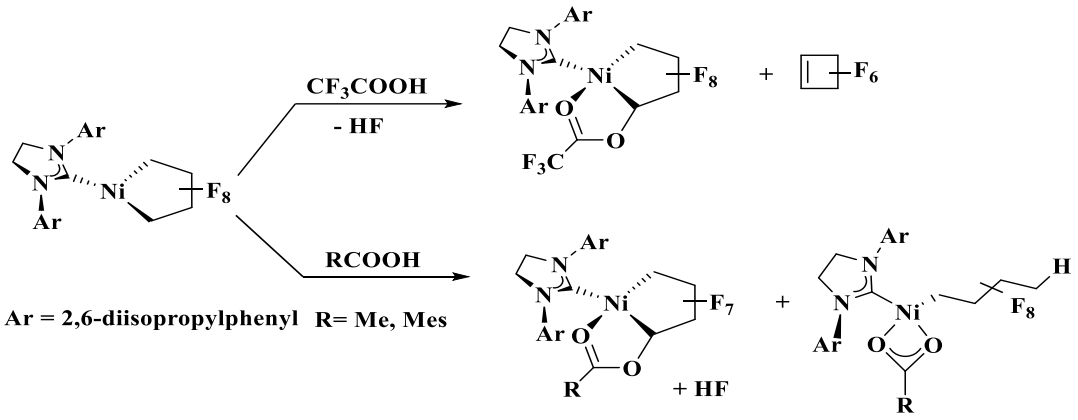

Scheme 1.18. Reactivity of NHC-perfluorometallacyclopentane with Brønsted acids.[63]

Interestingly, replacement of some fluorines with hydrogens can have a significant effect on the C-F bond reactivity of nickelacyclopentanes. Giffin, Baker et al. showed that metallacycles derived from trifluoroethylene underwent both Cα-F and Cβ-F bond cleavage on treatment with Lewis acids (**Scheme 1.19**).[64] Moreover, the nature of the Lewis acid dictated the final product formed, a result attributed to the nucleophilicity of the counteranion.

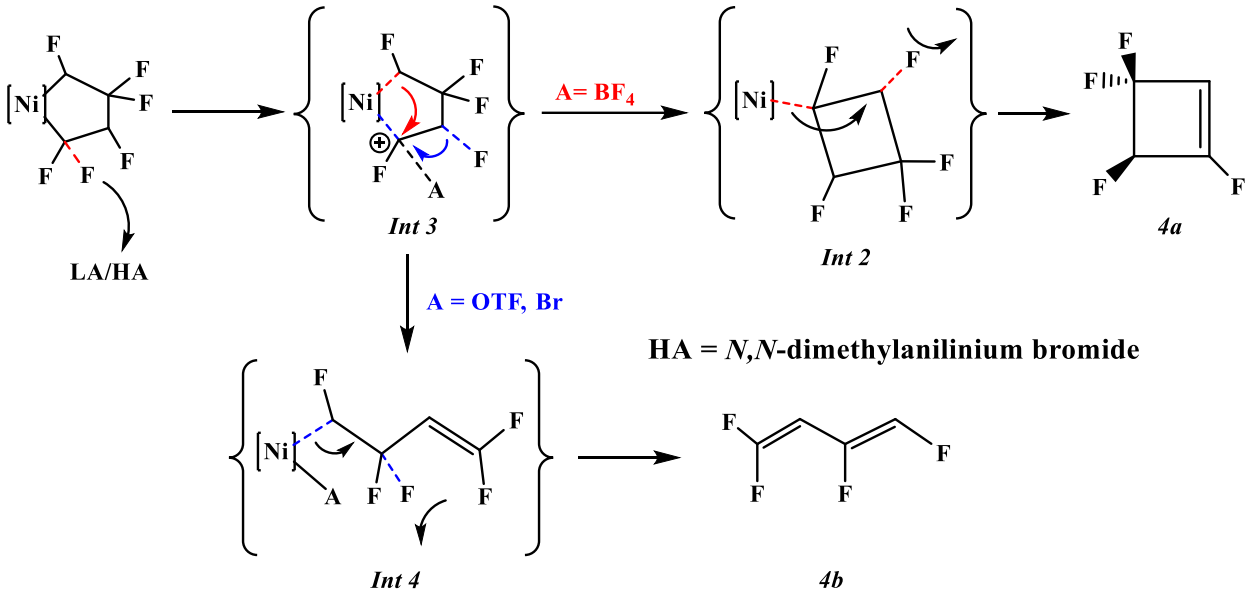

Scheme 1.19. Reactivity of nickelacyclopentane derived from trifluoroethylene.[64]

1.4 **Nickel -Catalyzed Fluoroalkene Reactions**

1.4.1 Ni-catalyzed hydrodimerization of TFE

While working at Du Pont, Baker *et al.* developed a catalytic method with perfluoronickelacyclopentane and $Ni[P(OR)_3]_4$ intermediates for the hydrodimerization of TFE (**Scheme 1.20**).[65] First, oxidative coupling of two TFE molecules using $Ni[P(OR)_3]_4$ forms the nickel perfluorometallacycle with loss of two phosphite ligands. Addition of H_2 to nickel generates the dihydrogen intermediate, which then protonates the α-carbon with formation of a putative nickel hydride. Finally, the HFC is released through reductive elimination to give HFC-338pcc and reform the Ni(0) phosphite complex. Although elevated temperatures and pressures are required for hydrogenolysis of the robust Ni–R^F bond with the ancillary π-acidic phosphite ligands, Werner *et al.* demonstrated that related perfluoronickelacycles, $Ni(C_4F_8)L_2$, in which L= PPh_3, or L_2= DPPP, DPPE do not undergo hydrogenolysis in the presence of H_2 at 20 atm.[55] Recently, our

group showed that the low-coordinate NHC nickel metallacycle undergoes Ni–C^F bond hydrogenolysis under much milder conditions (7 psig H_2 and 25 °C vs. 500 psig H_2 and 100 °C).[63]

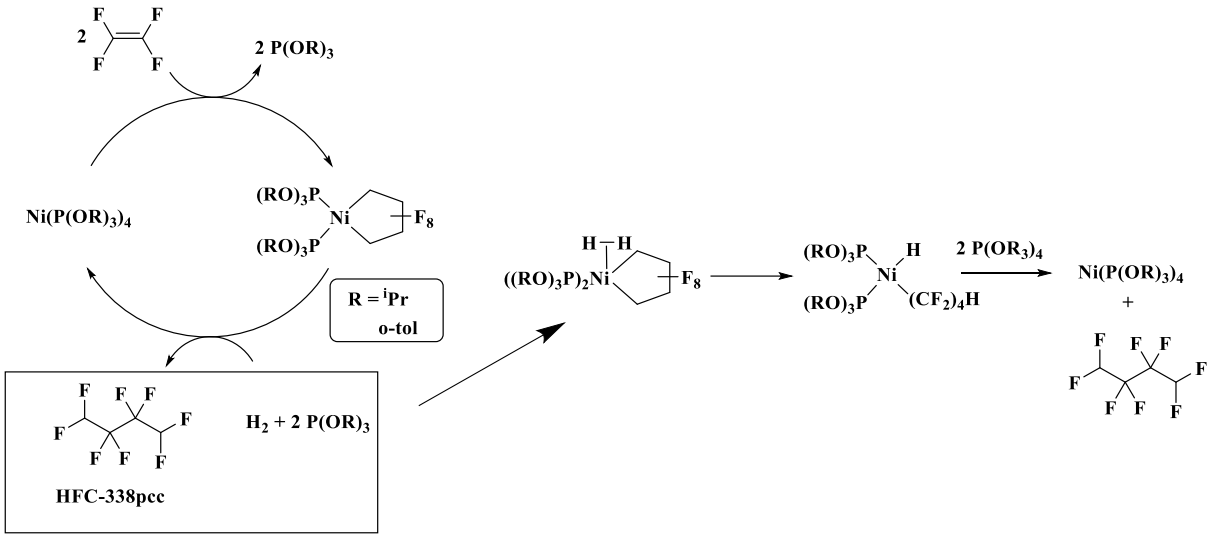

Scheme 1.20. Synthesis of nickel perfluorometallacycle complex via catalytic hydrodimerization of tetrafluoroethylene using valent Ni phosphite complex.[65]

1.4.2 Ni-catalyzed hydrodefluorodimerization of vinylidene fluoride (VDF)

A further example of fluorometallacycle C_β-F bond activation was discovered by Sicard[66] using bulky NHC ligands such as 1,3-di(1-adamantyl)imidazolidene (IAd). In this case, β-fluoride elimination from the presumed (but unobserved) metallacyclopentane intermediate affords the butenyl-nickel fluoride-bridged dimer. Addition of a silane converts Ni-F to Ni-H and subsequent reductive elimination yields the new C_4 HFO in a catalytic hydrodefluorodimerization process (**Scheme 1.21**).

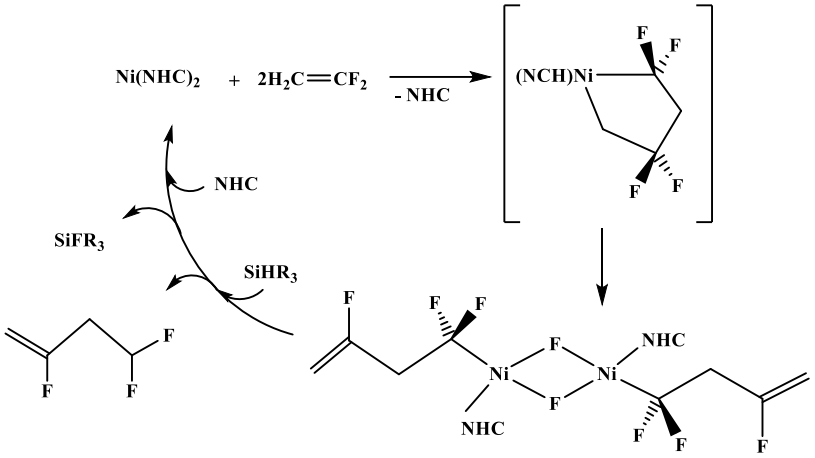

Scheme 1.21. Reaction steps for Ni-NHC complex-catalyzed VDF hydrodefluorodimerization.[66]

1.4.1 Other Nickel catalyzed fluoroalkene homologation reactions

In the presence of catalytic $Ni(cod)_2$ and bulky NHC ligand IPr, the Ogoshi group achieved a cross-trimerization reaction of aldehydes, ethylene and TFE (**Scheme 1.22a**).[67] The procedure yields a range of 4,4,5,5-tetrafluoro-1-pentanone derivatives in fair to excellent yields when done selectively. Oxidative cyclization of ethylene and TFE generates a key intermediate, the five-membered mixed nickelacycle. This partially fluorinated nickelacycle, which can be isolated using PCy_3 as an auxiliary ligand, reacts with enones in to yield the cross-trimerization product. Moreover, it can also be used as an important reaction intermediate in the ethylene and TFE co-trimerization to give 5,5,6,6-tetrafluoro-1-hexene (**Scheme 1.22b**).[68] In another report, a range of 1,3-dienes with a 3,3,4,4-tetrafluorobutyl chain were formed by cross-tetramerization of ethylene, TFE and alkynes using a catalytic amount of $Ni(cod)_2$ and PCy_3. Partially fluorinated five- and seven-membered nickelacycles are key intermediates in these catalytic reactions (**Scheme 1.23**).[69]

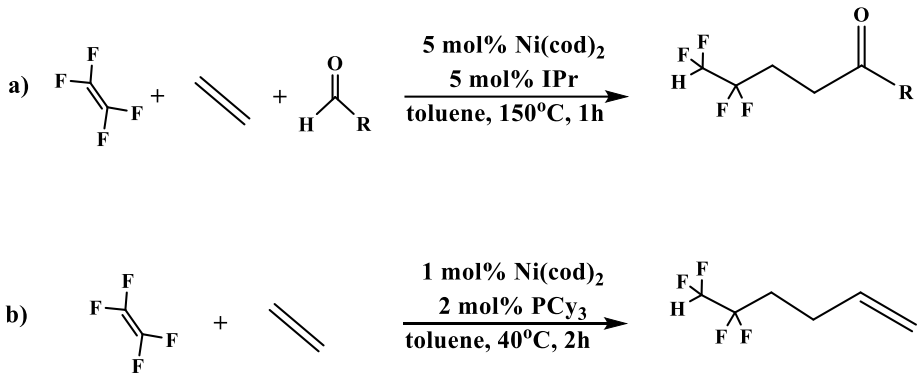

Scheme 1.22. Ni-catalyzed selective cross trimerization reactions.[67,68]

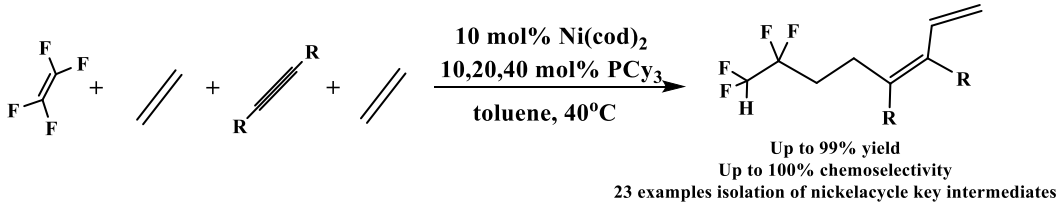

Scheme 1.23. Ni-catalyzed selective cross tetramerization reaction.[69]

1.4.2 Reactions of cobalt hydrides with tetrafluoroethylene

In her investigation of Co-H reactivity with TFE, Ghostine reported the first examples of metal hydride perfluorometallacycle complexes (**Scheme 1.24**).[70] Presumably the 18e- count of these complexes prevents the usually facile C-H reductive elimination. The complicated reactions of P-ligated Co(I) carbonyl hydride complexes with TFE begin with loss of one CO ligand and insertion of TFE into the Co-H bond. The resulting Co-CF_2CF_2H complex can then lose CO, coordinate a second TFE, and rearrange to the Co-H perfluorocobaltacyclopentane. In a competing reaction, the Co-CF_2CF_2H complex can react with the Co-H starting material to give hydrogenated

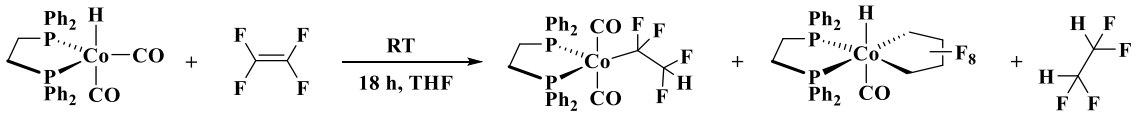

Scheme 1.24. Reaction of P-ligated Co carbonyl hydride with TFE.[70]

TFE and the zerovalent Co-Co bonded dimer. Although irradiation did not result in the expected reductive elimination, suitable choice of ligands may promote this reaction, allowing for a second route to hydrodefluorodimerization (**Scheme 1.25**). In contrast to the Ni-catalyzed VDF route above, the Co-catalyzed route would undergo C-H reductive elimination first, followed by β-F elimination to afford the fluoroalkene product. Silane reaction with the resulting Co-F would then regenerate the catalyst.

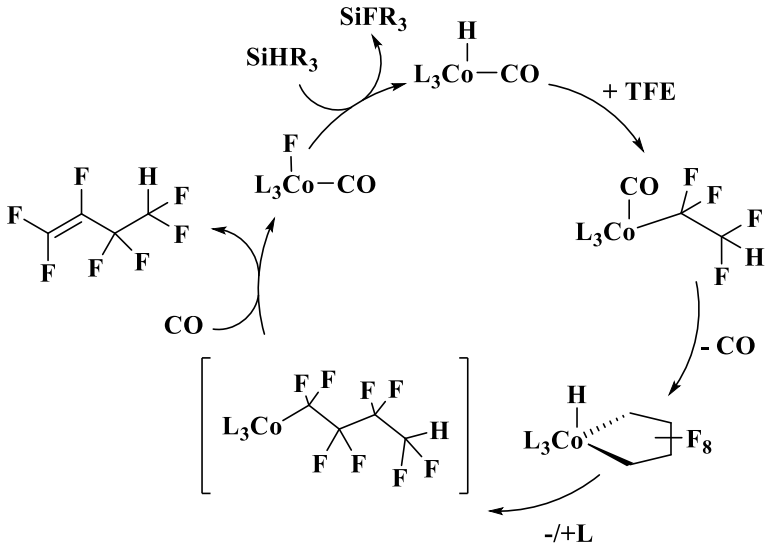

Scheme 1.25. Proposed catalytic cycle for HFO generation via cobalt hydride perfluorometallacyle.[70]

1.5 Summary and Thesis Outline

The goals of my thesis project were to prepare the first examples of d^4 perfluorometallacycle complexes using manganese and to assess the catalytic activity of manganese hydride complexes as amine-borane dehydrogenation catalysts. In **Chapter 2** the synthesis and partial characterization of a series of new Mn(III) perfluorometallacyles derived from $MnBr(P\text{-}P)_2$ and tetrafluoroethylene (TFE) are presenteded but these products are unstable in the absence of TFE. **Chapter 3** focuses on the photolysis of a series of nitrogen-, phosphine- and NHC-substituted manganese bromide carbonyl complexes with fluoroalkenes TFE, CTFE and PMVE from which new Mn(I) fluoroalkyl

complexes $Mn(CF_2CFHX)(DPPE)(CO)_3$ were obtained with X = F, Cl, and OCF_3. Formation of Mn-H from H atom abstraction from solvent by Mn(0) radicals was confirmed by reactions of the fluoroalkenes with $Mn_2(CO)_{10}$ that gave the known $Mn(CF_2CFHX)(CO)_5$ complexes with X = F, Cl and OCF_3. Finally prolonged photolysis of $MnBr(CO)_5$ + 3 equiv of DPPE with TFE gave mixtures that appear to include the d^4 fluorometallacycle, $MnBr(1,4\text{-}C_4F_8)(DPPE)(CO)$. In **Chapter 4** we assess the reactivity of $MnH(H_2)(dmpe)_2$ as an amine-borane dehydrogenation catalyst that compares with $FeH_2(dmpe)_2$ and $[FeH(H_2)(dmpe)_2]^+$. Lastly, in **Chapter 5** the findings of this thesis are placed in context and upcoming directions based on this work are discussed.

1.6 References

1) van Leeuwen, P. W. N. M. *Homogeneous Catalysis – Understanding the Art*, Springer, **2004**.
2) Gebbink, R. J. M.; Moret, M.-E., Eds. *Non-Noble Metal Catalysis: Molecular Approaches and Reactions*, John Wiley & Sons, **2018**.
3) Ribaucourt, A.; Cossy, J. *ACS Catal.* **2020**, *10*, 10127-10148.
4) Santoro, O.; Zhang, X.; Redshaw, C. *Catalysts* **2020**, *10*, 800.
5) West, J.; Huang, D.; Sorensen, E. *Nat. Commun.* **2015**, *6*, 10093.
6) Nesbit, M. A.; Suess, D. L. M.; Peters, J. C. *Organometallics* **2015,** *34* (19), 4741-4752.
7) (a) Mazzacano, T. J.; Mankad, N. J. *J. Am. Chem. Soc.* **2013**, *135* (46), 17258-17261. (b) Dombray, T.; Werncke, C. G.; Jiang, S.; Grellier, M.; Vendier, L.; Bontemps, S.; Sortais, J.-B.; Sabo-Etienne, S.; Darcel, C. *J. Am. Chem. Soc.* **2015**, *137* (12), 4062-4065. (c) Li, H.; Obligacion, J. V.; Chirik, P. J. *ACS Catal.* **2018,** *8* (11), 10606-10618. (d) Arevalo, R.; Pabst, T. P.; Chirik, P. J. *Organometallics* **2020,** *39* (14), 2763-2773.
8) Carney, J. R.; Dillon, B. R. Thomas, S. P. *Eur. J. Org. Chem.* **2016**, *23*, 3912-3929.
9) Mukherjee, A.; Milstein, D. *ACS Catal.* **2018**, *8*, 11435-11469.

10) Koten, G.; Milstein, D., Eds. *Organometallic Pincer Chemistry*. *Top. Organomet. Chem.* **2013**, *40*.

11) Mukherjee, A.; Nerush, A.; Leitus, G.; Shimon, L. J. W.; Ben David, Y.; Jalapa, N. A. E.; Milstein, D. *J. Am. Chem. Soc.* **2016,** *138* (13), 4298-4301.

12) Mastalir, M.; Glatz, M.; Gorgas, N.; Stöger, B.; Pittenauer, E.; Allmaier, G.; Veiros, L. F.; Kirchner, K. *Chem. Eur. J.* **2016**, *22*, 12316−12320.

13) Fu, S.; Shao, Z.; Wang, Y.; Liu, Q. *J. Am. Chem. Soc.* **2017,** *139* (34), 11941-11948.

14) (a) Staubitz, A.; Robertson, A. P. M.; Sloan, M. E.; Manners, I. *Chem. Rev.* **2010**, *110*, 4023−4078. (b) Staubitz, A.; Robertson, A. P. M.; Manners, I. *Chem. Rev.* **2010**, *110*, 4079−4124.

15) (a) Stephens, F. H.; Pons, V. Baker, R. T. *Dalton Trans.* **2007**, 2613-2626. (b) Hamilton, C. W.; Baker, R. T.; Staubitz, A.; Manners, I. *Chem. Soc. Rev.* **2009**, *38*, 279−293.

16) (a) Rossin, A.; Peruzzini, M. *Chem. Rev*. **2016**, *116*, 8848−8872. (b) Johnson, H. C.; Hooper, T. Weller, A. S. *Top. Organomet. Chem.* **2015**, *49*, 153-220.

17) (a) Pons, V.; Baker, R. T.; Szymczak, N. K.; Heldebrant, D. J.; Linehan, J. C.; Matus, M. H.; Grant, D. J.; Dixon, D. A., *Chem. Commun.* **2008**, 6597-6599. (b) Baker, R. T.; Gordon, J. C.; Hamilton, C. W.; Henson, N. J.; Lin, P.-H.; Maguire, M.; Murugesu, M.; Scott, B. L.; Smythe, N. C. *J. Am. Chem. Soc.* **2012**, *134*, 5598-5609. (c) Bhunya, S.; Zimmerman, P. M.; Paul, A. *ACS Catal.* **2015**, *5*, 3478−3493.

18) Denney, M. C.; Pons, V.; Hebden, T. J.; Heinekey, D. M.; Goldberg, K. I. *J. Am. Chem. Soc.* **2002**, *128*, 12048-12049.

19) Gluer, A.; Förster, M.; Celinski, V. R.; auf der Gunne, J. S.; Holthausen, M. C.; Schneider, S. *ACS Catal.* **2015**, *5*, 7214-7217.

20) Kalviri, H. A.; Gärtner, F.; Ye, G.; Korobkov, I.; Baker, R. T. *Chem. Sci.* **2015**, *6*, 618−624.

21) Keaton, R. J.; Blacquiere, J. M.; Baker, R. T. *J. Am. Chem. Soc.* **2007**, *129*, 1844-1845.

22) Bhattacharya, P.; Krause, J. A.; Guan, H. *J. Am. Chem. Soc.* **2014**, *136*, 11153-11161.

23) Staubitz, A.; Sloan, M. E.; Robertson, A. P. M.; Friedrich, A.; Schneider, S.; Gates, P. J.; auf der Gunne, J. S.; Manners, I. *J. Am. Chem. Soc.* **2010**, *132*, 13332-13345.

24) Anke, F.; Han, D.; Klahn, M.; Spannenberg, A.; Beweries, T. *Dalton Trans.* **2017**, *46*, 6843-6847.

25) Sharpe, H. R.; Geer, A. M.; Blundell, T. J.; Hastings, F. R.; Fay, M. W.; Rance, G. A.; Lewis, W.; Blake, A. J.; Kays, D. L. *Catal. Sci. Technol.* **2018**, *8*, 229-235.

26) Blanksby, S. J.; Ellison, G. B. *Acc. Chem. Res.* **2003**, *36* (4), 255–263.

27) a) Chambers, R.D. Fluorine in Organic Chemistry, 2nd Ed., Blackwell: Oxford, **2004**. b) Kirsch, P. Modern Fluoroorganic Chemistry: Synthesis, Reactivity, Applications, 1st ed., Wiley-VCH:Weinheim, Germany, **2004**.

28) Stone, F. G. A. *Pure Appl. Chem.* **1972**, *30*, 551.

29) Braun, T.; Hughes, R. P. *Organometallic Fluorine Chemistry*, Springer, **2015**.

30) Wang, Z. Reagents, Swarts reaction. In Comprehensive Organic Name Reactions and Reagents, **2010**.

31) Norman, C. S.; Decanio, S. J.; Fan, L. *Glob. Environ. Chang.* **2008**, *18*, 330–340.

32) a) Lemal, D. M. *J. Org. Chem.* **2004**, *69*, 1–11. b) Sicard, A. J.; Baker, R. T. *Chem. Rev.* **2020**, *120* (17), 9164-9303.

33) Rao, V. N. M.; Sievert, A. C.; Nappa, M. J. WO **2008**/030440 A2 2008.

34) Potts, J. E.; Ashcraft, A. C.; Wise, E. W.; Va, W. US Patent 3,472,826, **1969**.

35) Egorova, K. S.; Ananikov, V. P. *Organometallics* **2017**, *36*, 4071–4090.

36) Cramer, R.; Kline, J. B.; Roberts, J. D. *J. Am. Chem. Soc.* **1968**, *21* (9), 2519–2524.

37) Parshall, G. W.; Jones, F. N. *J. Am. Chem. Soc.* **1965**, *87*, 5356.

38) Treichel, P. M.; Pitcher, E.; Stone, F. G. A.; Pitcher, E. *Inorg. Chem.* **1962**, *1* (3), 511–517.

39) Wilford, J. B.; Stone, F. G. A. *Inorg. Chem.* **1965**, *4* (1), 2–6.

40) Treichel, P. M.; Morris, J. H.; Stone, F. G. A. *J. Chem. Soc.* **1963**, 720–723.

41) Burrell, A. B.; Roper, W. R. *Organometallics* **1990**, *3* (3), 1905–1910.

42) Wilford, J. B.; Stone, F. G. A. *Inorg. Chem.* **1965**, *4*, 93-97.

43) Beveridge, A. D.; Clark, H. C. *J. Organomet. Chem.* **1967**, *11*, 601.

44) Clark, H. C.; Tsai, J. H. *Inorg. Chem.* **1966**, *5* (8), 1407–1415.

45) Clark, H. C.; Cotton, J. D.; Tsai, J. H. *Inorg. Chem.* **1966**, *5* (8), 1407–1415.

46) Crabtree, R. H. *The Organometallic Chemistry of the Transition Metals*, 6th Ed.; John Wiley & Sons, Inc: Yale University, New Haven, Connecticut, **2014**.

47) Stone, F. G. A. *Leaving no Stone Unturned: Pathways in Organometallic Chemistry*, Wiley-VCH, 1993.

48) (a) Manuel, T. A.; Stafford, S. L.; Stone, F. G. A. *J. Am. Chem. Soc.* **1961**, *104* (2), 2–3. (b) Hoehn, H. H.; Pratt, L.; Watterson, K. F.; Wilkinson, G.; *J. Chem. Soc.* **1960**, 2738–2745.

49) Coyle, T. D.; King, R. B.; Pitcher, E.; Stafford, S. L.; Treichel, P.; Stone, F. G. A. *J. Inorg. Nucl. Chem.* **1961**, *20* (1–2), 172–173.

50) Cundy, C. S.; Green, M.; Stone, F. G. A. *J. Chem. Soc. A* **1970**, 1647–1653.

51) Green, M.; Osborn, R. B. L.; Rest, A. J.; Stone, F. G. A. *J. Chem. Soc. A* **1968**, *502*, 2525–2530.

52) Mukhedkar, V. A.; Mukhedkar, A. J. *J. Inorg. Nucl. Chem.* **1981**, *43* (11), 2801–2805.

53) Ohashi, M.; Shibata, M.; Saijo, H.; Kambara, T.; Ogoshi, S. *Organometallics* **2013**, *32* (13), 3631–3639.

54) Kuwae, R.; Kawakami, K.; Tanaka, T. *Inorg. Chim. Acta* **1977**, *22*, 39-42.

55) Gasafi-Martin, W.; Oberendfellner, G.; von Werner, K. *Can. J. Chem.* **1996**, *74* (11), 1922–1924.

56) Kaplan, P. T.; Xu, L.; Chen, B.; McGarry, K. R.; Yu, S.; Wang, H.; Vicic, D. A. *Organometallics* **2013**, *32*, 7552–7558.

57) Kühnel, M. F.; Lentz, D. *Dalton Trans.* **2010**, *39*, 9729-10004.

58) Lentz, D.; Akkerman, F.; Kickbusch, R.; Patzschke, M. *Z. Anorg. Allg. Chem.* **2004**, *630*, 1363.

59) Baker, R. T.; Beatty, P. R.; Farnham, B. W.; Wallace, L. R. US Patent 5,545,769, **1996**.

60) Ghostine, K.; Gabidullin, B.M.; Baker, R. T. *Polyhedron* **2020**, *185*, 114587.

61) Burch, R. R.; Calabrese, J. C.; Ittel, S. D. *Organometallics* **1988**, *7*, 1642.

62) (a) Giffin, K. A.; Harrison, D. J.; Korobkov, I.; Baker, R. T. *Organometallics* **2013**, *32* (24), 7424–7430. (b) Giffin, K. A.; Korobkov, I.; Baker, R. T. *Dalton Trans.* **2015**, *44*, 19587–19596.

63) Andrella, N. O.; Sicard, A. J.; Gorelsky, S. I.; Korobkov, I.; Baker, R. T. *Chem. Sci.* **2015**, *6*(11), 6392–6397.

64) Giffin, K. A.; Pua, L. A.; Piotrkowski, S.; Gabidulin, B. M.; Korobkov, I.; Hughes, R. P.; Baker, R. T. *J. Am. Chem. Soc.* **2017**, *139*, 4075.

65) (a) Baker, R. T.; Beatty, R. P.; Farnham, W. B.; Wallace, R. L. US Patent 5,670,679, **1997**. (b) Baker, R. T.; Beatty, R. P.; Farnham, W. B.; Wallace, R. L. US Patent

5,760,282, **1998**. (c) Baker, R. T.; Beatty, R. P.; Sievert, A. C.; Wallace, R. L. US Patent 6,242,658, **2001**.

66) Sicard, A. J. University of Ottawa MSc thesis, **2016**.

67) Ohashi, M.; Shirataki, H.; Kikushima, K.; Ogoshi, S. *J. Am. Chem. Soc.* **2015**, *137*, 6496-6499.

68) Ohashi, M.; Kawashima, T.; Taniguchi, T.; Kikushima, K.; Ogoshi, S. *Organometallics* **2015**, *34*, 1604-1607.

69) Kawashima, T.; Ohashi, M.; Ogoshi, S. *J. Am. Chem. Soc.* **2017**, *139*, 17795-17798.

70) Ghostine, K., University of Ottawa MSc thesis, **2018**.

Chapter 2: Synthesis and Reactivity of Phosphorus-Ligated Manganese Bromide Complexes with Tetrafluoroethylene (TFE)

2.1 **Introduction**

As discussed in Chapter 1, both d^6 and d^8 perfluorometallacyclopentanes have been prepared and their reactivity studied. The goal of this chapter was to prepare a variety of monovalent manganese bromide phosphine complexes and investigate their reactivity with TFE to afford the first examples of d^4 fluorometallacyclopentanes. In addition, reactions of manganese phosphine halide complexes with C_2 fluoroalkenes have the potential to afford new C_4 fluoroalkenes in a catalytic process if silanes can be used to convert Mn-F back to Mn-H (**Scheme 2.1**).

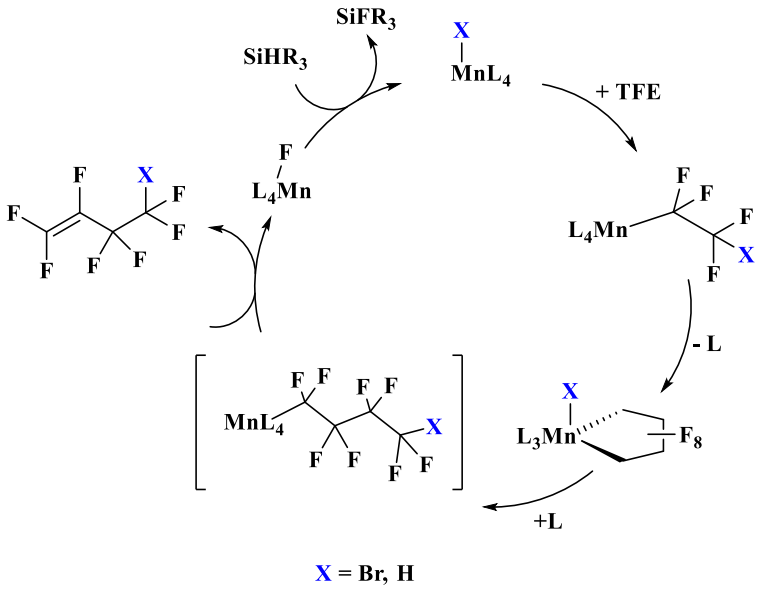

Scheme 2.1. Proposed catalytic cycle for Mn-catalyzed C_4 fluoroalkene formation from TFE.

Low-valent metal phosphine complexes are typically prepared by reduction of metal phosphine halides.[1] For example, reduction of Co dihalide polyphosphine complexes (**Figure 2.1**) with $NaBH_4$ in ethanol affords monovalent Co-H complexes.[2,3] However, examples of carbonyl-

free, monovalent Mn phosphine hydride complexes prepared by this method are limited to the bis(diphosphine) complexes, $MnH(P\text{-}P)_2L$ in which P-P = dmpe and depe and L = H_2 or N_2 [dmpe = 1,2-bis(dimethylphosphino)ethane and depe = 1,2-bis(diethylphosphino)ethane].[4,5] Other examples include $MnH(NO)_2(PEt_3)_2$.[6] As these non-bulky, electron-rich diphosphines are likely to react with TFE, we investigated less basic DPPE and sterically bulky DiBPE diphosphines [DPPE = 1,2-bis(diphenylphosphino)ethane and DiBPE = 1,2-bis(diisobutylphosphino)ethane] as well as monodentate, π-acidic triethylphosphite.

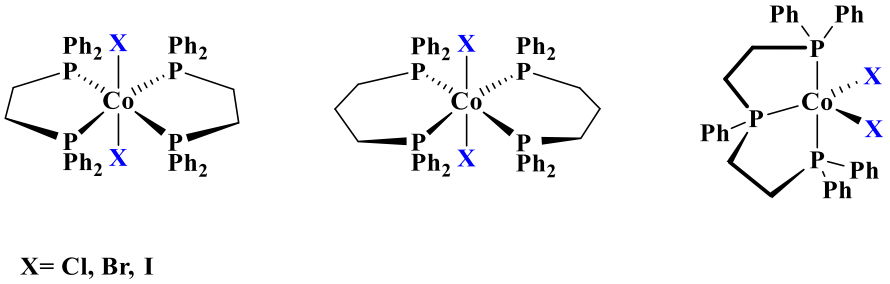

Figure 2.1. Three cobalt dihalide complexes that can be reduced to monovalent 18 e- $CoX(P\text{-}P)_2$ or 16 e- CoX(P-P-P) products.[2,3]

2.2 Results and Discussion

2.2.1 Synthesis of Mn(I) complexes

Manganese dibromide complexes were successfully prepared following a literature procedure[7] by addition of 2 equiv of DPPE, DiBPE or 4 equiv of $P(O^iPr)_3$ to a suspension of $MnBr_2$ in THF solvent to give a colorless solution of paramagnetic $MnBr_2(P\text{-}P)_2$ or $MnBr_2(P)_4$. A number of reducing agents were then employed to generate monovalent Mn-Br or Mn-H analogs. While KC_8 led to decomposition (confirmed by black solid formation), other insoluble metals such as Zn, Mg and Mn showed no reaction either at room temperature or heating at 60°C. Using soluble sodium benzophenone or sodium naphthalenide generated yellow solutions and insoluble NaBr, indicative of reduction. Unfortunately, the purity of the paramagnetic products of these reactions

was not easily assessed but further reaction with TFE broad resonances also indicating a mixture of products. Fearing that further reduction to Mn(0) could be a factor, we employed the milder reductant cobaltocene [Co(η^5-C_5H_5)$_2$]. In this case, the purple colour of the reductant was soon replaced with the orange colour of the cobaltocenium cation. Although the resulting d^6 MnBr products were still paramagnetic, treatment with CO now gave single diamagnetic products MnBr(DPPE)$_2$(CO), **2-2A** and MnBr(DPPP)$_2$(CO), **2-2B** as shown in (**Scheme 2.2**) and (Fig. A.1-A.2).

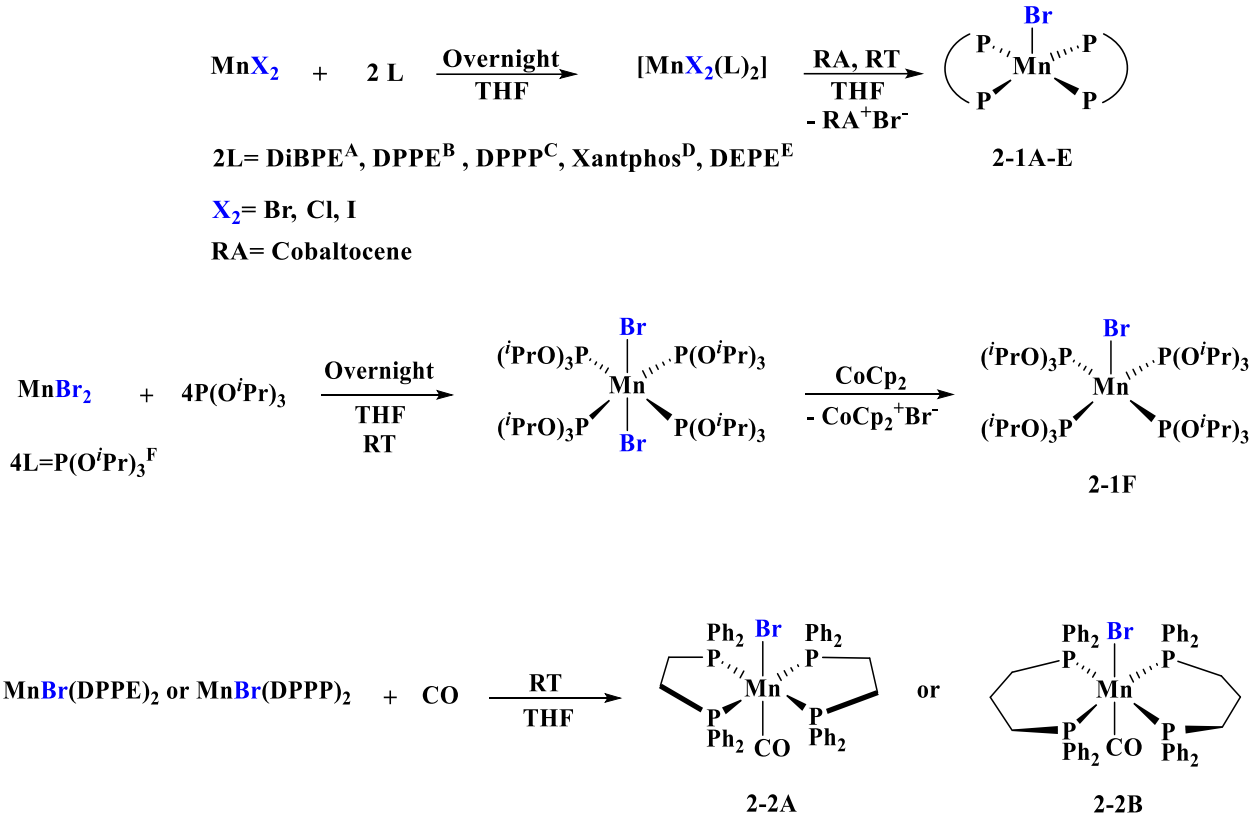

Scheme 2.2. Synthesis of MnBr complexes (**2-1A-F**) using mono- and bidentate phosphorus ligands, and reactions of **2-1B** and **2-1C** with CO.

2.2.2 Reaction of TFE with MnBr(DiBPE)$_2$ (2-1A): Double C-F bond activation by a basic diphosphine

Treatment of **2-1A** with TFE in THF solution gave a rapid colour change to orange (**Scheme 2.3**). The ^{19}F NMR spectrum (**Figure 2.2**) included three resonances: a doublet at -1.6 (J = 675.5 Hz),

a singlet at -101.0 and a doublet at -147.9 ppm (J = 43.5 Hz). The ^{31}P NMR spectrum displayed two doublet resonances at 17.2 (J = 43.5 Hz) and -71.4 ppm (J = 675.5 Hz) (Fig. A.3). Work-up of the reaction mixture by solvent removal and hexane washing removed free ligand and afforded a yellow powder. Recrystallization from THF/hexanes provided a single crystal that identified **2-3** as the reaction product of the basic bis(phosphine) with TFE (**Scheme 2.3**).

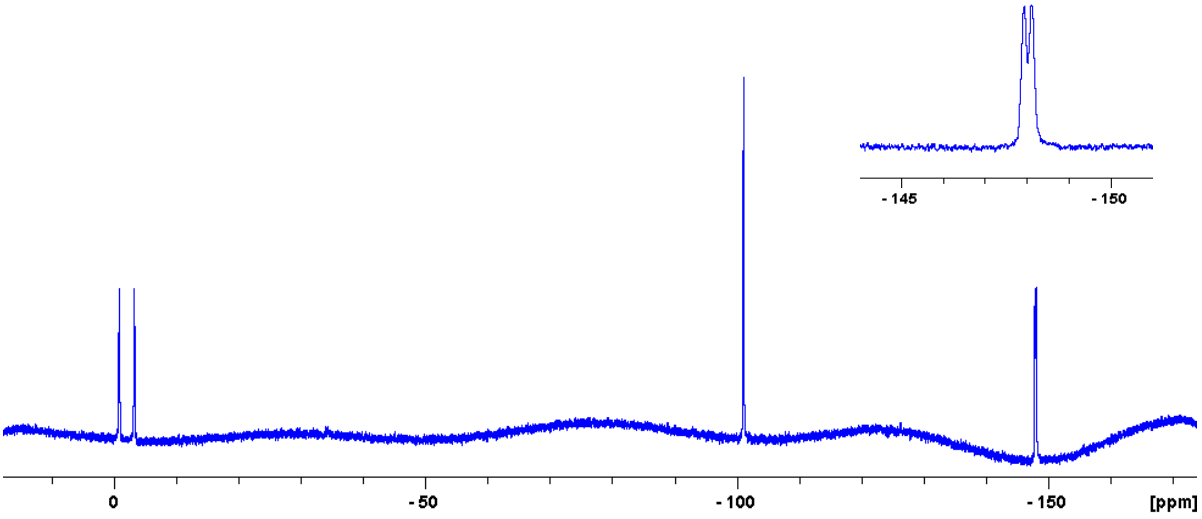

Figure 2.2. ^{19}F NMR spectrum of **2-3** from reaction of bis(phosphine) DiPBE with TFE.

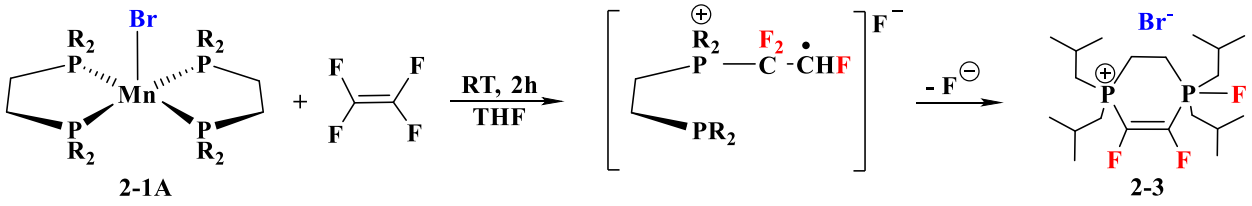

Scheme 2.3. Double C-F bond activation of TFE by bis(phosphine) DiBPE.

The molecular structure of **2-3** consists of a bromide salt of a -CF=CF-bridged phosphorane-fluorophosphonium cation derived from the double C-F bond activation of TFE (**Figure 2.3**). The initially formed fluoride salt presumably undergoes salt metathesis with the [$CoCp_2$]Br, forming **2.3** and [$CoCp_2$]F. Unlike TFE, the C=C bond length of 1.30(3) Å is

appreciably shorter than the C-F bonds 1.44(3) Å, 1.40(3) Å (*cf.* C=C = 1.311 and C-F = 1.319 Å in TFE).[8] Moreover, the bond distances between P2–C7 and P1–F1 are 1.73(2) Å and 1.70(1) Å, respectively. With the structure determined, we can now assign the above NMR resonances. The fluorophosphonium center gives rise to the doublet ^{31}P and ^{19}F NMR resonances with J_{PF} = 675.5 Hz and the other doublet^{19}F resonance is due to the C-F next to the phosphonium center ($^{2}J_{FP}$ = 43.5 Hz).

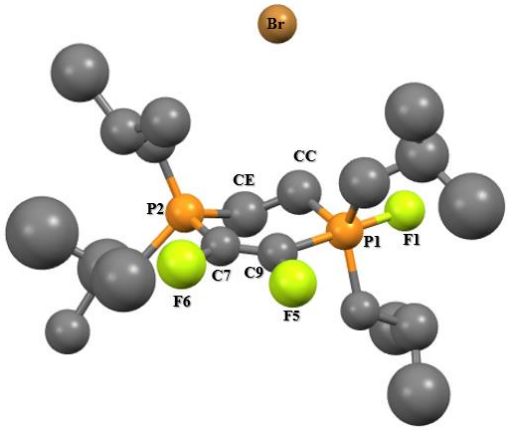

Figure 2.3. ORTEP representation of the molecular structure of **2-3**. Thermal ellipsoids are set at the 40% probability level and hydrogen atoms are omitted for clarity. Selected bond lengths [Å] and angles [deg]. C9–F5 1.44(3), C7–F6 1.40(3), P2–C7 1.73(2), P1–F1 1.70(1), C7–C9 1.30(3), C7–P2–CE 101(1), C9–P1–CC 92(1), P1–C9–F5 113(1), P2–C7–F6 113(2), C7–C9–F5 109(2), F6–C7–C9 125(2) (Table A.1).

*2.2.3 Reaction of TFE with MnBr(DPPE)$_2$ (**2-1B**): Formation of (CpCo)$_2$(μ-η^4,η^4-C$_5$H$_5$-CF$_2$CF$_2$-C$_5$H$_5$-) (**2-4**) and MnBr(1,4-C$_4$F$_8$)(DPPE) (**2-5**).*

To avoid reaction of TFE with the bis(phosphine) we next turned to less electron-rich alkyl-diarylphosphine ligand DPPE. Monitoring the reaction of **2-1B** with TFE by NMR spectroscopy showed appearance of both free (-12 ppm) and coordinated (93.3 ppm) dppe in the ^{31}P NMR and one sharp and two broad ^{19}F NMR resonances (**Figure 2.4**). Following solvent removal under vacuum, however, no ^{31}P and only a single ^{19}F NMR resonance remained. The latter species was characterized by single crystal X-ray diffraction as (CpCo)$_2$(μ-η^4,η^4-C$_5$H$_5$-CF$_2$CF$_2$-C$_5$H$_5$-) (**2-4**),

the product of reaction of TFE with unreacted cobaltocene (**Figure 2.5**). The broad ^{19}F NMR peaks, however, appear in similar regions as the C_α and C_β fluorines in metallocyclopentanes.[9] In this case, however, formation of the proposed metallacycle (**2.5)** is presumably reversible, perhaps driven by the extra equivalent of dppe (**Scheme 2.4**). Similar results were obtained with dppp, **2-6** and Xantphos ligands (**2-7**) (Figs. A.4 and A.5).

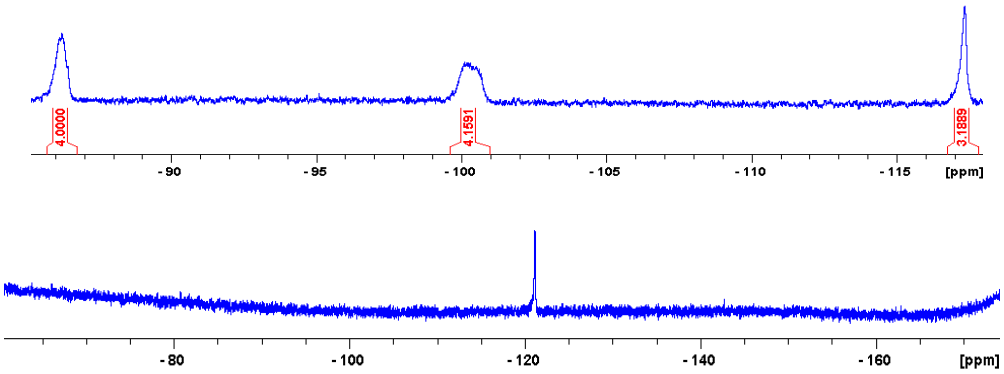

Figure 2.4. ^{19}F NMR spectra of the reaction of **2-1B** with TFE after 2 h. Bottom spectrum was obtained after removal of solvent and dissolution in C_6D_6.

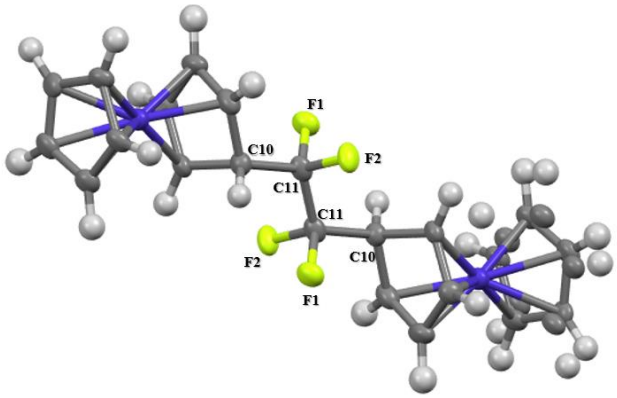

Figure 2.5. ORTEP representation of the molecular structure of $(CpCo)_2(\mu\text{-}\eta^4,\eta^4\text{-}C_5H_5\text{-}CF_2CF_2\text{-}C_5H_5\text{-})$ (**2-4**). Thermal ellipsoids are set at the 40% probability level. Hydrogen atoms are omitted for clarity. Selected bond lengths [Å] and angles [deg]. C11–C11 1.533(7), C11–F1 1.360(6), C11–F2 1.374(5), C10–C11–F1 111.1(2), C10–C11–F2 108.1(4), F1–C11–C11 107.1(4), F2–C11–C11 107(4) (Table A.2).

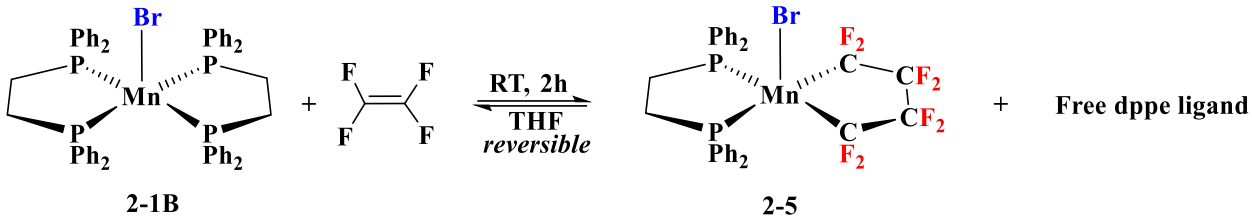

Scheme 2.4. Synthesis of MnBr(1,4-C_4F_8)(DPPE), **2-5.**

The molecular structure of **2.4** is consistent with electron transfer from two Cp_2Co metalloradicals to the TFE molecule, forming a novel C_2F_2-bridged di(cyclopentadiene). Each Co(I) center is coordinated to one Cp anion and to the new di(cyclopentadiene) as a η^4-1,3-diene. This bonding mode is confirmed by the shorter C-C bond distances and the non-planarity of the 5-membered rings in the di(cyclopentadiene).

*2.2.4 Formation of MnBr(1,4-C_4F_8)[P(O^{i}Pr)$_3$]$_3$ (**2-8**).*

Reaction of MnBr[P(OiPr)$_3$]$_4$ (**2-1F**) with TFE gave a similar reaction with broad ^{19}F NMR resonances at -86.5 and -101 ppm (Figs. A.6 and A.7), although the ^{31}P NMR data [integration of coordinated (139 ppm) *vs.* free (140 ppm) phosphite signals is 3:1] are now consistent with an octahedral 16 e- structure for **2-8** (**Scheme 2.5**). Unfortunately, even after removal of the excess phosphite under vacuum, metallacycle formation was again reversible, with only the ^{19}F NMR signal due to **2.4** being observed on dissolution of the resulting solid.

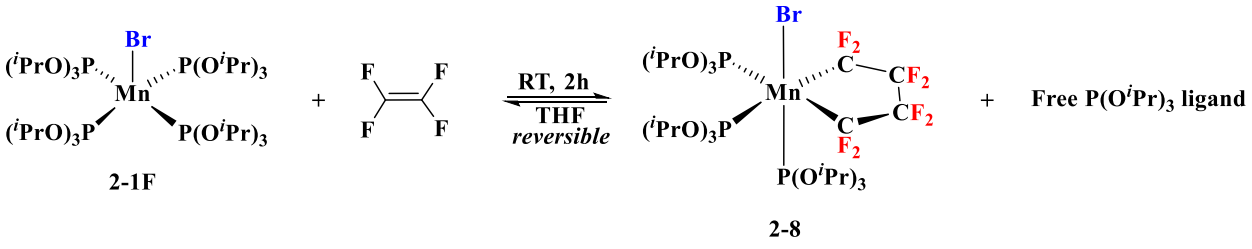

Scheme 2.5. Synthesis of MnBr[P(O^{i}Pr)$_3$]$_3$(1,4-C_4F_8), **2-8.**

2.3 **Conclusions**

In conclusion, although characterization relies solely on *in situ* NMR measurements in the presence of TFE, it appears that formation of the first examples of d^4 perfluorometallacycles is a reversible process, presumably due to the instability of the trivalent Mn metallacycles vs. monovalent phosphorus-ligated Mn bromide. Although not the focus of our investigation, we also identified two interesting new structures derived from TFE reactions with reducing agent Cp_2Co, and bulky dialkyl bis(phosphine) DiPBE. Due to instability of manganese bromide d^4 metallacycle complexes, we turned our investigations in Chapter 3 to manganese bromide carbonyl complexes that may better stabilize d^4 fluorometallacycles based on the d^6 examples.

2.4 **Experimental**

2.4.1 General considerations

MBraun glove box and Schlenk techniques were used to carry out the experiments under nitrogen. A J. C. Meyer solvent purification system was used to dry the diethyl ether, toluene, tetrahydrofuran (THF) and hexanes using activated alumina columns. Stirring over activated alumina (ca. 10 wt.%) was used to dry the benzene-d_6 (C_6D_6) overnight, followed by filtration. Dichloromethane (DCM) and acetonitrile-d_3 (CD_3CN) were refluxed over calcium hydride, stirred over activated alumina (ca. 5 wt.%) overnight and filtered. Activated 4 Å molecular sieves (heated at ca. 250 ^oC for >10 h under vacuum) were added to all solvents stored in the glovebox. All glassware was heated in an oven for >2 h at 150 ^oC.

Commercial chemicals used were 1,2-bis(diphenylphosphino)ethane (DPPE, 99%, Aldrich), manganese(II) bromide ($MnBr_2$, 98%, Aldrich), triisopropylphosphite $P(O^iPr)_3$, 95%, Aldrich), 1,3-bis(diphenylphosphino)propane (DPPP, 97% Aldrich,), 1,2-

bis(diisobutylphosphino)ethane (Cytec-Solvay, DiBPE), 1,2-bis(diethylphosphino)ethane (Strem, DEPE) and 4,6-bis(diphenylphosphino)-10H-phenoxazine (Xantphos, 97%, Aldrich). Pyrolysis was used to prepare tetrafluoroethylene from polytetrafluoroethylene (powdered, Scientific Polymer Products) under vacuum using a modified literature procedure [10-20 mTorr, 25 g scale, 650 °C, R(+)-limonene (97%, Aldrich) for product stabilization producing 97-98% pure TFE].[10] Cobaltocene[11] and $MnBr(P\text{-}P)_2$[7] were also prepared using modified literature procedures. A 300 MHz Bruker Avance instrument was used to record the ^{1}H, $^{31}P\{^{1}H\}$ ^{19}F, and $^{13}C\{^{1}H\}$ NMR spectra at room temperature (21-23 °C). ^{1}H NMR chemical shifts are reported relative to residual proton peaks of the deuterated solvents (CD_3CN: 1.94 ppm; C_6D_6: 7.16 ppm), while ^{19}F and ^{31}P NMR shifts are reported relative to 1,3- bis(trifluoromethyl)benzene (BTB) at -63.5 ppm and phosphoric acid (85 % aqueous solution) at 0 ppm. Electrospray ionization mass spectral data were collected using an Applied Biosystem API2000 triple quadrupole mass spectrometer. Mass spectra were also collected using a Kratos Analytical – Concept magnetic sector electron impact mass spectrometer.

Samples for X-ray crystallography were affixed on thin glass fibres with the help of paraffin oil. Bruker AXS KAPPA single-crystal diffractometer (λ= 0.71073Å) furnished with a sealed Mo tube source and APEX II CCD detector was used to collect the data. APEX II software package from BRUKER AXS was used to collect and process the raw data.

2.4.2 Synthesis and characterization

Synthesis of $MnBr(DiBPE)_2$, 2-1A. Using a literature procedure for a similar complex (other ligands),[7] solid $MnBr_2$ (100 mg, 0.46 mmol) was suspended in 15 mL of THF and stirred for 1 h to dissolve all solid of $MnBr_2$ in vial with a stir bar. After that, 1,2-bis(diisobutylphosphino)ethane (296 mg, 0.93 mmol) in 5 mL of THF was added dropwise and,

after stirring for 12 h, gave a colourless solution. One equivalent of cobaltocene (88 mg, 0.46 mmol) in 5 mL of THF was then added slowly to give a dark yellow solution after stirring overnight. The reaction mixture was filtered through a glass frit to remove orange cobaltocenium bromide and the filtrate dried in vacuo to yield a dark yellow powder. Yield: 350 mg, 88 %. No signals were observed in the $^{31}P\{^{1}H\}$ NMR spectrum of paramagnetic **2-1A**.

Synthesis of MnBr(DPPE)$_2$, 2-1B. This complex was prepared as above using 100 mg of $MnBr_2$ (0.46 mmol), 363 mg of 1,2-bis(diphenylphosphino)ethane (0.93 mmol) and 88 mg of cobaltocene (0.46 mmol). After 12 h stirring, a gradual colour change to dark yellow was observed at room temperature. The reaction mixture was filtered, solvent removed, and the residue dried to obtain a final dark yellow product. Yield: 370 mg, 80%. No signals were observed in the $^{31}P\{^{1}H\}$ NMR spectrum of paramagnetic **2-1B**.

Synthesis of MnBr[P(O^{i}Pr)$_3$]$_4$, 2-1F. This complex was prepared[7] as above using 100 mg of $MnBr_2$ (0.46 mmol), 389 mg of dried triisopropyl phosphite (1.86 mmol) and 88 mg of cobaltocene (0.46 mmol). After 12 h, a gradual colour change to dark yellow was observed at room temperature. The reaction mixture was filtered, solvent removed, and the residue dried to obtain a final dark yellow product. Yield: 340 mg, 70%. No signals were observed in the $^{31}P\{^{1}H\}$ NMR spectrum of paramagnetic **2-1F**.

Synthesis of MnBr(CO)(DPPE)$_2$, 2-2A. To an NMR tube containing $MnBr(DPPE)_2$ was bubbled CO gas, giving a color change from dark yellow to orange. $^{31}P\{^{1}H\}$ NMR (121 MHz, C_6D_6) 31.5 (s, 2P), -12 ppm (free dppe).

Synthesis of MnBr(CO)(DPPP)$_2$, 2-2B. To an NMR tube containing $MnBr(DPPP)_2$ was bubbled CO gas, giving a color change from dark yellow to orange. $^{31}P\{^{1}H\}$ NMR (121 MHz, C_6D_6) 27.7 (s, 2P), -13 ppm (free dppp).

Reactions of phosphorus-ligated manganese bromide with TFE.

These reactions were carried out by dissolving 25-40 mg of the Mn-Br complex in 0.5 mL of THF in an NMR tube fitted with a septum cap and then TFE was added by a 1 mL syringe through the septum cap. NMR spectra were recorded after 2 h of reaction after which time the THF solvent was removed and the resulting residue dissolved in C_6D_6 for additional NMR analysis.

a) **Synthesis of [(i-Bu)$_2$P(μ-CH$_2$CH$_2$)(μ-CF=CF)PF(i-Bu)$_2$]Br, 2-3.** Solid MnBr(DiBPE)$_2$, **2-1A**, (25 mg, 0.03 mmol) was dissolved in ca. 0.5 mL of THF in an NMR tube fitted with a septum cap. Then, 1 mL of TFE gas was injected via syringe through the septum cap. The colour of the reaction mixture changed immediately from dark yellow to orange with precipitation of a solid. The solution was filtered through Celite and evaporated under vacuum to yield oxidized bis(phosphine) product **2-3** as a yellow powder. Yield: 15 mg. ^{19}F NMR (282 MHz, C_6D_6) -1.6 (d, J_{FP} = 675.5 Hz,1F), - 101(s, 1F), - 147.9 ppm (d, $^2J_{FP}$ = 43.5 Hz, 1F). ^{31}P{^{1}H} (121 MHz, C_6D_6) 17.2 (d, $^2J_{PF}$ = 43.5 Hz, 1P), -71.4 ppm (d, J_{PF} = 675.5 Hz, 1P).

b) **MnBr(DPPE)$_2$ + TFE** (Generation of MnBr(1,4-C_4F_8)(DPPE), **2-5**). Solid MnBr(DPPE)$_2$, **2-1B** (40 mg, 0.04 mmol) was dissolved in ca. 0.5 mL of THF in an NMR tube fitted with a septum cap. Then, 1 mL of TFE gas was added via syringe through the septum cap. The reaction mixture changed immediately from dark yellow to orange with precipitation. ^{19}F NMR (282 MHz, C_6D_6) - 86.3 (br s, 4F, $C_\alpha F_2$), - 100 (br s, 4F, $C_\beta F_2$), - 117.3 ppm [s, 4F, (**2-4**)]. ^{31}P{^{1}H} (120 MHz, THF, C_6D_6) 93.3 ppm (s). The resulting solution was filtered through Celite and evaporated under vacuum to yield a yellow powder. Yield: 25 mg. This solid showed no ^{31}P NMR resonances and ^{19}F NMR showed just **2-4**. Similar reactions generated the DPPP (**2.6**) and Xantphos (**2.7**) metallacycles (Figs. A.4 and A.5).

c) **MnBr[P(O^{i}Pr)$_3$]$_4$ + TFE** (Generation of MnBr(1,4-C_4F_8)[P(O^{i}Pr)$_3$]$_3$, **2-8**). Solid MnBr[P(O^{i}Pr)$_3$]$_4$, **2-1F** (25 mg, 0.03 mmol) was dissolved in ca. 0.5 mL of THF in an NMR tube fitted with a septum cap. Then, 1 mL of TFE gas was inserted via syringe through the septum cap. The reaction mixture changed immediately from dark yellow to orange with precipitation. ^{19}F NMR (282 MHz, THF, C_6D_6) δ - 87 (br s, 4F, $C_\alpha F_2$), - 101.5 (br s, 4F, $C_\beta F_2$), - 121[s, 4F, (**2-4**)]. ^{31}P{^{1}H} (121 MHz, THF, C_6D_6) δ 139 ppm (s). The solution was filtered through Celite and evaporated under vacuum to yield a yellow powder. Yield: 13 mg. This solid showed no ^{31}P NMR resonances and ^{19}F NMR showed just **2-4**.

2.5 **References**

1) (a) King, R. B.; Kapoor, P. N.; Kapoor, R. N. *Inorg. Chem.* **1971**, *10*, 1841-1850. (b) Vinal, R. S.; Reynolds, L. T. *Inorg. Chem.* **1964**, *3*, 1062-1063.
2) Kruse, W.; Atalla, R. H. *Chem. Commun.* **1968**, *15*, 921–922.
3) (a) Horrocks, W. D. Jr.; Van Hecke, G. R.; DeWitt Hall, D. *Inorg. Chem.* **1967,** *6* (4), 694-699. (b) Yamamoto, A.; Kitazume, S.; Pu, L. S.; Ikeda, S. *J. Am. Chem. Soc.* **1971,** *93* (2), 371-380.
4) (a) Girolami, G. S.; Howard, C. G.; Wilkinson, G.; Dawes, H. M.; Thornton-Pett, M.; Motevalli, M.; Hursthouse, M. B. *J. Chem. Soc., Dalton Trans.* **1985**, 921-929. (b) Girolami, G. S.; Wilkinson, G.; Thornton-Pett, M.; Hursthouse, M. B. *J. Am. Chem. Soc.* **1983**, *105*, 6752-6753.
5) Perthuisot, C.; Fan, M.; Jones, W. D. *Organometallics* **1992**, *11*, 3622-3629.
6) Gusev, D. G.; Nietlispach, D.; Vymenits, A. B.; Bakhmutov, V. I.; Berke, H. *Inorg. Chem.* **1993**, *32*, 3270-3276.
7) Girolami, G. S.; Wilkinson, G.; Galas, A. M. R.; Thornton-Pett, M.; Hursthouse, M. B. *J. Chem. Soc., Dalton Trans*. **1985**, *7*, 1339–1348.
8) Hellwege, K. H.; Hellwege, A. M. (Ed.). *Landolt-Bornstein: Group II: Atomic and Molecular Physics Volume 7: Structure Data of Free Polyatomic Molecules.* Springer-Verlag: Berlin, **1976**.
9) Cundy, C. S.; Green, M.; Stone, F. G. A. *J. Chem. Soc. A* **1970**, 1647–1653.
10) Hunadi, R. J.; Baum, K. *Synthesis* **1982**, 39, 454.

11) Maier, T. M.; Sandl, S.; Shenderovich, I. G.; von Wangelin, A. J.; Weigand, J. J.; Wolf, R. *Chem. Eur. J.* **2019**, *25* (1), 238–245.

Chapter 3: Reactions of Substituted Manganese Bromide Carbonyl Complexes with Fluoroalkenes

3.1 **Introduction**

In chapter 2, we proposed that bis(phosphine) Mn(I) bromide d^4 fluorometallacycles were generated from TFE but reverted back to the starting complex upon solvent removal in vacuum. This chapter focuses on the reactivity of manganese pentacarbonyl bromide, $MnBr(CO)_5$, **3-1** and its P-, N-, and C-donor ligand-substituted analogs with TFE and two commercially available fluoroalkenes, chlorotrifluoroethylene (CTFE) and perfluoro(methyl vinyl ether) (PMVE). Surprisingly, when we used $MnBr(DPPE)(CO)_3$ these photolytic reactions afforded products resulting from insertion of the fluoroalkenes into a Mn-H[1] that was generated *in situ* [DPPE = 1,2-bis(diphenylphosphino)ethane]. While previous work on insertion of CTFE into $MnH(CO)_5$ indicated formation of both regioisomers,[1b] only the Mn-CF_2CFHCl isomer was obtained in our experiments, presumably due to the increased steric bulk of the $Mn(DPPE)(CO)_3$ fragment (*vs.* $Mn(CO)_5$). By comparison with results from a previous Baker group MSc thesis,[2] we also determined that Mn-H generation from H atom abstraction in THF is accompanied by formation of α-fluoroalkylated THF,[3-5] $O[-(CH_2)_3CH(CF_2CFXH)-]$, in which X = F, Cl, OCF_3. Switching to methyl *t*-butyl ether solvent, exhaustive photolysis of $MnBr(CO)_5$, + 3 equiv of DPPE with TFE gave a mixture containing a new product proposed to be the first stable d^4 fluorometallacycle, $MnBr[-(CF_2)_4-](DPPE)(CO)$. Finally, exhaustive photolysis of $Mn(CF_2CFHCl)(DPPE)(CO)_3$ with CTFE in C_6D_6 generated additional products also proposed to be d^4 fluorometallacycles. Reactions of the fluoroalkenes with zerovalent $Mn_2(CO)_{10}$ were also carried out in order to clarify the reaction pathways.

3.2 **Synthesis of Donor Ligand Analogues of $MnBr(CO)_5$**

Not only several bi- and tridentate phosphine ligands, but also nitrogen donors and an *N*-heterocyclic carbene were used to replace CO groups in manganese pentacarbonyl bromide $MnBr(CO)_5$, **3-1.** Using modified literature procedures, three phosphine-substituted complexes were prepared.[6-10] By adapting another technique from the literature, we synthesized two bidentate nitrogen donor-[11,12] and one NHC-ligated analogue.[13]

Under toluene reflux, equimolar amounts of **3-1** and bidentate phosphine DPPE gave previously reported $MnBr(DPPE)(CO)_3$ (**3-2)**.[6] The $^{31}P\{^1H\}$ NMR spectrum indicated a single isomer (**Scheme 3.1**) with a singlet at 67.8 ppm. Using 2 equiv of DPPE with **3-1** afforded $MnBr(DPPE)_2(CO)$, **3-3** with CO trans to Br as confirmed by a ^{31}P NMR singlet at 72 ppm.[7,8] With tridentate ligand 1,1-bis(diphenylphosphinoethyl)phenyl phosphine (triphos) the dicarbonyl complex (**3-4**) displayed two broad ^{31}P NMR singlets at 116.7 and 83.4 ppm in a 1:2 ratio, confirming the κ^3-coordination of the triphos ligand (Fig. A.8).[9,10]

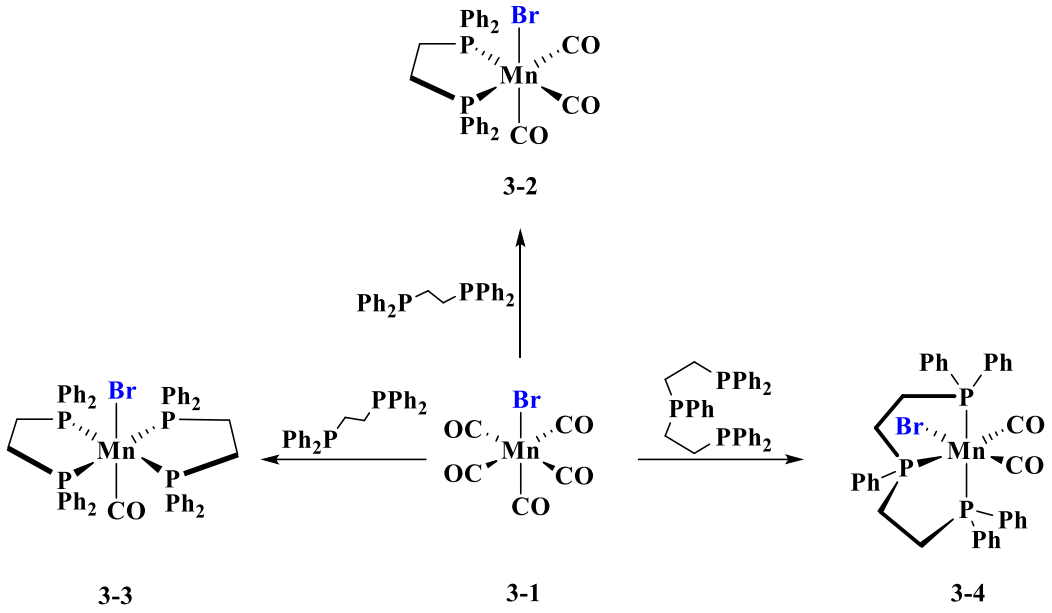

Scheme 3.1. Phosphorus-ligated manganese bromide carbonyl complexes.[6-10]

Substitution reactions with 2,2′-bipyridine (bipy, **3-5**), phenanthroline (phen, **3-6**),[11,12] and IPr (**3-7**),[13] was also successful (**Scheme 3.2**). The IPr complex was isolated in 46% yield as an orange solid that is stable in air. According to literature procedures in the IR spectra,[13] they showed that three CO bands at 2078, 1995, 1938 cm^{-1} are consistent with the cis-configurations. For $MnBr(bipy)(CO)_3$ (**3-5**) and $MnBr(phen)(CO)_3$ (**3-6**), the three CO ligands are found from two strong $^{\nu}$CO stretching bands which be around at 1920 and 2030 cm^{-1} in their FTIR spectra as mention in literature.[12] Similar results were obtained for the phen analog.

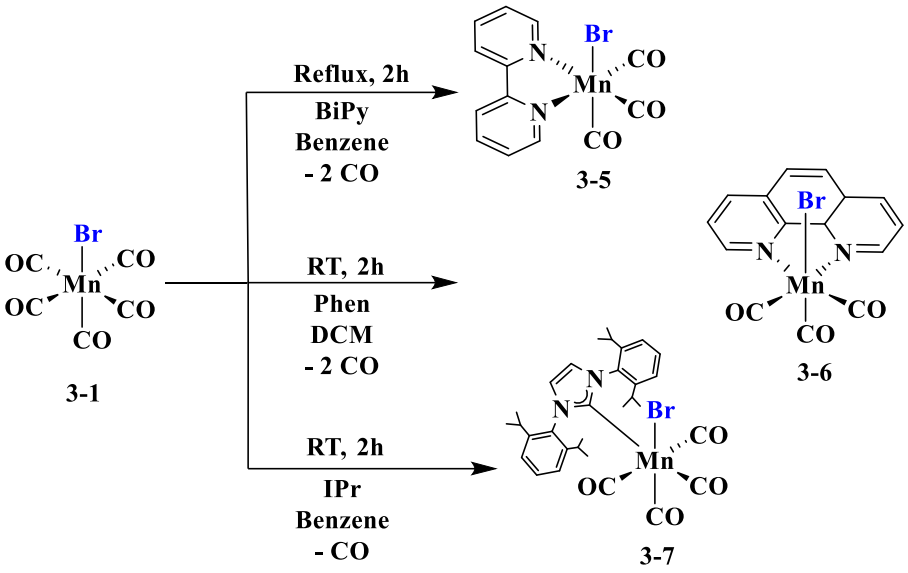

Scheme 3.2. Reaction of $MnBr(CO)_5$ with NHC and nitrogen ligands.[11-13]

3.3 **Reactions of $MnBr(CO)_5$ and its Ligated Analogs with Fluoroalkenes**

Complex **3-1** and the various substituted manganese(I) carbonyl bromide complexes were treated with fluoroalkenes TFE, PMVE and CTFE and subsequently photolyzed using a Hg UV lamp. Initial experiments using toluene solvent gave only broad resonances between -80 and -120 ppm so we switched to THF.

3.3.1 TFE reactions: Formation of Mn[-CF_2CF_2H-](DPPE)$(CO)_3$ and O[-$(CH_2)_3CH(CF_2CF_2H)$-]

Monitoring the reaction of TFE with DPPE analog **3-2** in THF under UV radiation using ^{19}F NMR indicated formation of three different products (**Figure 3.1**). A comparison with the proton-decoupled ^{19}F NMR spectrum identified one product as the DPPE Mn-tetrafluoroethyl complex (**3-8**), resulting from insertion of TFE into Mn-H [*cf.* CF_2 at -115.1 (d mult, $^3J_{FP}$ = 67 Hz) and CF_2H at -134.8 ppm (ddtr, $^2J_{FH}$ = 54, $^4J_{FP}$ = 22.5, $^3J_{FF}$ = 6 Hz] (**Scheme 3.3**). The $^{31}P\{^1H\}$ NMR

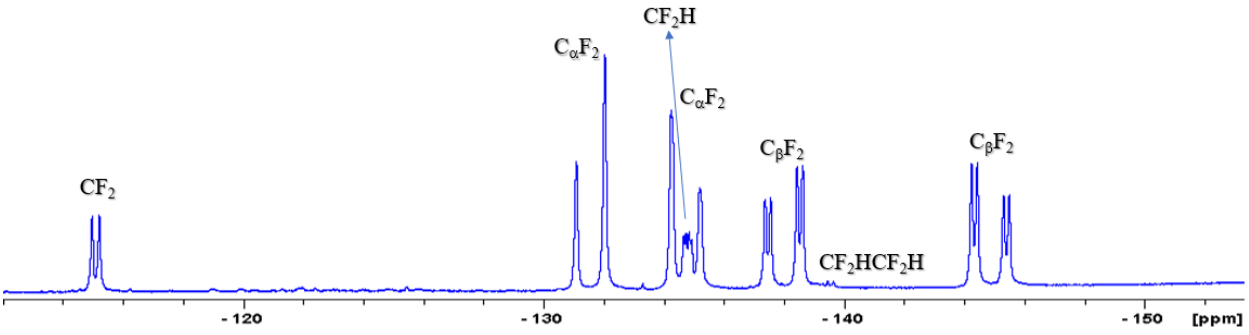

Figure 3.1. ^{19}F NMR spectrum from photolysis of MnBr(DPPE)(CO)$_3$, **3-2** with TFE in THF after 7 h.

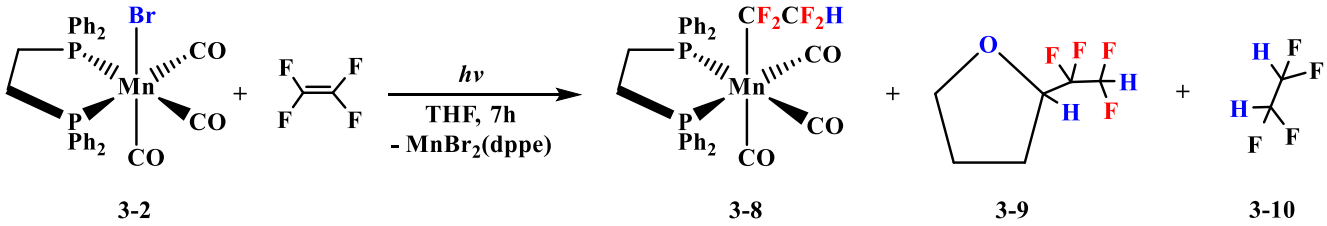

3-2 **3-8** **3-9** **3-10**

Scheme 3.3. Reaction of MnBr(DPPE)(CO)$_3$, **3-2** with TFE.

spectrum of **3-8** contained a triplet of triplets at -6.7 ppm as expected for the R^F group *cis* to the 2 Ps (Fig. A.9) and the CF_2*H* triplet of triplets resonance in the ^{1}H NMR spectrum was observed at δ 5.1($^2J_{HF}$ = 53, $^3J_{FH}$ = 5 Hz) (Fig. A.10). In addition to a trace of hydrogenated TFE (**3-10**, 1,1,2,2,-tetrafluoroethane), the major product contained two diastereotopic CF_2 groups that we initially assigned to a Mn-H fluorometallacycle based on data for an analogous CoH(P^{i}Bu$_3$)(CO)$_3$ + TFE reaction from an earlier Baker group MSc thesis.[2] Having seen that our product was *exactly* the same as the one from the Co reaction (**Figure 3.2**), however, we eventually confirmed its structure as α-fluoroalkylated THF,[3-5] O[-(CH$_2$)$_3$CH(CF$_2$CF$_2$H)-], **3-9**. A ^{19}F-^{19}F COSY NMR spectrum confirmed the expected correlations (Fig. A.11). Analogous photolytic reactions of TFE with **3-1** yielded larger amounts of hydrogenated TFE but no evidence of the unsubstituted Mn carbonyl tetrafluoroethyl insertion product[1] (Fig. A.12).

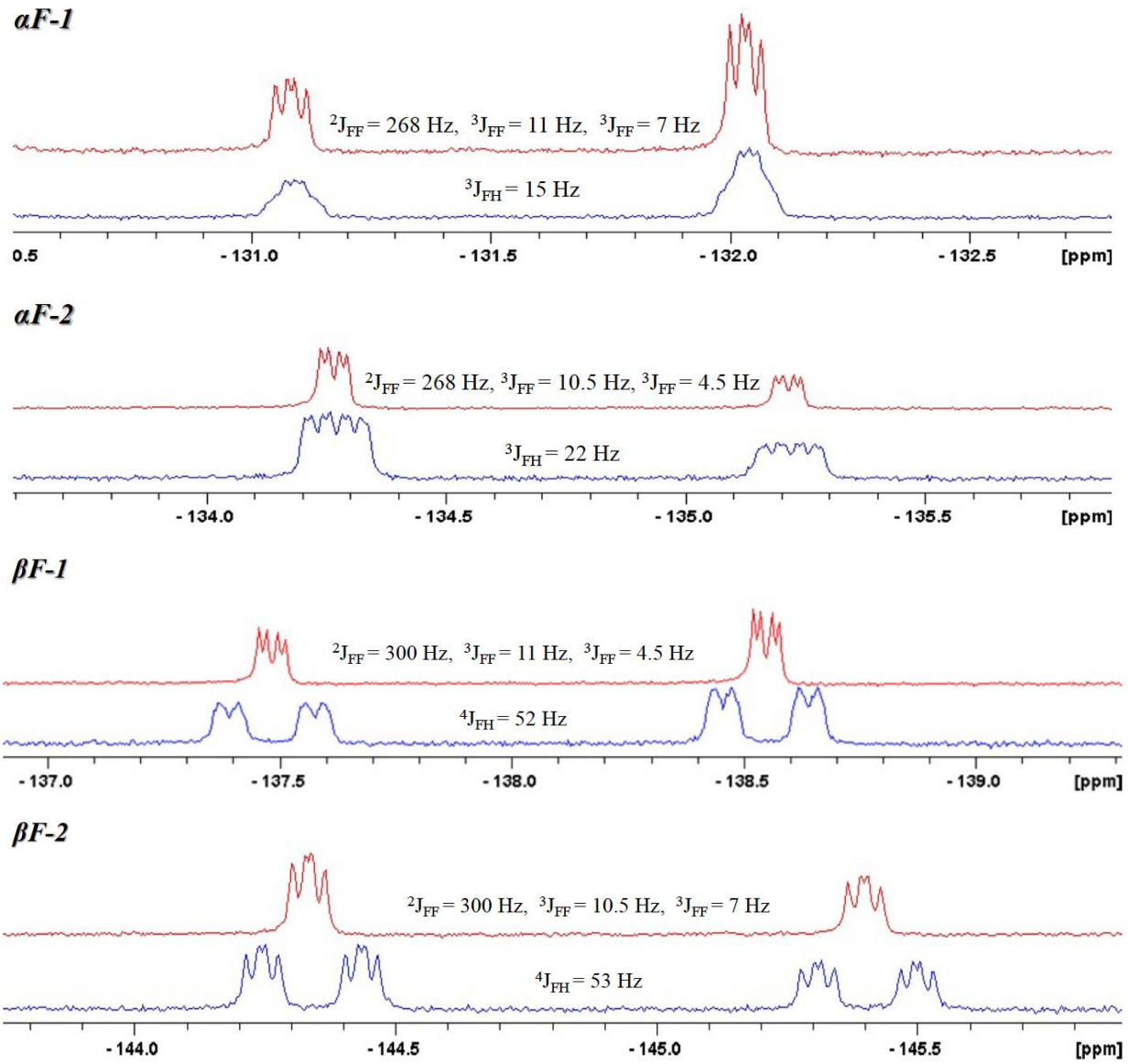

Figure 3.2. High resolution ^{19}F NMR spectrum of O[-$(CH_2)_3CH(CF_2CF_2H)$-], **3-9** (red = proton decoupled).

Surprisingly, photolysis of MnBr(triphos)$(CO)_2$ (**3-4)** with TFE in THF gave mainly fluoroalkylated THF complex (**3-9**) although the reaction was much slower (Fig. A.13). Finally, reactions of TFE with the N-ligated and NHC-substituted analogs also gave primarily **3-9** (Figs. A.14-16).

3.3.2 PMVE reactions: Formation of Mn[$CF_2CFH(OCF_3)$](DPPE)$(CO)_3$ and diastereomers of O{-$(CH_2)_3$CH[$CF_2CFH(OCF_3)$]-}

As shown by the ^{19}F NMR spectra (**Figure 3.3**), irradiation of **3-2** gave diastereomers of fluoroalkylated THF, O{-$(CH_2)_3$CH[$CF_2CFH(OCF_3)$]-} (**3-11** and **3-12)** as well as insertion product, Mn[$CF_2CFH(OCF_3)$](DPPE)$(CO)_3$ (**3-13**) (**Scheme 3.4**). The overlapping diastereotopic CF_2 resonances for **3-11** and **3-12** are at -128.5 (ddd, $^2J_{FF}$ = 265, $^3J_{FH}$ = 20, $^3J_{FF}$ = 12.5 Hz, 1F) and -125.8 ppm (d mult, $^2J_{FF}$ = 265 Hz, 1F) for the major isomer, and -128.7 (dd, $^2J_{FF}$ = 267, $^3J_{FH}$ = 22 Hz, 1F), and -126.7 ppm (d mult, $^2J_{FF}$ = 267 Hz, 1F) for the minor one. While the OCF_3 resonances are overlapping at -56.5 and -56.6 ppm, the doublet CF resonances are at -142.4 (d, $^2J_{FH}$ = 52 Hz, 1F) and -150.3 ppm (d, $^2J_{FH}$ = 54 Hz, 1F) for the minor and major isomers, respectively. All expected correlations were confirmed by the ^{19}F-^{19}F COSY NMR spectrum (Fig. A.17). For insertion product **3-13**, a single doublet ^{19}F NMR resonance is observed for the diastereotopic CF_2 group, presumably due to their chemical shifts being the same. The $^{31}P\{^1H\}$ NMR spectrum of **3-13** contained triplet of doublets at 1.3 ppm (Fig. A.18-A.19). Using alternate ligated starting Mn complexes with bipy (**3-5**), (phen) (**3-6**) or (IPr) (**3-7**) gave primarily **3-11** and **3-12** but no insertion products (Figs. A.20-22).

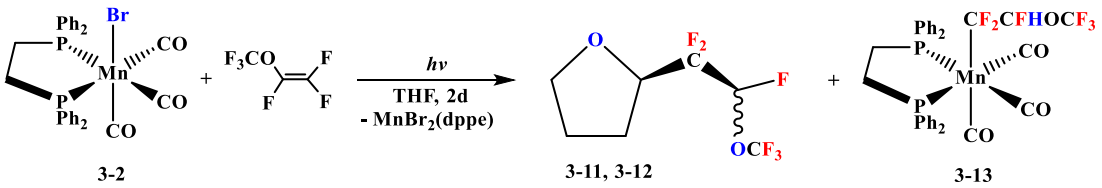

3-2 3-11, 3-12 3-13

Scheme 3.4. Photolysis reaction of $MnBr(DPPE)(CO)_3$ (**3-2**) with PMVE in THF.

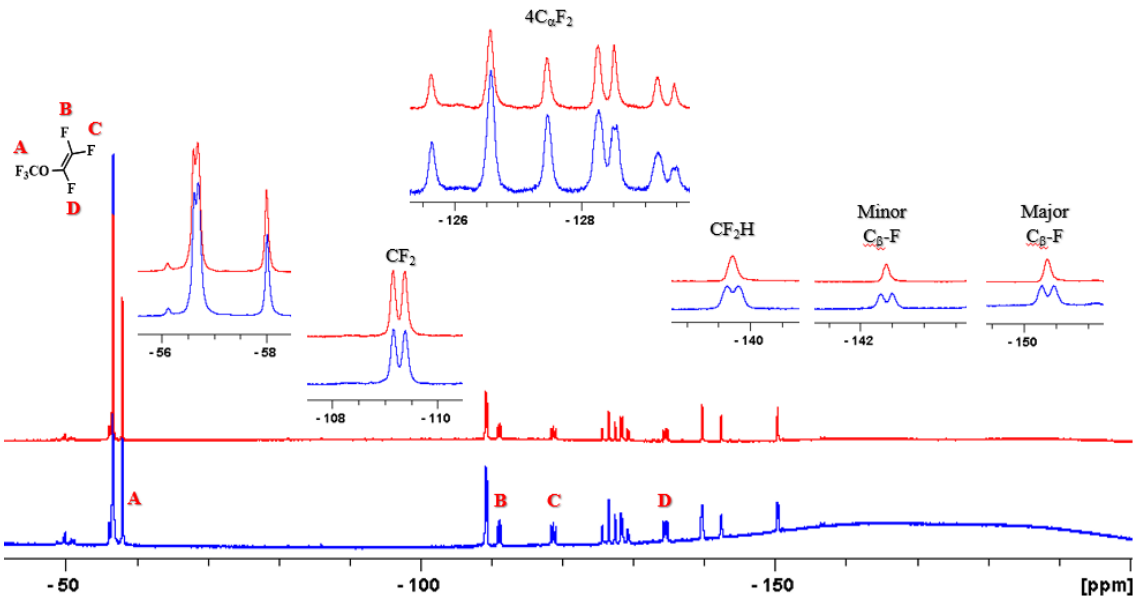

Figure 3.3. ^{19}F and $^{19}F\{^{1}H\}$ NMR spectrum of diastereomers, O{-$(CH_2)_3$CH[CF_2CFH(OCF_3)]-}, (**3-11** and **3-12**) and Mn[CF_2CFH(OCF_3)](DPPE)$(CO)_3$, (**3-13**) derived from irradiation of MnBr(dppe)$(CO)_3$ (**3-2**) with PMVE in THF after 2 d (red = proton-decoupled).

3.3.3 CTFE reactions: Formation of Mn[CF_2CHFCl](DPPE)$(CO)_3$ and diastereomers of O[-$(CH_2)_3$CH(CF_2CFHCl)-]

Photolysis of MnBr(DPPE)$(CO)_3$ (**3-2**) with CTFE in THF afforded analogous products to those from PMVE; namely diastereomers of fluoroalkylated THF, O[-$(CH_2)_3$CH(CF_2CFHCl)-], (**3-14** and **3-15**) and the insertion product, Mn[CF_2CHFCl](DPPE)$(CO)_3$ (**3-16**; **Scheme 3.5**). As for the PMVE products, overlapping diastereotopic C*F*$_2$ resonances for **3-14** and **3-15** in the ^{19}F NMR are at -128.2 (ddd, $^{2}J_{FF}$ = 254.5, $^{4}J_{FH}$ = 20, $^{3}J_{FF}$ = 16 Hz, 1F) and -125.6 ppm (ddd, $^{2}J_{FF}$ = 254.5, $^{4}J_{FH}$ = 12, $^{3}J_{FF}$ = 12 Hz, 1F) for the major isomer, and -127.2 (ddd, $^{2}J_{FF}$ = 265, $^{4}J_{FH}$ = 18.5, $^{3}J_{FF}$ = 10 Hz, 1F) and -126.1 ppm (ddd, $^{2}J_{FF}$ = 265, $^{4}J_{FH}$ = 14, $^{3}J_{FF}$ = 14 Hz, 1F) for the minor one (**Figure 3.4**). The doublet C*F* resonances are at -160.01 (dtr, $^{3}J_{FH}$ = 41.5, $^{3}J_{FF}$ = 14 Hz, 1F) and -152.3 (dtr, $^{3}J_{FH}$ = 41, $^{3}J_{FF}$ = 12 Hz, 1F) for the minor and major isomers, respectively. All the expected correlations were confirmed by the ^{19}F-^{19}F COSY NMR spectrum (Fig. A.23).

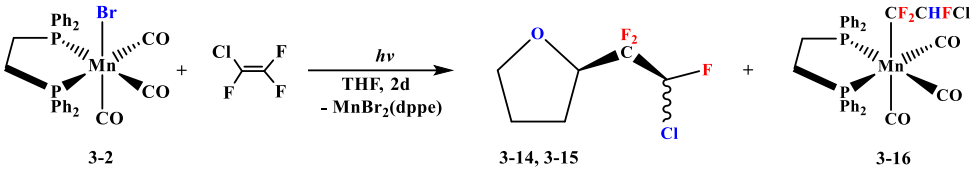

Scheme 3.5. Photolytic reaction of CTFE with MnBr(DPPE)$(CO)_3$ (**3-2**).

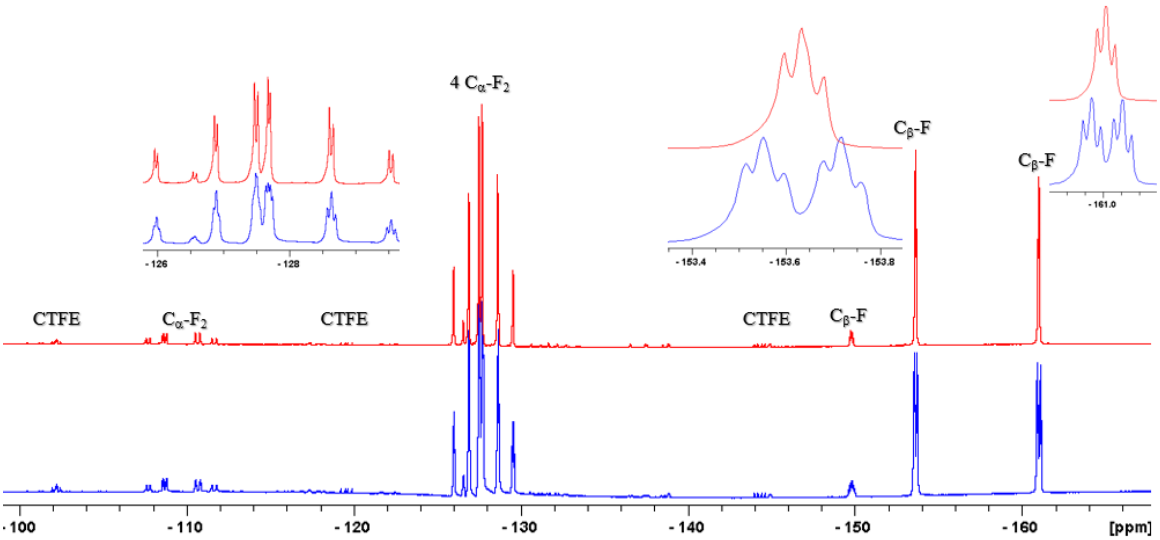

Figure 3.4. ^{19}F and $^{19}F\{^1H\}$ NMR spectra of photolytic reaction of CTFE with MnBr(DPPE)$(CO)_3$ (**3-2**) (red = proton-decoupled).

In contrast to the PMVE analog, the ^{19}F NMR spectrum of insertion product **3-16** showed diastereotopic Cα*F*$_2$ resonances at -107.2 and -110.0 ($^2J_{FF}$ = 276 Hz) with significant coupling to P (58 and 78 Hz, respectively), intermediate $^3J_{FF}$ (18 and 12 Hz) and small coupling to H (4 and 10 Hz; **Figure 3.5**). The Cβ*F* at -148.4 ppm exhibits the typical large $^2J_{FH}$ coupling of 50 Hz, the $^{31}P\{^1H\}$ NMR ddd resonance shows coupling to the three inequivalent Fs and the -CFCl*H* was observed in the ^1H NMR spectrum at δ 5.5 (ddd, $^4J_{FH}$ = 58, 10, 4 Hz) (Fig. A.24). Again, reactions of CTFE with the bipy (**3-5**), phen (**3-6**) or IPr (**3-7**) analogues gave no insertion products (Figs. A.25-27).

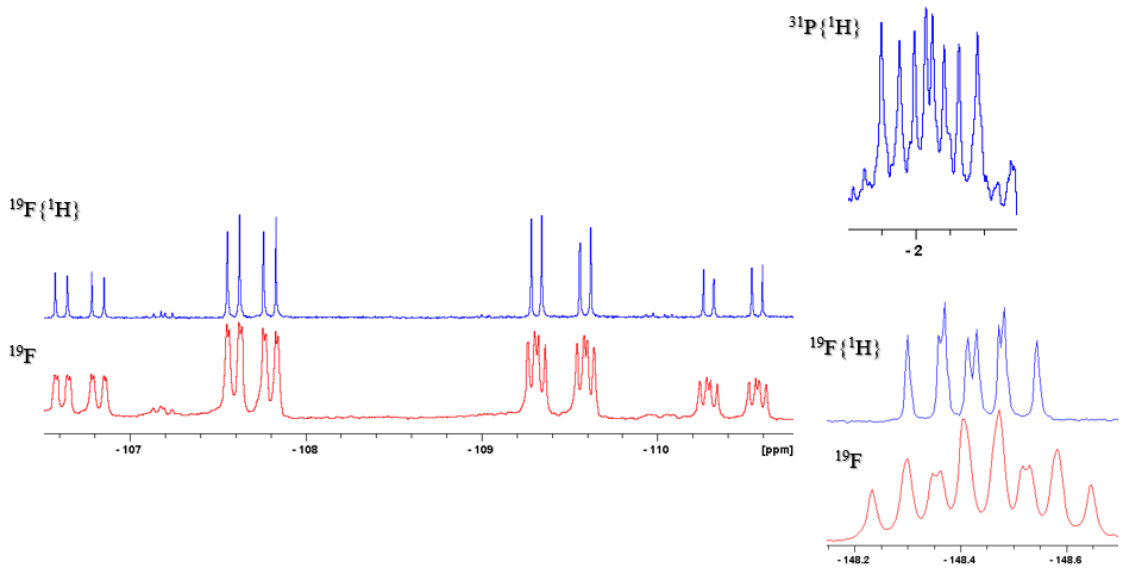

Figure 3.5. High resolution ^{19}F, $^{19}F\{^{1}H\}$ and $^{31}P\{^{1}H\}$ NMR spectra of $Mn[CF_2CHFCl](DPPE)(CO)_3$ (**3-16**).

3.3.4 Reaction of dimanganese decacarbonyl, $Mn_2(CO)_{10}$ with fluoroalkenes.

As discussed in the next section, we suspected that Mn-H formation resulted from H atom abstraction from THF by a zerovalent Mn intermediate. As a result, we investigated reactions of zerovalent $Mn_2(CO)_{10}$ with our fluoroalkene substrates. Indeed, heating $Mn_2(CO)_{10}$ and TFE at 65 °C in THF gave monoalkyl-substituted tetrahydrofuran, $O[-(CH_2)_3CH(CF_2CF_2H)-]$, (**3-9**) and *unsubstituted* insertion product, $Mn(CF_2CF_2H)(CO)_5$, (**3-17**)[1] in one of the cleanest reactions according to the ^{19}F NMR spectra (Fig. A.28). Unfortunately, this reaction gave the same results under UV irradiation (Fig. A.29). Turning to PMVE, the thermal reaction with $Mn_2(CO)_{10}$ also cleanly gave diastereomers of $O[-(CH_2)_3CH(CF_2CFH)(OCF_3)-]$, **3-11** and **3-12** (Fig. A.30) whereas irradiation of the same reaction yielded only unsubstituted insertion product $Mn[CF_2CF(OCF_3)H](CO)_5$, (**3-18**) and hydrogenation product, $HCF_2CF(OCF_3)H$ (Fig. A.31). Finally, CTFE gave a sluggish reaction at 65°C with only small amounts of hydrogenation product, HCFClCFClH, and $O[-(CH_2)_3CH(CF_2CFHCl)-]$, **3-14** and **3-15** being formed (Fig. A.32). Remarkably, irradiation of the same reaction gave a number of broad ^{19}F NMR resonances due to

an uncharacterized mixture of products with no evidence of insertion or metallacycle products (Fig. A.33).

3.3.5 Alternate ether solvents

Interestingly, addition of TFE to the monocarbonyl complex, $MnBr(DPPE)_2(CO)$, **3-3** in diethyl ether solvent (DEE) also gave insertion product (**3-8**), hydrogenated TFE (**3-10**) and monoalkylation of DEE, $EtO[CH(CF_2CF_2H)CH_3]$, **3-19** (Figs. A.34 and 35; **Scheme 3.6**). Turning to methyl *t*-butyl ether (MTBE), photolysis of **3-2** and TFE still afforded Mn-H insertion products

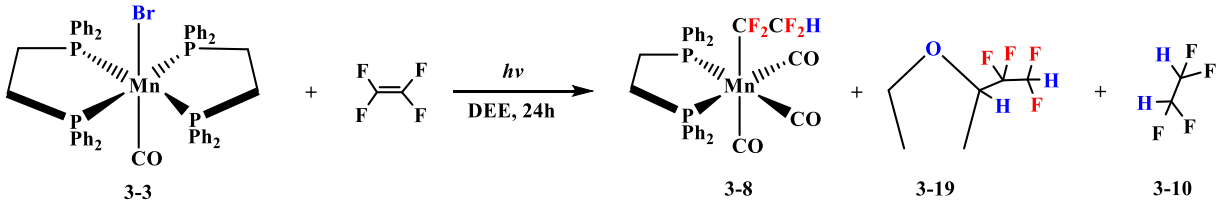

Scheme 3.6. Reaction of $MnBr(DPPE)_2(CO)$, **3-3** with TFE in diethyl ether.

but no evidence of solvent fluoroalkylation. Finally, exhaustive photolysis (3 d) of $MnBr(CO)_5$ + 3 equiv. of DPPE with TFE in MTBE afforded a mixture of new products, one of which (**3-20**) featured four different CF_2 resonances coupled to P (Fig. A.36). Although separation of the product and further characterization is required, the ^{19}F NMR spectra suggest formation of a Mn fluorometallacycle, presumably still containing the Mn-Br bond (**Scheme 3.7; Figure 3.6**).

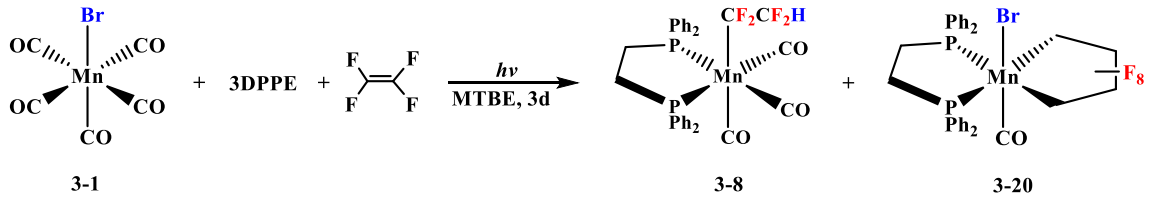

Scheme 3.7. Reaction of $MnBr(CO)_5$ (**3-1**) + 3 equiv. of DPPE with TFE in MTBE.

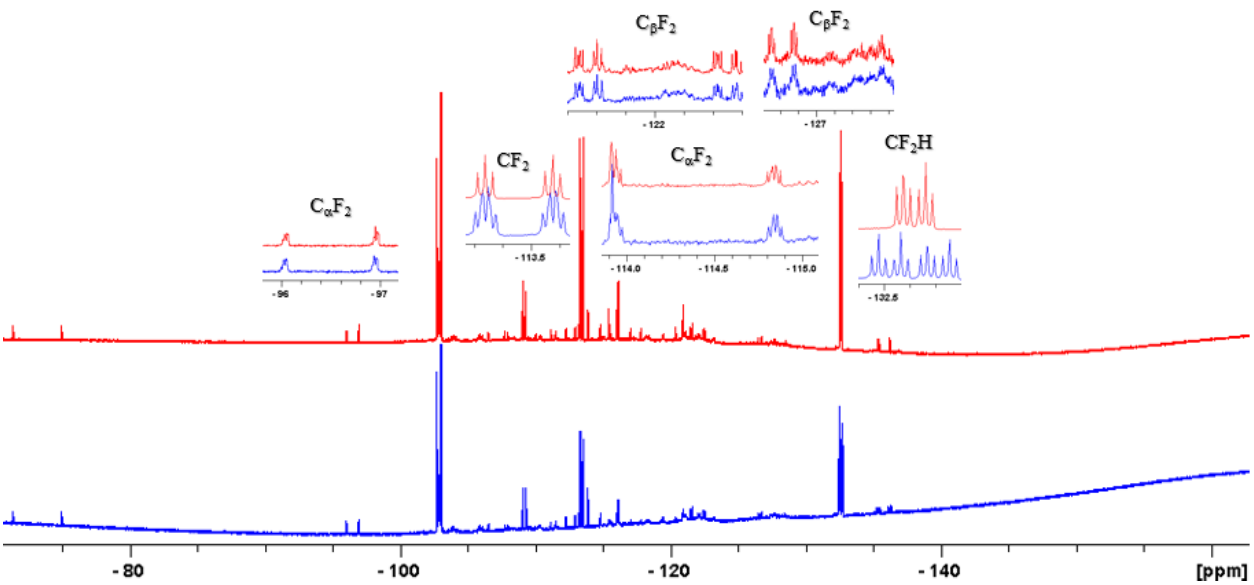

Figure 3.6. ^{19}F NMR spectra (282 MHz, C_6D_6) of Mn[CF_2CF_2H](DPPE)$(CO)_3$ (**3-8**) and possibly MnBr[-CF_2)$_4$-](DPPE)(CO) (**3-20**) (red = proton-decoupled).

*3.3.6 Isolation of Mn[CF_2CFHCl](DPPE)$(CO)_3$ (**3-16**) and further photolysis with CTFE*

On scale-up of the reaction of MnBr(DPPE)$(CO)_3$ (**3-2**) with CTFE in THF, we found that solvent removal followed by washing with hexane gave solid insertion product **3-16** in high purity. Subsequent dissolution of this product in C_6D_6 and exhaustive photolysis for 7 d afforded a mixture of products that included the unsubstituted insertion product, Mn(CF_2CFHCl)$(CO)_5$, **3-21**. The ^{19}F NMR spectrum (**Figure 3.7**) also shows one product that closely resembles the Co hydride metallacycles characterized previously in the Baker group.[2]

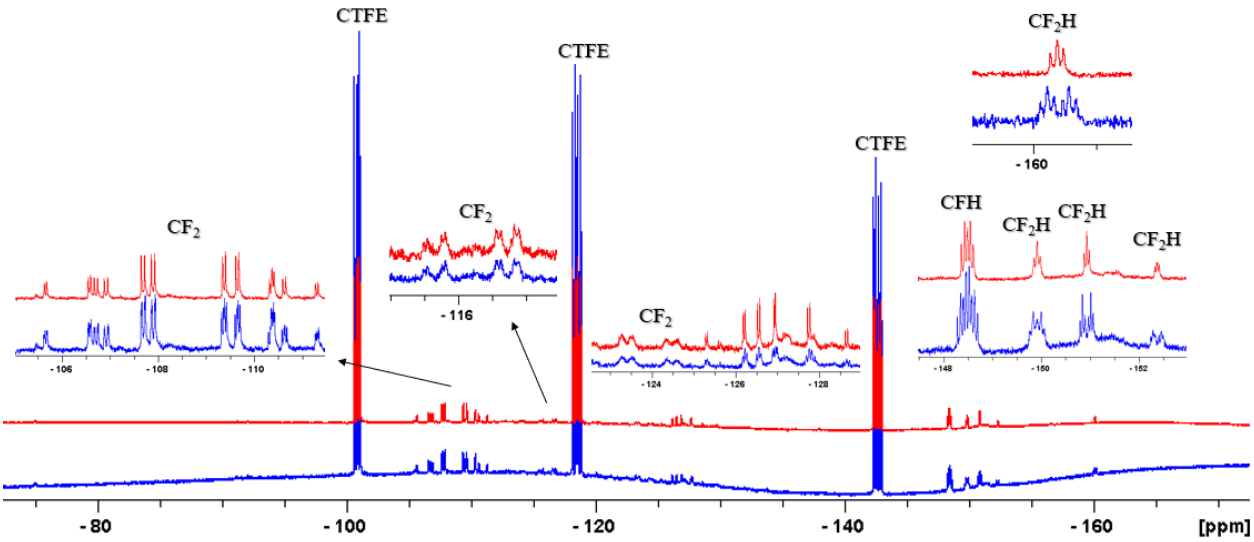

Figure 3.7. ^{19}F and $^{19}F\{^{1}H\}$ NMR spectrum of reaction mixture from $Mn(CF_2CFHCl)(DPPE)(CO)_3$ (**3-16**) + CTFE in C_6D_6 (red = proton-decoupled).

3.1 **Proposed Reaction Pathways**

Multiple studies were carried out to obtain a better understanding of the reaction pathways involved in reactions of fluoroalkenes with manganese bromide carbonyl complexes. Based on the data gathered, we suggest a likely reaction pathway using $MnBr(DPPE)(CO)_3$, **3-2** and TFE as an example (**Scheme 3-8**). First, photolysis of **3-2** results in CO loss, generating five-coordinate 16 e- intermediate **I**. Addition of the strong electron-acceptor TFE may then weaken the covalent Mn-Br bond which undergoes abstraction by another equivalent of **I**, affording zerovalent $Mn(DPPE)(CO)_2(CF_2{=}CF_2)$ and divalent $MnBr_2(DPPE)(CO)_2$ which likely loses its CO ligands as a result of the electrophilic Mn(II) center's inability to back-bond. Hydrogen atom abstraction from the THF solvent by the zerovalent Mn intermediate then forms the Mn-H, as confirmed by the thermal $Mn_2(CO)_{10}$ reactions. Insertion of the coordinated TFE into Mn-H followed by CO trapping affords $Mn(CF_2CF_2H)(DPPE)(CO)_3$, **3-8**. In contrast to Ghostine's Co

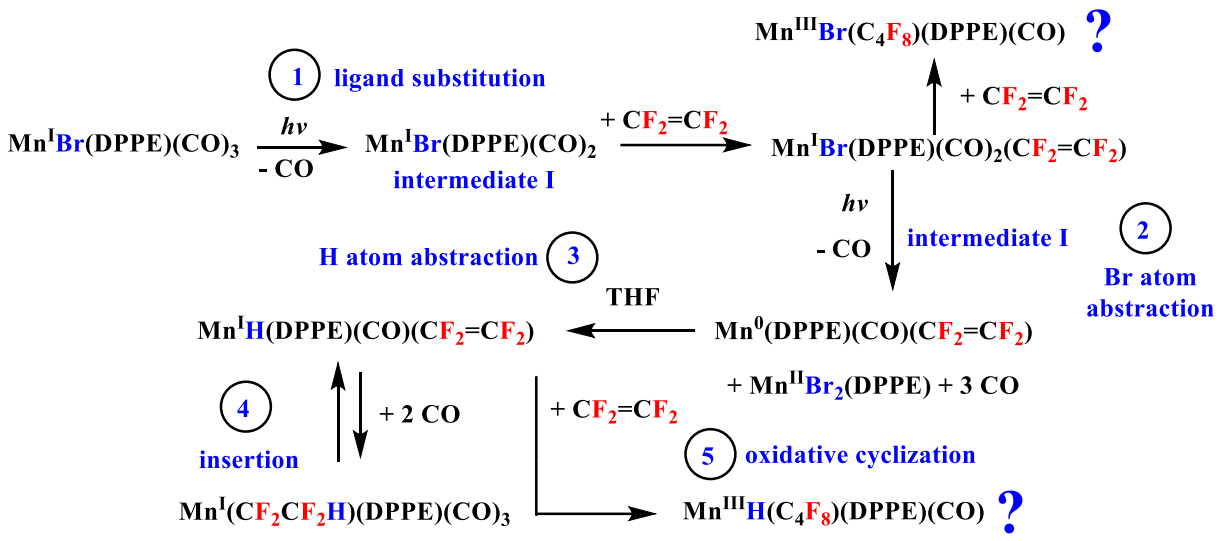

Scheme 3.8. Proposed pathways for TFE reaction with $MnBr(DPPE)(CO)_3$ (**3-2**).

chemistry[2] the Mn insertion product **3-8** does not readily coordinate additional TFE en route to a Mn-H metallacyle although monitoring exhaustive photolysis experiments by ^{19}F NMR provides evidence for further incorporation of the fluoroalkene.

While Cα-H atom abstraction from THF is well known, the radical is typically short-lived.[14] Nonetheless, previous studies have demonstrated the α-fluoroalkylation of THF using fluoroalkenes initiated by gamma rays using Co-60[3,4] and radical initiators.[5] Although similar reactions have been reported for dimethyl ether,[5] we showed that while H atom abstraction from methyl *t*-butyl ether still occurs, the ensuing radical does not add efficiently to fluoroalkenes as *t*-BuO-$CH_2CF_2CF_2H$ was not observed as a major product by ^{19}F NMR. Although formation of **3-18** suggests that a stable d^4 metallacycle may be attainable, attempts to isolate this product have not yet been successful.

3.2 **Conclusions**

The reactions of $MnBr(CO)_5$ (**3-1**) and its ligated analogs with fluoroalkenes would have been difficult to sort out had a previous Baker group researcher not already characterized similar

fluorometallacycles derived from DPPE- and tripod-Co hydride carbonyl complexes.[2] Nonetheless, it is surprising that under photolysis conditions only the DPPE derivative (**3-2**) affords Mn products derived from the fluoroalkenes. Further insight into the reaction pathways was provided by the $Mn_2(CO)_{10}$ / fluoroalkene reactions which demonstrated the ability of zerovalent $[Mn(CO)_n]$ radicals to abstract H atoms from THF, diethyl ether and methyl *t*-butyl ether. The latter solvent, however, does not readily add to the fluoroalkenes, making it the solvent of choice for *in situ* Mn-H generation.

The mixture of products observed by photolysis of $Mn_2(CO)_{10}$ with CTFE showed some similarities with those from the photolytic $MnBr(CO)_5$ reaction, thus identifying another role for the ancillary ligands in directing the reactions towards the desired Mn-H insertion products. In contrast to the Co DPPE and κ^2-tripod examples,[2] the Mn fluoroalkyl complexes have proven to be reluctant to bind additional TFE and form the Mn hydride fluorometallacycles. In light of Lentz's result with the CpMn system (**Scheme 1.12**) and his isolation of a d^3 fluorometallacycle, we believe that formation of stable d4 Mn fluorometallacycles is possible. However, additional experimentation will be required to find efficient routes to these targets so that their reactivity can be explored and compared to their more electron-rich counterparts.

3.3 **Experimental Section**

3.3.1 General Considerations

MBraun glove box and Schlenk techniques were used to carry out all experiments under nitrogen. A J. C. Meyer solvent purification system was used to dry the diethyl ether, toluene, tetrahydrofuran (THF) and hexanes using activated alumina columns. Stirring over activated alumina (ca. 10 wt.%) was used to dry the benzene-d_6 (C_6D_6) overnight followed by filtration.

Dichloromethane (DCM) and acetonitrile-d_3 (CD_3CN) were refluxed over calcium hydride, stirred over activated alumina (ca. 5 wt.%) overnight and filtered. Activated 4 Å molecular sieves (heated at ca. 250 ^oC for >10 h under vacuum) were added to all solvents stored in the govebox. All glassware was heated in an oven for >2 h at 150 ^oC.

Commercial chemicals used were 1,2-bis(diphenylphosphino)ethane (DPPE, 99%, Aldrich), bromopentacarbonylmanganese(I) ($MnBr(CO)_5$, 98%, Aldrich), dimanganese decacarbonyl ($Mn_2(CO)_{10}$, 98%, Aldrich), 1,10-phenanthroline (phen, 99%, Aldrich), 2,2′-bipyridine (bipy, 99%, Aldrich), and bis(2-diphenylphosphinoethyl)phenylphosphine (triphos, 97%, Aldrich). The *N*-heterocyclic carbene IPr was prepared by modifying the literature procedure.[15] Pyrolysis was used to prepare tetrafluoroethylene from polytetrafluoroethylene (powdered, Scientific Polymer Products) under vacuum using a modified literature procedure [10-20 mTorr, 25 g scale, 650 ^oC, R(+)-limonene (97%, Aldrich) for product stabilization producing 97-98% pure TFE].[16] A 300 MHz Bruker Avance instrument was used to record the spectra of ^1H, $^{31}P\{^1H\}$ ^{19}F, and $^{13}C\{^1H\}$ NMR at room temperature (21-23 ^oC). ^1H NMR chemical shifts are reported relative to residual proton peaks of the deuterated solvents (CD_3CN: 1.94 ppm; C_6D_6: 7.16 ppm), while ^{19}F and ^{31}P NMR shifts are reported relative to 1,3- bis(trifluoromethyl)benzene (BTB) at -63.5 ppm and phosphoric acid (85 % aqueous solution) at 0 ppm. IR data were collected on a Thermo Scientific Nicolet 6700 FT-IR spectrometer.

3.3.2 Synthesis and Characterization

Synthesis of $MnBr(DPPE)(CO)_3$, (3-2). This complex was prepared using 234 mg (0.85 mmol) of $MnBr(CO)_5$ and 339 mg (0.85 mmol) of 1,2-bis(diphenylphosphino)ethane in 20 mL of toluene. After 18 h reflux at 120°C the solvent was removed and the residue was washed with

hexane and dried to give a yellow solid. Yield: 550 mg, 96%. $^{31}P\{^{1}H\}$ (121 MHz, C_6D_6) 68.0 ppm (s, 2P).

Synthesis of MnBr(DPPE)$_2$(CO), (3-3). In a modification of a literature procedure,[7,8] $MnBr(CO)_5$ (200 mg, 0.72 mmol) and 1,2 bis(diphenylphosphino)ethane (578 mg, 1.5 mmol) were dissolved in 20 mL of benzene in a Schlenk tube. The reaction mixture was irradiated with stirring for 3 h under N_2 giving a gradual colour change from orange to yellow. After 3 h the yellow solution was filtered and solvent removed to afford a yellow solid. Further purification was accomplished by precipitation from toluene with ethanol. Yield: 247 mg, 49.4% $^{31}P\{^{1}H\}$ (121 MHz, CD_2Cl_2) 65.6 ppm (s).

Synthesis of *cis, mer*-MnBr(triphos)(CO)$_2$, (3-4). In a modification of a literature procedure,[9,10] solid $MnBr(CO)_5$ (100 mg, 0.36 mmol) and 1,1,1-tris(diphenylphosphino-methyl)ethane (194 mg, 0.36 mmol) in 20 mL of toluene were heated at 120ºC for 18 h giving an orange solution. After cooling the solution, orange needles were filtered off and the reaction mixture was then dried in vacuo to yield a dark orange powder that was recrystallized from dichloromethane/ hexane. Yield: 280 mg, 95 %. $^{31}P\{^{1}H\}$ (121 MHz, C_6D_6) 83.4 (s, 2P), 116.7 ppm (s, 1P).

Synthesis of MnBr(bipy)(CO)$_3$, (3.5). In a modification of a literature procedure,[11,12] a mixture of $MnBr(CO)_5$ (100 mg, 0.36 mmol) and 2,2′-bipyridine (56 mg, 0.36 mmol) were heated in 20 mL of benzene at reflux for 2 h in a Schlenk tube yielding a yellow-orange solution. This solution was dried and washed thoroughly with hexanes. The resulting yellow solid was recrystallized from CH_2Cl_2 and hexanes to give orange crystals. Yield 95 mg, 70% . ^{1}H NMR was confirmed from the literature.

Synthesis of MnBr(phen)(CO)$_3$, (3-6). In a modification of a literature procedure,[11,12] using 100 mg (0.36 mmol) of MnBr(CO)$_5$ and 66 mg (0.36 mmol) of 1,10-phenanthroline were stirred for 20 h at RT in a Schlenk tube. When the solution changed to orange, it was dried in vacuo and the resulting yellow solid was dissolved in diethyl ether and cooled at -35 ^{o}C. The resulting solid was filtered off and dried. Yield 88 mg, 53%. Selected IR (KBr): $^{\nu}$CO = 2021, 1941 cm^{-1}.

Synthesis of MnBr(IPr)(CO)$_4$, (3-7). In a modification of a literature procedure,[13] solid MnBr(CO)$_5$ (275 mg, 1 mmol) and 1,3-bis(2,6-diisopropylphenyl)imidazol-2-ylidene (388.74 mg, 1 mmol) were suspended in 20 mL of benzene and stirred for 2 h in a Schlenk tube with a stir bar giving a yellow-orange solution. The solvent was then removed and the yellow-orange solid was extracted with hexane and filtered. After cooling at -35^{o}C, a yellow precipitate formed which was isolated by filtration to afford the final product. Yield 310 mg, 46% . ^{1}H NMR was confirmed from the literature.

Reactions of Complexes 3-1 - 3-7 with Fluoroalkenes

These reactions were carried out by dissolving 25-50 mg of the Mn-Br complex in 0.5 mL of THF in an NMR tube fitted with a septum cap and then TFE, PMVE or CTFE gas was added using a 1 mL syringe through the septum cap. The NMR tube was then irradiated using a Hg UV lamp and monitored by ^{19}F NMR spectroscopy.

Scale-up of Selected Reactions

a) **MnBr(CO)$_5$ (3-1) + TFE: Isolation of O[-(CH$_2$)$_3$CH(CF$_2$CF$_2$H)-] (3-9).** Solid MnBr(CO)$_5$ (100 mg, 0.36 mmol) was dissolved in ca. 20 mL of THF in a small RB-Schlenk with stir bar. Then, the flask was degassed with three freeze-pump-thaw cycles and TFE gas was added on a Schlenk line. The flask was sealed and irradiated with UV light for 24 h giving a colorless solution and light tan precipitate. ^{19}F NMR (282 MHz, THF) **3-10**: -139.5 (d, $^2J_{FH}$ = 54 Hz,

$H(CF_2)_2H$, 4F). The mixture was filtered through Celite and evaporated under vacuum to afford a white powder. Yield: 80 mg. ^{19}F NMR (282 MHz, THF) **3-9**: -145.4 ppm (dddd, $^2J_{FF}$ = 300, $^4J_{FH}$ = 53, $^3J_{FF}$ = 10.5, 7 Hz, 2F, $C_\beta F$), -138.0 ppm (dddd, $^2J_{FF}$ = 300, $^4J_{FH}$ = 52, $^3J_{FF}$ = 11, 4.5 Hz, 2F, $C_\beta F$), -135.2 (dddd, $^2J_{FF}$ = 268, $^3J_{FH}$ = 22, $^3J_{FF}$ = 10.5, 4.5 Hz, 2F, $C_\alpha F$), -132.0 ppm (dddd, $^2J_{FF}$ = 268, $^3J_{FH}$ = 15, $^3J_{FF}$ = 11, 7 Hz, 2F, $C_\alpha F$).

b) **$MnBr(DPPE)(CO)_3$ (3-2) + TFE in THF: Isolation of $Mn[CF_2CF_2H](DPPE)(CO)_3$, (3-8).** Solid $MnBr(DPPE)(CO)_3$(40 mg, 0.06 mmol) was dissolved in ca. 0.5 mL of THF in an NMR tube fitted with a septum cap. Then, 1 mL of TFE gas was added via syringe through the septum cap. The reaction mixture changed immediately from yellow to orange with precipitation. The resulting solution was filtered and evaporated under vacuum to yield an orange powder. Washing with hexane, refiltering and drying afforded ca. 30 mg of **3-8.** ^{19}F NMR (282 MHz, THF) -115.1 (ddtr, $^3J_{FP}$ = 67, $^3J_{FF}$ = 6, $^3J_{FH}$ = 4 Hz, Mn–C$F_2$$CF_2H$), -134.8 ppm (ddtr, $^2J_{FH}$ = 54, $^4J_{FP}$ = 22.5, $^3J_{FF}$ = 6 Hz, Mn-CF_2CF_2H, 2F). $^{31}P\{^1H\}$ NMR (121 MHz, THF) -6.7 ppm (trtr, $^3J_{PF}$ = 67 Hz, $^4J_{PF}$ = 22.5 Hz, 2P). ^1H NMR (300 MHz, C_6D_6) δ 5.1 (trtr, $^2J_{HF}$ = 54, $^3J_{HF}$ = 4 Hz, Mn-CF_2CF_2*H*).

c) **$MnBr(Bipy)(CO)_3$ (3-5) + PMVE in THF: Isolation of O[-$(CH_2)_3CH(CF_2CFH)(OCF_3)$-], 3-11 and 3-12.** Solid $MnBr(Bipy)(CO)_3$ (35 mg, 0.08 mmol) was dissolved in ca. 0.5 mL of THF in an NMR tube fitted with a septum cap. Then, 1 mL of PMVE gas was inserted via syringe through the septum cap. The colour of the reaction changed immediately from orange to yellow with precipitation of a solid. The solution was filtered and evaporated under vacuum to yield a yellow powder. Yield: 20 mg. ^{19}F NMR (282 MHz, THF) major isomer : -150.3 (d, $^3J_{FH}$ = 54 Hz, 2F, $C_\beta F$), -128.5 (ddd, $^2J_{FF}$ = 265, $^4J_{FH}$ = 20, $^3J_{FF}$ = 12.5 Hz, 2F, $C_\alpha F$), -125.8 (d mult, $^2J_{FF}$ = 265 Hz, 2F, $C_\alpha F$), -56.5 ppm (s, OCF_3), minor isomer: -142.4 (d,

$^{3}J_{FH}$ = 52 Hz, 2F, CβF), -128.7 (dd, $^{2}J_{FF}$ = 267, $^{3}J_{FH}$ = 22 Hz, 2F, CαF), -126.7 (d mult, $^{2}J_{FF}$ = 267 Hz, 2F CαF), -56.6 ppm (s, OCF_3).

e) **MnBr(DPPE)(CO)$_3$ (3-2) + PMVE in THF: Isolation of Mn[CF$_2$CFH(OCF$_3$)](DPPE)(CO)$_3$ (3-13).** Solid MnBr(DPPE)(CO)$_3$ (25 mg, 0.04 mmol) was dissolved in ca. 0.5 mL of THF in an NMR tube fitted with a septum cap. Then, 1 mL of PMVE gas was inserted via syringe through the septum cap. Upon UV irradiation, the colour of the reaction changed immediately from yellow to light yellow with precipitation of a solid. The solution was filtered and evaporated under vacuum to yield a yellow powder. Yield: 15 mg. ^{19}F NMR (282 MHz, THF) **3-13**: -55 (br s, OC*F*$_3$, 3F), -107.68 (d mult, $^{2}J_{FP}$ = 62.5 Hz, Mn-C*F*$_2$CFH(OCF$_3$), 2F), -138.09 ppm (d, $^{2}J_{FH}$ = 51 Hz, Mn-CF$_2$C*F*H(OCF$_3$), 2F), ^{31}P{^{1}H} NMR (121 MHz, THF) 1.28 ppm (trd, $^{3}J_{PF}$ = 62.5, $^{4}J_{PF}$ = 22.5 Hz, 2P). ^{1}H NMR (300 MHz, C_6D_6) δ 5.5 (trtr, 1H, Mn-CF$_2$CF$_2$*H*).

f) **MnBr(Phen)(CO)$_3$ (3-6) + CTFE in THF: Isolation of O[-(CH$_2$)$_3$CH(CF$_2$CFHCl)-], 3-14 and 3-15**. Solid MnBr(Phen)(CO)$_3$ (35 mg, 0.08 mmol) was dissolved in ca. 0.5 mL of THF in an NMR tube fitted with a septum cap. Then, 1 mL of CTFE gas was inserted via syringe through the septum cap. Upon UV irradiation the colour of the reaction changed immediately from orange to yellow with precipitation of a solid. After 2 d the solution was filtered and evaporated under vacuum to yield a yellow powder. Yield: 20 mg. ^{19}F NMR (282 MHz, THF) major isomer: -152.3 (dtr, $^{3}J_{FH}$ = 41, $^{3}J_{FF}$ = 12 Hz, 1F, Cβ*F*), -128.2 (ddd, $^{2}J_{FF}$ = 254.5, $^{4}J_{FH}$ = 20, $^{3}J_{FF}$ = 16 Hz, 1F, Cα*F*$_2$), -125.6 ppm (ddd, $^{2}J_{FF}$ = 254.5, $^{4}J_{FH}$ = 12, $^{3}J_{FF}$ = 12 Hz, 1F, Cα*F*$_2$), minor isomer: -160.01 (dtr, $^{3}J_{FH}$ = 41.5, $^{3}J_{FF}$ = 14 Hz, 1F, Cβ*F*), -127.2 (ddd, $^{2}J_{FF}$ = 265, $^{4}J_{FH}$ = 18.5, $^{3}J_{FF}$ = 10 Hz, 1F, Cα*F*$_2$). -126.1 ppm (ddd, $^{2}J_{FF}$ = 265 Hz, $^{4}J_{FH}$ = 14, $^{3}J_{FF}$ = 14 Hz, 1F, Cα*F*$_2$).

g) **$MnBr(DPPE)(CO)_3$ (3-2) + CTFE in THF: Isolation of $Mn[-CF_2CHFCl-](DPPE)(CO)_3$ (3-16).** Solid $MnBr(DPPE)(CO)_3$ (40 mg, 0.06 mmol) was dissolved in ca. 0.5 mL of THF in an NMR tube fitted with a septum cap. Then, 1 mL of CTFE gas was added via syringe through the septum cap. Upon UV irradiation the reaction mixture changed immediately from yellow to light yellow with precipitation. After 2 d the resulting solution was filtered and evaporated under vacuum to yield yellow powder. Yield: 35 mg. ^{19}F NMR (282 MHz, C_6D_6) -107.2 (dddd, $^2J_{FF}$ = 276, $^2J_{FP}$ = 58, $^3J_{FF}$ = 19.5, $^3J_{FH}$ = 4 Hz, 1F, CαF_2), -110.0 (dddd, $^2J_{FF}$ = 276, $^2J_{FP}$ = 79, $^3J_{FF}$ = 17, $^3J_{FH}$ = 11 Hz, 1F, CαF_2), -148.4 ppm (dddd, $^2J_{FH}$ = 49, $^4J_{FP}$ = 33, $^3J_{FF}$ = 19.5, 17 Hz, 1F, CβF). $^{31}P\{^1H\}$ NMR (121 MHz, THF) 3.7 ppm (ddd, $^3J_{FP}$ = 78, 58, $^4J_{FP}$ = 33 Hz). ^1H NMR (300 MHz, C_6D_6) δ 5.5 (ddd, 1H, $^2J_{FH}$ = 49, $^3J_{FH}$ = 11, 4 Hz, Mn-CF_2CFCl*H*).

Reactions of $Mn_2(CO)_{10}$ with Fluoroalkenes. In a typical reaction 10 mg of $Mn_2(CO)_{10}$ was dissolved in 0.5 mL of THF, DEE, MTBE or CPME in an NMR tube fitted with a septum cap and then TFE, PMVE or CTFE gas was added via a 1 mL syringe through the septum cap. The NMR tube was then heat at 65 ºC and the ^{19}F NMR spectrum monitored over 1-3 d.

a) **$Mn_2(CO)_{10}$ + TFE: Generation of unsubstituted insertion product, $Mn(CF_2CF_2H)(CO)_5$, (3-17).**[1] The reaction colour changed from light yellow to dark yellow after heating at 65 °C overnight. NMR data after 3 d: ^{19}F NMR (282 MHz, THF) -65.06 (br s, Mn–CF_2CF$_2$H, 2F), -124.1 ppm (br d, $^2J_{FH}$ = 58 Hz, Mn-CF_2CF_2H, 2F). This reaction also generated monoalkyl-substituted tetrahydrofuran, O[-$(CH_2)_3$CH(CF_2CF_2H)-], (**3-9**) when performed in THF solvent. The reaction gave the same results under a Hg UV lamp.

c) **$Mn_2(CO)_{10}$ + CTFE in THF: Generation of diastereomeric hydrogenation products, HCFClCFClH.** The reaction colour changed from light yellow to dark yellow after heating

overnight. NMR data after 3 d showed THF adducts and the *meso* and *d,l*-hydrogenation products: ^{19}F NMR (282 MHz, THF): -132.7 (d, $^{2}J_{FH}$ = 49 Hz, HC*F*ClC*F*ClH, 2F), -158.3 ppm (d, $^{2}J_{FH}$ = 49 Hz, HC*F*ClC*F*ClH, 2F). This reaction gave several broad peaks under irradiated condition using a UV lamp.

Alternate ether solvents

a) **MnBr(DPPE)$_2$(CO), (3-3) + TFE in DEE: generation of Mn[CF$_2$CF$_2$H](DPPE)(CO)$_3$, 3-8, EtO[CH(CF$_2$CF$_2$H)CH$_3$], 3-19 and hydrogenated TFE, 3-10.** Solid MnBr(DPPE)$_2$(CO) (30 mg, 0.03 mmol) was dissolved in ca. 0.5 mL of DEE in an NMR tube fitted with a septum cap. Then, 1 mL of TFE gas was added via syringe through the septum cap. The reaction mixture changed immediately from yellow to orange under UV lamp for 24 h. NMR data after 1d for **3-19**: ^{19}F NMR (282 MHz, Et$_2$O) -143.5 (dddd, $^{2}J_{FF}$ = 300, $^{4}J_{FH}$ = 53.7, $^{3}J_{FF}$ = 10.5, 7 Hz, 1F, C$_\beta$*F*$_2$), -138.4 (dddd, $^{2}J_{FF}$ = 300, $^{4}J_{FH}$ = 52.8, $^{3}J_{FF}$ = 11, 4.5 Hz, 1F, C$_\beta$*F*$_2$), -133.2 (br dddd, $^{2}J_{FF}$ = 268, $^{3}J_{FH}$ = 22, $^{3}J_{FF}$ = 10.5, 4.5 Hz, 2F, C$_\alpha$*F*$_2$), -128.8 ppm (br dddd, $^{2}J_{FF}$ = 268, $^{3}J_{FH}$ = 15, $^{3}J_{FF}$ = 11, 7 Hz, 2F, C$_\alpha$*F*$_2$).

b) **MnBr(DPPE)(CO)$_3$ (3-2) + TFE in MTBE: generation of Mn[CF$_2$CF$_2$H](DPPE)(CO)$_3$, (3-8) without evidence of solvent fluoroalkylation.** Solid MnBr(DPPE)(CO)$_3$(30 mg, 0.06 mmol) was dissolved in ca. 0.5 mL of MTBE in an NMR tube fitted with a septum cap. Then, 1 mL of TFE gas was added via syringe through the septum cap. The reaction mixture changed from yellow to orange under UV lamp after 1 d. ^{9}F NMR data after 1d just showed formation of Mn-H insertion product **3-8**.

Exhaustive Photolysis reactions

a) **MnBr(CO)$_5$ + 3 equiv. DPPE + TFE in MTBE: Proposed generation of MnBr[-(CF$_2$)$_4$-](DPPE)(CO) (3-20)**. Solid MnBr(CO)$_5$ (20 mg, 0.07 mmol) and bis(diphenylphosphino)ethane

(86 mg, 0.2 mmol) were dissolved in ca. 5 mL of MTBE in a small RB-Schlenk with stir bar. Then, TFE gas was added via a 5 mL syringe through the septum cap. The flask was sealed and irradiated with UV light for 3 d giving a colorless solution and yellow precipitate. After 3 d stirring and solvent removal, the product was washed with hexane to afford a light yellow powder. Yield: 55 mg. NMR data after 3 d:^{19}F NMR (282 MHz, C_6D_6) -121.5 (ddd, 2F, $^2J_{FF}$ = 270, $^3J_{FF}$ = 15 Hz, $^2J_{FP}$ = 36 Hz, $C_\beta F_2$), -117.14 (dddd, 2F, $^2J_{FF}$ = 270, $^3J_{FF}$ = 16 Hz, $^2J_{FP}$ = 36 $C_\beta F_2$), -114.4 (dddd, 2F, $^2J_{FF}$ = 255, $^3J_{FF}$ = 9, 3 Hz, $C_\alpha F_2$), -96.37 ppm (ddd, 2F, $^2J_{FF}$ = 255, $^3J_{FF}$ = 9, 8, 6 Hz, $C_\alpha F_2$). ^{31}P{^{1}H} NMR (121 MHz, C_6D_6) -4.60 ppm (ddd, $^3J_{FP}$ = 89, $^4J_{FP}$ = 56.6 Hz), -5.61 ppm (trtr, $^3J_{PF}$ = 67 Hz, $^4J_{PF}$ = 22.5 Hz, 2P), 41(s), -15(free dppe).

b) **Mn(CF_2CHFCl)(DPPE)$(CO)_3$ (3-16) + CTFE in C_6D_6: Generation of Mn(CF_2CHFCl)(DPPE)$(CO)_3$ (3-16) and unsubstituted insertion product, Mn(CF_2CFHCl)$(CO)_5$, (3-21)**. Solid Mn(CF_2CHFCl)(DPPE)$(CO)_3$ was dissolved in ca. 0.5 mL of C_6D_6 in an NMR tube fitted with a septum cap and CTFE gas was added via a 1 ml syringe through the septum cap. The NMR tube was then irradiated using UV light for 7 d. The reaction mixture changed from colorless to light yellow. ^{19}F NMR (282 MHz, C_6D_6) **3-21:** -106.1 (ddd, 1F, $^2J_{FF}$ = 259, $^3J_{FF}$ = 14, $^3J_{FH}$ = 4.5 Hz, Mn-*CF_2*CFCl), -110.9 (ddd, 1F, $^2J_{FF}$ = 259, $^3J_{FF}$ = 13.5, $^2J_{FH}$ = 6 Hz, Mn-*CF_2*CFCl), -149.9 ppm (ddd, 1F, $^2J_{FH}$ = 46, $^3J_{FF}$ = 14, 13.5 Hz, Mn-CF_2*CF*Cl).

3.7 References

1)(a) Treichel, P. M.; Pitcher, E. Stone, F. G. A. *Inorg. Chem.* **1962**, *1*, 511-517. (b) Wilford, J. B.; Treichel, P. M.; Stone, F. G. A. *J. Organomet. Chem.* **1964**, *2*, 119-128.

2) Ghostine, K. University of Ottawa MSc thesis, **2018**.

3) a) Inukai, K. *J. Synth. Org. Chem., Jpn.* **1970**, *28*, 1285-1292. b) Ueda, T.; Muramatsu, H.; Inukai, K. *Nippon Kagaku Kaishi* **1975**, 100-106.

4) Abroskina, T. N.; Sorokin, A. D.; Kudryavtsev, R. V.; Cheburkov, Yu. A. *Bull. Acad. Sci. USSR* **1974**, *23*, 1741-1744.

5) Chauvin, A.; Greiner, J.; Pastor, R.; Cambon, A. *J. Fluorine Chem.* **1985**, *27*, 385-399.

6) Pope, S. J. A.; Reid, G. *J. Chem. Soc., Dalton Trans.* **1999**, 1615-1622.

7) King, W. A.; Scott, B. L.; Eckert, J.; Kubas, G. J. *Inorg. Chem.* **1999**, *38*, 1069-1084.

8) King, W. A.; Luo, X.-L.; Scott, B. L.; Kubas, G. J.; Zilm, K. W. *J. Am. Chem. Soc*. **1996**, *118*, 6782.

9) Coville, N. J.; Butler, I. S. *J. Organomet.Chem.* **1973**, *57*, 355–362.

10) Bond, A. M.; Colton, R.; Gable, R. W.; Mackay, M. F.; Walter, J. N. *Inorg. Chem.* **1997** *36*, 1181-1193.

11) Jimenez, J.; Chakraborty, I.; Mascharak, P. K. *Eur. J. Inorg. Chem.* **2015**, 5021–5026.

12) Chakraborty, I.; Carrington, S. J.; Mascharak, P. K. *ChemMedChem* **2014**, *9*, 1266–1274.

13) Martin, T. A.; Ellul, C. E.; Mahon, M. F.; Warren, M. E.; Allan, D.; Whittlesey, M. K.. *Organometallics* **2011**, *30*, 2200-2211.

14) Das, R.; Venkataram, B. *Res. Chem. Intermed.* **2005**, *31*, 167-192.

15) Nolan, S. P. *Beilstein J. Org. Chem.* **2015**, *11*, 2318–2325.

16) Hunadi, R. J.; Baum, K. *Synthesis* **1982**, *39*, 454.

Chapter 4: Investigations of $MnH_3(dmpe)_2$ as an Amine-borane Dehydrogenation Catalyst

4.1 Introduction

Ammonia-borane (H_3N-BH_3, AB) is a compound in which toxic Lewis base ammonia and reactive Lewis acid borane unite to form a stable solid, held together by strong dihydrogen bonds (N-H•••H-B), that is soluble in water.[1-6] In the thermolysis of AB, initial cleavage of the B-N bond at about 100 °C produces free borane that then serves as a dehydrogenation catalyst.[7,8] Nonetheless, the hydrogen stream from this process is typically contaminated with ammonia, diborane and borazine.[9] Over the last two decades several catalysts have been discovered that can generate > 2 equiv. of H_2, as well as amorphous graphene-like BNH_x (**Scheme 4.1**).[10-16] Moreover, this solid product has been converted back to AB using hydrazine in ammonia solvent.[17]

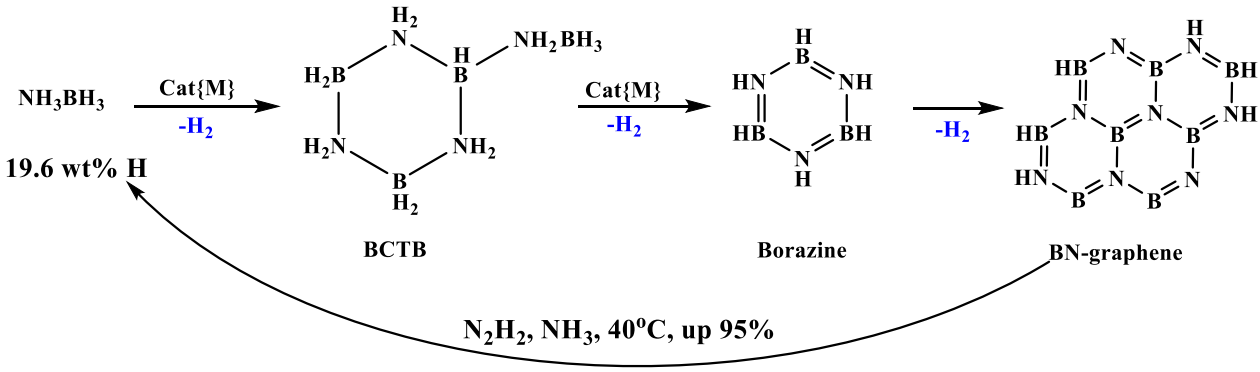

Scheme 4.1. Selectivity in metal catalyzed AB dehydrogenation.[10-16]

Several transition metal catalysts, on the other hand, have been identified[18-23] to produce a single equivalent of H_2 from AB along with insoluble polyaminoboranes, H_3N-$(BH_2NH_2)n$-BH_3, that are potential non-volatile precursors to BN.[24] In the presence of cyclohexene, AB dehydrogenation with these latter catalysts does not result in the usual trapping of the reactive

aminoborane monomer as BCy_2NH_2 (Cy = cyclohexyl).[25] While several theories have been proposed to describe this phenomenon,[25-27] further study is needed.

The development of robust metal complex catalysts capable of $>10^3$ turnovers has been hindered by the strongly reducing reaction conditions associated with AB dehydrogenation, especially for those containing earth-abundant metals.[28,29] Recently, a very active Fe pincer catalyst (TOF = 30 h^{-1} at RT) has been reported by Schneider et al.[23] However, a trace of free borane in the solution can deactivate this catalyst (Fe-H → Fe-BH_4). Adding ca. 4 equiv. of NMe_2Et per iron more than doubled catalytic turnovers from 120 to 330.

An alternate approach to accessing stable first row metal amine-borane dehydrogenation catalysts is to employ 18 e- complexes (**Scheme 4.2**). An initial report by Shubina *et al.* showed that two 18e- Co hydrides gave different selectivity for AB dehydrogenation at 55°C in THF with **1** affording cyclic products and >2 equiv H_2 and **1** giving insoluble poly(aminoborane) and 1 equiv of H_2 (**Scheme 4.3**). Their combined experimental and computational study suggested that dissociation of the N-donor in **1** allowed for substrate coordination whereas **2** just underwent protonation of the Co-H by the N-H of AB, followed by hydride abstraction, yielding aminoborane monomer and regenerating the catalyst (**Scheme 4.4**). Formation of Co-H-B intermediate **I** generates a nucleophilic amido N that is then regenerated upon each insertion of the aminoborane monomer.[28]

Recently, in as yet unpublished work, the Baker group showed that 18e- Fe(II) complex, $FeH_2(dmpe)_2$ (**4-1**; **Scheme 4.5**), is a robust catalyst for the dehydrogenation of ammonia-borane (AB) to both poly(aminoborane) and cyclic products, giving more than 10^3 turnovers at 50 °C in 1,2-dimethoxyethane over several days without evident catalyst decomposition. The catalyst also

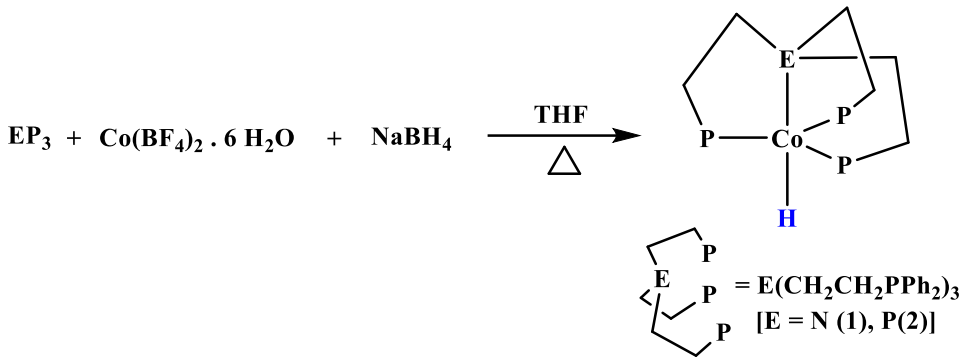

Scheme 4.2. 18e- Co hydride AB dehydrogenation catalysts.[28]

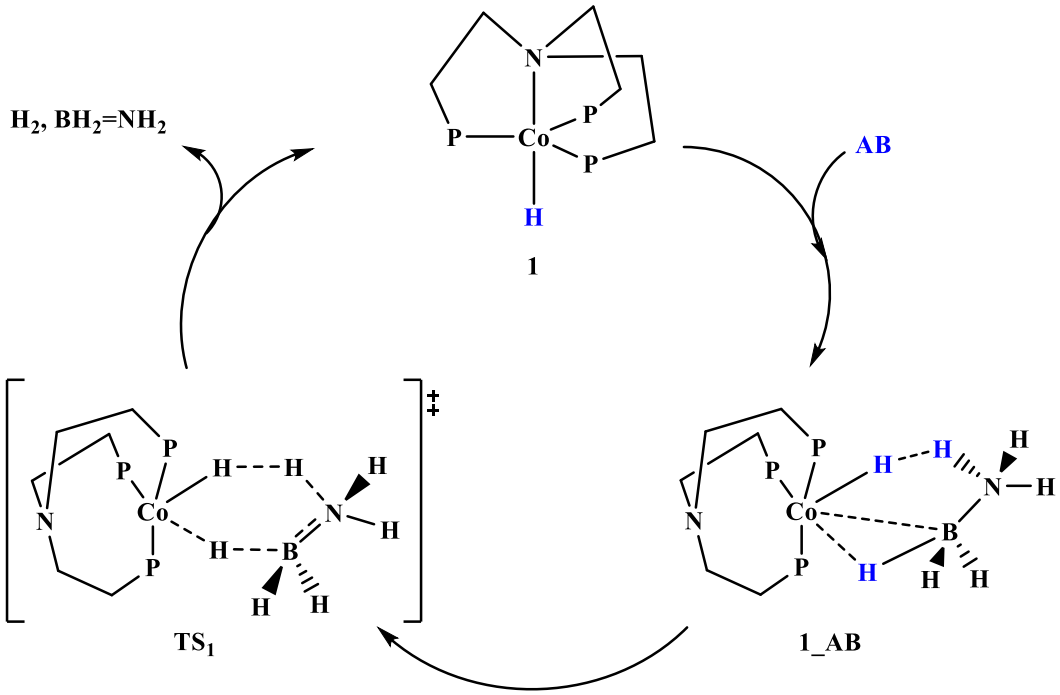

Scheme 4.3. Proposed catalytic cycle of AB dehydrogenation mediated by Co-H catalyst 1.[28]

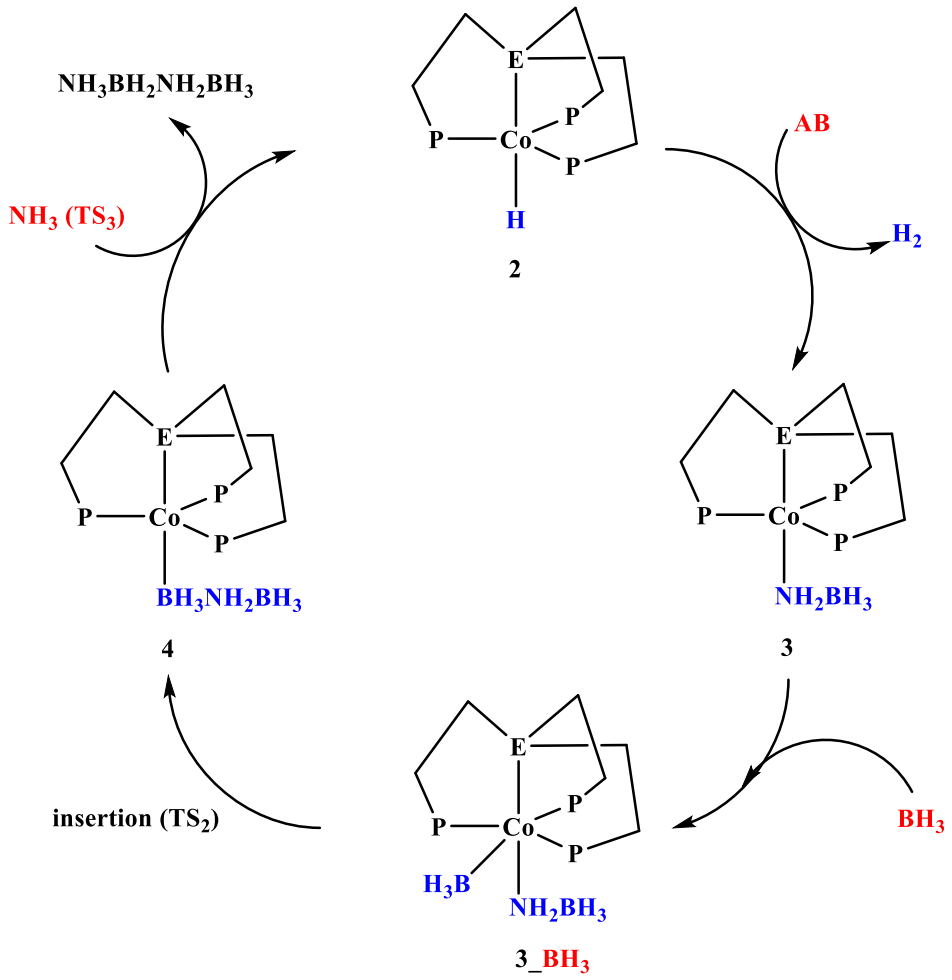

Scheme 4.4. Proposed reaction pathway for poly(aminoborane) production using Co-H catalyst **2**.[28]

tolerates triethylamine, which alters the product selectivity, and the *trans*-FeH(κ^1-BH_4)$(dmpe)_2$ (**4-2**) resting state of the catalyst does not give rise to catalyst deactivation. Deuterium labeling and DFT studies also indicated an initial N-H bond activation step. In contrast, the dihydrogen complex $[FeH(H_2)(dmpe)_2]^+$ (**4-3**) obtained by protonation of **4-1**, gave mostly cyclic aminoborane and iminoborane products and a new catalyst resting state, $[Fe(\kappa^2$-$BH_4)(dmpe)_2]^+$ (**4-4**), was identified and structurally characterized. Although computational studies indicated a concerted B-H/N-H bond activation mechanism for this cationic catalyst, NMR studies indicated a competing hydride abstraction reaction that then generates neutral *trans*-FeH(κ^1-BH_4)$(dmpe)_2$ (**4-2**), the same resting

state observed using **4-1**! To alleviate this complication, we chose to prepare the manganese analog, $MnH(H_2)(dmpe)_2$ (**4-5**)[30] and assess its catalytic activity and selectivity with AB, methylamine-borane (MAB) and dimethylamine-borane (DMAB).

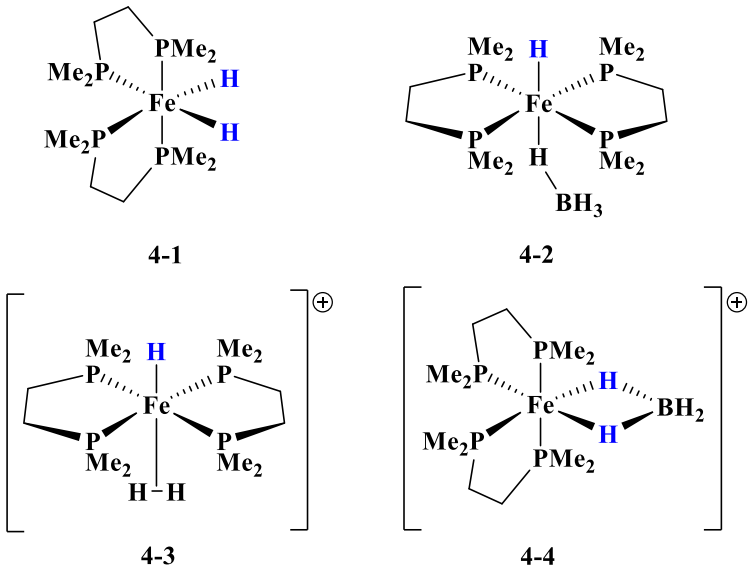

Scheme 4.5. Iron AB dehydrogenation catalysts and resting states.

Manganese hydride complex (**4-5**) was synthesized successfully using a literature procedure.[30] Reduction of $MnBr_2(dmpe)_2$ using $LiAlH_4$ affords the $(Al_2H_8)^{2-}$-bridged dimer that is then hydrolyzed to **4-5** (**Scheme 4.6**). The product exhibits a singlet at 82.7 ppm in the $^{31}P\{^1H\}$ NMR and a quintet due to the Mn-H at δ -12.6 ppm (J_{PH} = 28 Hz) in the ^1H NMR spectrum (Figs. A.37, A.38). At low temperatures, slow interconversion of the hydride and dihydrogen ligands is seen for the depe analog and separate resonances can be observed at δ 10.9 (1H) and 11.4 (2H) at -100 °C.[30c]

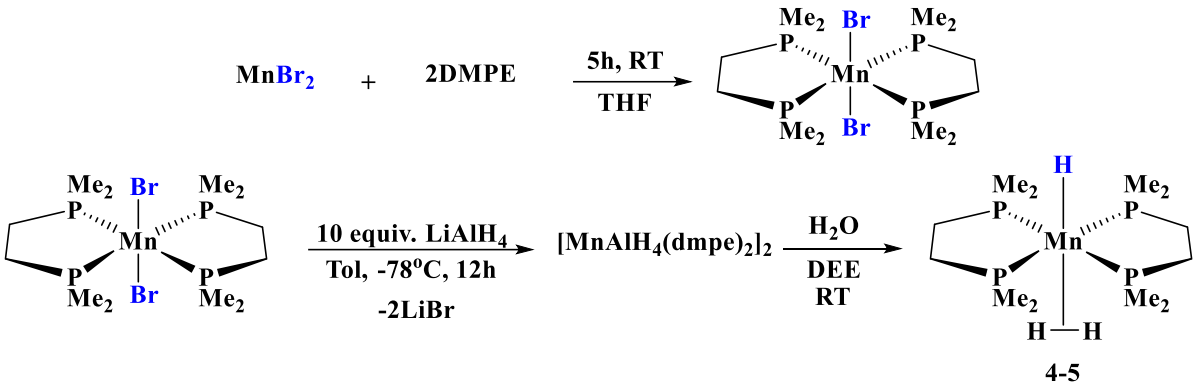

Scheme 4.6. Synthesis of manganese hydride-dihydrogen complex (**4-5**).[30]

4.2 **Amine-borane Dehydrogenation Catalyzed by 4-5**.

The AB dehydrogenation reactions were performed under the same reaction conditions [1-5 mol% catalyst at 50-55 °C in 1,2-dimethoxyethane (DME)] as those used previously for the iron analogues.

*4.2.1 Ammonia-borane dehydrogenation catalyzed by $MnH(H_2)(dmpe)_2$ (**4-5**).*

Exposure of a yellow DME solution of $MnH(H_2)(dmpe)_2$ **4-5** to 20 equiv of AB at 50 °C for 1 d produced hydrogen gas, a colorless solid and a purple solution. Monitoring the reaction by ^{11}B NMR spectroscopy showed some unreacted AB at -23 ppm, a doublet at 31.2 and a triplet at -12.0 ppm due to the B-N benzene (borazine) and cyclohexane (cyclotriborazane, CTB) analogues, respectively (**Figure 4.1**). In addition to a trace amount of the cyclic aminoborane tetramer, BCTB, the large doublet of quartets at -39 ppm is due to dmpe bis(borane) ($H_3B{\bullet}PMe_2CH_2CH_2Me_2P{\bullet}BH_3$), suggesting some catalyst decomposition that was not observed for the iron analogue. Finally, the large peak at 27 ppm is in the region of $HB(NH_2)_2$ but is due primarily, in fact, to the catalyst resting state, $Mn(\kappa^2\text{-}BH_4)(dmpe)_2$ (**4-6**). In fact, at full conversion,

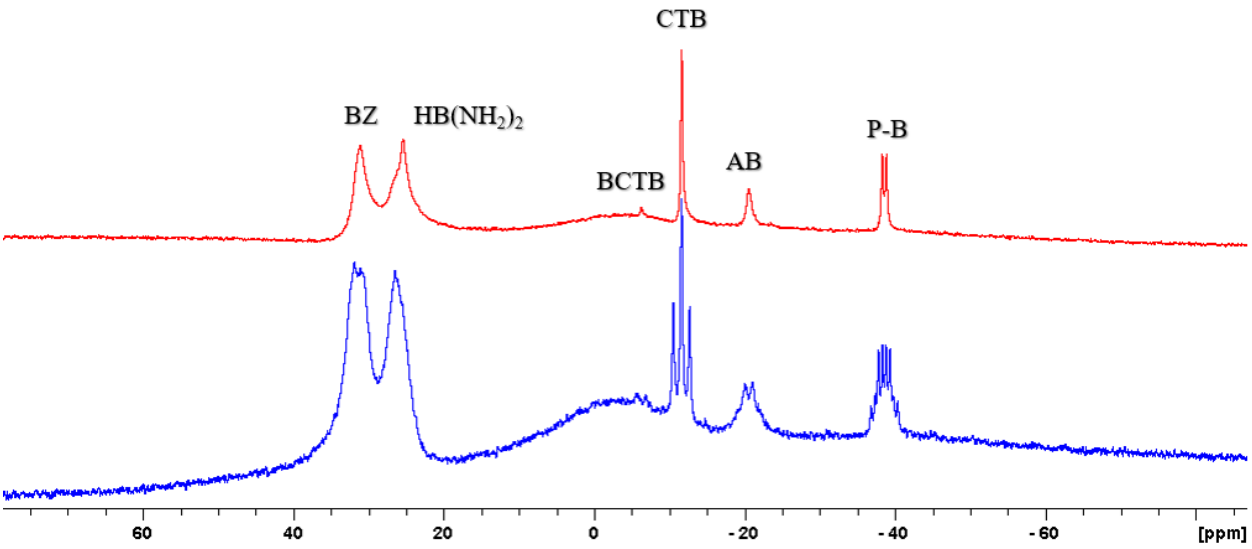

Figure 4.1. ^{11}B and $^{11}B\{^1H\}$ NMR spectra of catalytic dehydrogenation of AB with 5 mol% **4-5** in DME at 50 °C after 1 d (top: $^{11}B\{^1H\}$; bottom:^{11}B).

integration of this peak vs. the other products could be used to estimate the yield of insoluble poly(aminoborane). The $^{31}P\{^1H\}$ NMR spectrum of this reaction mixture confirms formation of dmpe bis(borane) (broad multiplet at 9.8 ppm) and includes two broad singlet resonances at 89 and 71 ppm in a 1:2 ratio due to **4-6** (Fig. A.39). Removal of the DME solvent from the above reaction followed by extraction into C_6D_6 afforded primarily complex **4-6** with a little dmpe bis(borane) (**Figure 4.2**). The ^{11}B NMR spectrum confirms the above assignments and ^1H NMR of **4-6** shows that any exchange between the terminal B-Hs (mult at δ 5.2) and the Mn-H-B bridges ('d' at δ -16) is slow on the NMR time scale.

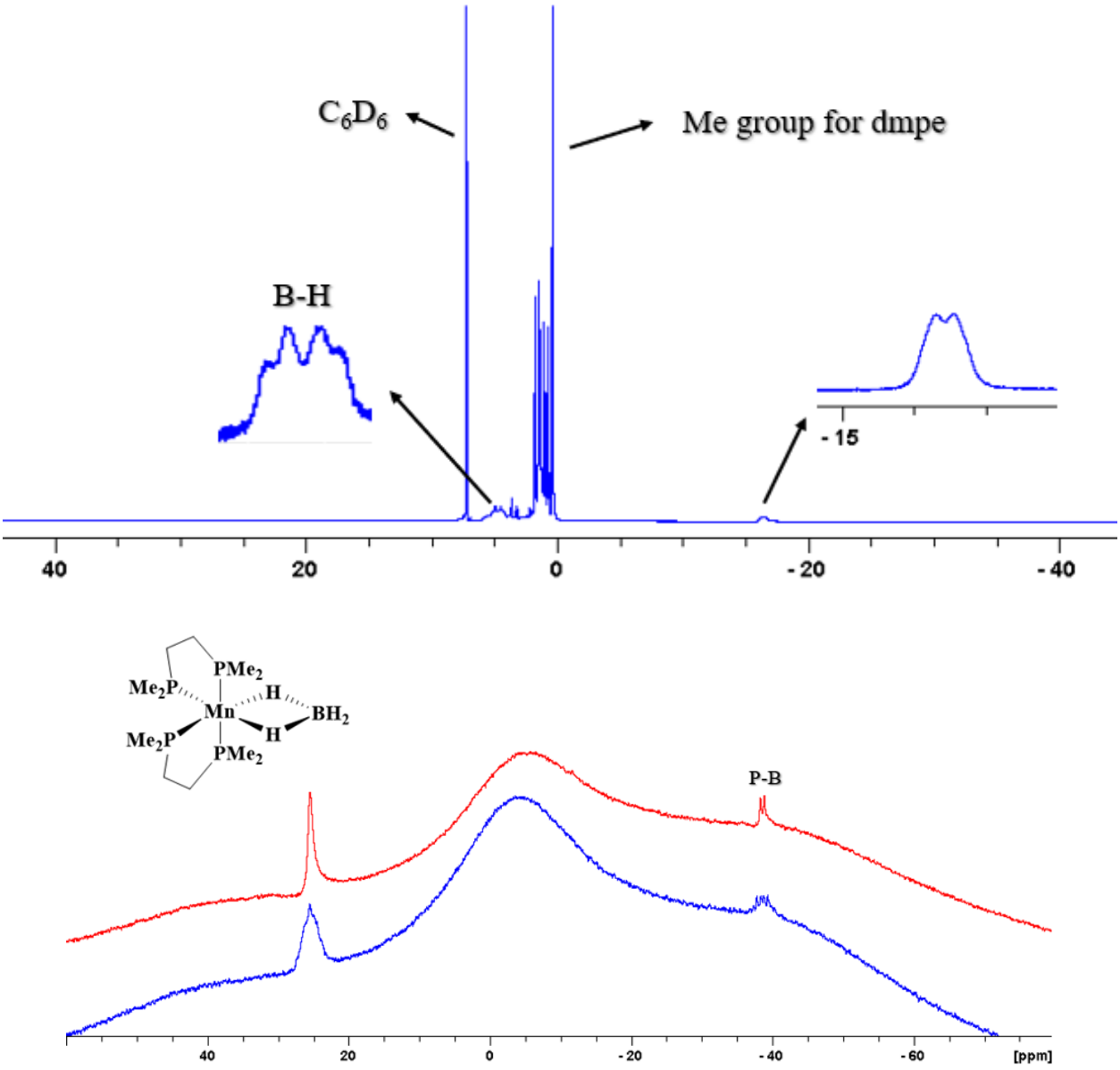

Figure 4.2. NMR spectra for $Mn(BH_4)(dmpe)_2$ (**4-6**) in C_6D_6 (top: ^1H; bottom: $^{11}B\{^1H\}$ and ^{11}B).

*4.2.1 Methylamine-borane dehydrogenation catalyzed by $MnH(H_2)(dmpe)_2$ (**4-5**).*

Catalyzed dehydrogenation of MAB using 5 mol% **4-5** was much slower than that for AB. In addition to *N*-trimethylborazine, several *N*-methylaminoborane oligomers (^{11}B NMR triplets at -2, -4 and -6 ppm) are also formed in preference to poly(*N*-methylamino-borane) which exhibits a very broad resonance centered at -5 ppm.[31] Note also the prominent resonance due the catalyst

resting state (**4-6**) at 24 ppm (**Figure 4.3**). This was confirmed by the ^{1}H and ^{31}P NMR spectra that also showed some unreacted **4-5** (Figs. A.40, A.41). Interestingly, less catalyst decomposition occurs using MAB vs. AB as seen by the relative amounts of *N*-trimethylborazine (**BZ**) and dmpe bis(borane) (**PB**).

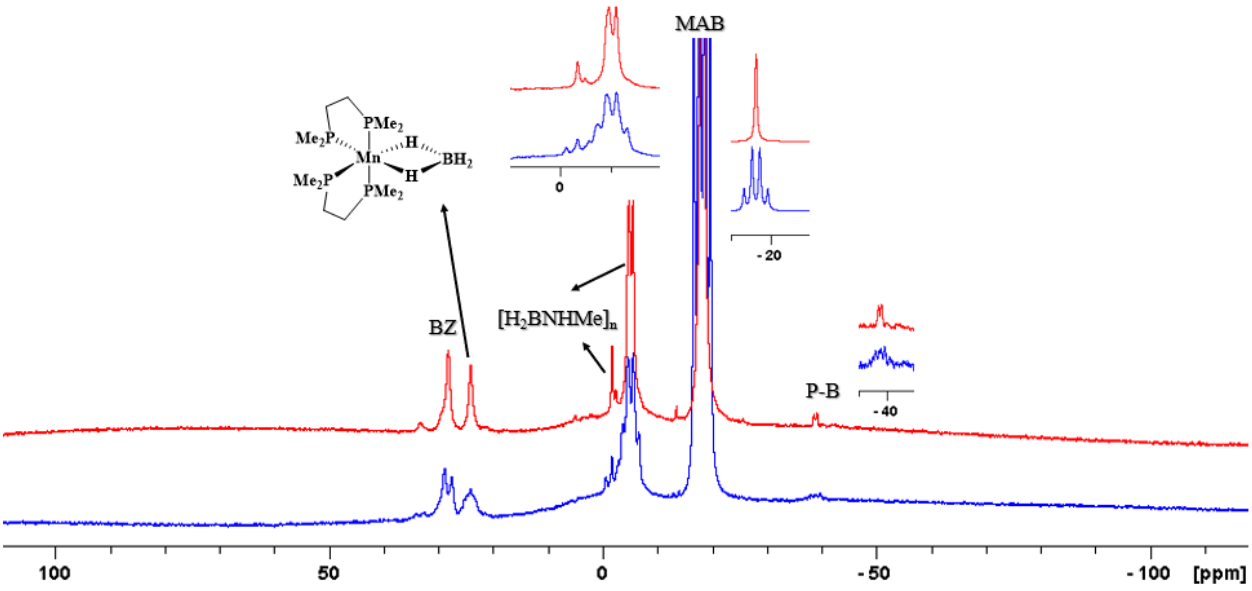

Figure 4.3. ^{11}B and $^{11}B\{^{1}H\}$ NMR spectrum of catalytic dehydrogenation of MAB with **4-5** in DME at 50 ^{o}C after 1 d (top: $^{11}B\{^{1}H\}$; bottom: ^{11}B).

*4.2.1 Dimethylamine-borane dehydrogenation catalyzed by $MnH(H_2)(dmpe)_2$ (**4-5**).*

Catalyzed dehydrogenation of DMAB using 5 mol% **4-5** was also very slow. In fact, the catalyst resting state is not even visible in the ^{11}B NMR spectrum that shows a typical mixture[32] of dimethylaminoborane monomer ($Me_2N{=}BH_2$, doublet at 33.1 ppm), cyclic dimer (triplet at 9.9 ppm) and intermolecular dehydrogenation product, $Me_2HNBH_2NMe_2BH_3$ (triplet at 6.2 ppm and quartet buried under DMAB peak) (**Figure 4.4**). Note also that catalyst decomposition predominates for DMAB as evidenced by the large **PB** peak and no evidence of **4-6**. In the same way, the ^{1}H NMR and $^{31}P\{^{1}H\}$ spectra confirmed the presence of the $Mn(BH_4)(dmpe)_2$ (Figs. A.42, A.43).

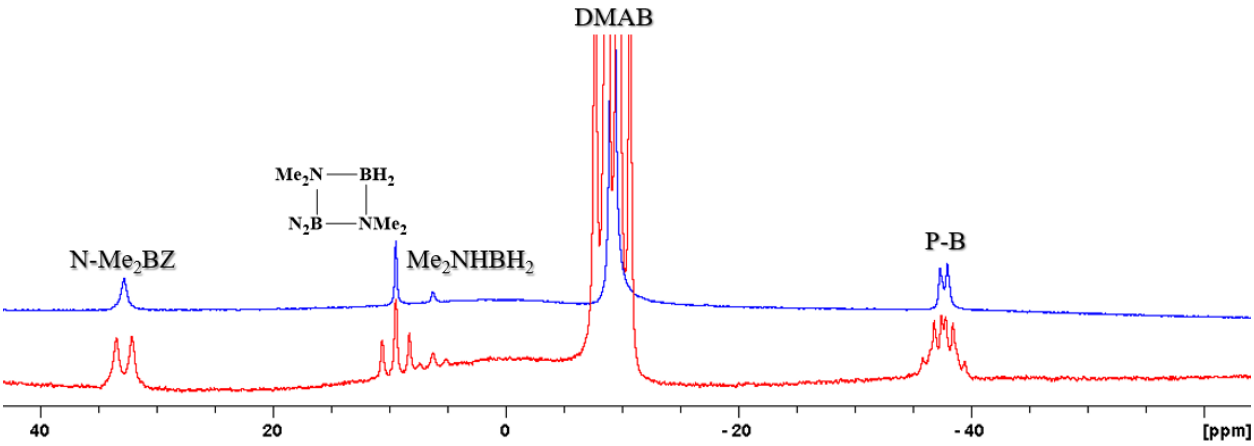

Figure 4.4. ^{11}B and $^{11}B\{^1H\}$ NMR spectra of DMAB dehydrogenation using 5 mol% **4-5** at 50 ^0C after 1 d (top: $^{11}B\{^1H\}$; bottom: ^{11}B).

4.3 **Conclusions**

One of the unique properties of *cis*-$FeH_2(dmpe)_2$ (**4-1**) as an amine-borane dehydrogenation catalyst is its greatly reduced activity with MAB (*vs* AB). Using the Ir POCOP catalyst, for example, these amine-boranes have been shown to react at nearly the same rate. In the present study we see that Mn catalyst **4-5** also shows a large rate drop-off going from AB to MAB in spite of its ready access to an open coordination site. The most disappointing property of the Mn catalyst, however, is its rapid formation of dmpe bis(borane) that will presumably lead to catalyst death. As a result it would be interesting to see if the stable pincer-ligand Mn hydride catalysts such as that used by Liu for the Guerbet reaction would better tolerate the reducing conditions associated with amine-borane dehydrogenation.

4.4 **Experimental Section**

4.4.1 General considerations

MBraun glove box and Schlenk techniques were used to carry out the experiments under nitrogen. A J.C. Meyer solvent purification system was used to dry the diethyl ether, toluene,

tetrahydrofuran (THF) and hexanes using activated alumina columns. Stirring over activated alumina (ca. 10 wt.%) was used to dry the benzene-d_6 (C_6D_6) overnight followed by filtration. Dichloromethane (DCM) and acetonitrile-d_3 (CD_3CN) were refluxed over calcium hydride, stirred over activated alumina (ca. 5 wt.%) overnight and filtered. Activated 4 Å molecular sieves (heated at ca. 250 ^oC for >10 h under vacuum) were used to store all solvents. All glassware was heated in an oven for >2 h at 150^oC.

Commercial chemicals used were ammonia borane (AB, NH_3-BH_3, Scitix, 91%), 1,2-bis(dimethylphosphino)ethane (DMPE, Strem, 98%), borane dimethylamine complex (DMAB, Me_2NH-BH_3, 97%, Aldrich). Methylamine-borane (MAB, $MeNH_2$-BH_3),[33] and *trans*-$MnH(H_2)(DMPE)_2$[30] were prepared modifying the literature procedures from the literature. Ammonia-borane and methylamine-borane were sublimed before use. A 300 MHz Bruker Avance instrument was used to record the spectra of ^1H, $^{31}P\{^1H\}$, ^{11}B, and $^{11}B\{^1H\}$ NMR at room temperature (21-23^oC). ^1H NMR chemical shifts are reported relative to residual proton peaks of the deuterated solvents (CD_3CN: 1.94 ppm; C_6D_6: 7.16 ppm), while $^{31}P\{^1H\}$, ^{31}P, ^{11}B, and $^{11}B\{^1H\}$ NMR shifts are reported relative to phosphoric acid and boron trifluoride diethyl etherate (85 % aqueous solution) at 0 ppm. $^{13}C\{^1H\}$ NMR spectra was recorded on a 400 MHz Bruker Avance instrument. Applied Biosystem API2000 triple quadrupole mass spectrometer was used to collect the mass spectral data of electrospray ionization and electron Impact. IR data was collected on a Thermo Scientific Nicolet 6700 FT-IR spectrometer.

Samples for X-ray crystallography were affixed on thin glass fibres with the help of paraffin oil. Bruker AXS KAPPA single-crystal diffractometer (**λ**= 0.71073Å) furnished with a sealed Mo tube source and APEX II CCD detector was used to collect the data. APEX II software package from BRUKER AXS was used to collect and process the raw data.

4.4.2 Synthesis and characterization

Synthesis of $MnBr_2(dmpe)_2$: In a modification of a literature procedure,[30] $MnBr_2$ (100 mg, 0.46 mmol) was suspended in 20 mL of THF and stirred for 1 h in a Schlenk tube with a stir bar in the glove box. Then 1,2-bis(dimethylphosphino)ethane (140 mg, 0.93 mmol) in 5 mL of THF was added dropwise and stirred for 5 h to give a colourless solution. The solution was dried in vacuo to yield a white solid powder. Yield: 220 mg (92%). No signals were observed in the $^{31}P\{^1H\}$ NMR spectrum for the paramagnetic product.

Synthesis of $[Mn(AlH_4)(dmpe)_2]_2$. Solid $MnBr_2(dmpe)_2$ (240 mg, 0.65 mmol) was added to a suspension of 10 equiv $LiAlH_4$ (250 mg, 6.57 mmol) in 15 mL of toluene at -78 ^oC. After warming to room temperature, the reaction solution turned yellow with gas evolution and solid formation. After stirring for 12 h the solvent was removed and the residue extracted with hexane and filtered. The filtrate was cooled at -20 °C to give $[Mn(AlH_4)(dmpe)_2]_2$ as a yellow powder. Yield after filtration and drying: 225 mg, 46 %. Product formation was confirmed by $^{31}P\{^1H\}$ NMR (singlet at 76 ppm) and ^1H NMR [Mn-H-Al at δ -15.02 (br s) in C_6D_6].

Synthesis of $MnH(H_2)(dmpe)_2$, 4-5. Following the above literature procedure,[30] a solution of 225 mg of $[Mn(AlH_4)(dmpe)_2]_2$ in 5 mL of diethyl ether was treated with distilled water dropwise until gas evolution ceased. The reaction mixture was then filtered, dried and extracted with hexane. The extract was concentrated and cooled at -20 ^oC to obtain the yellow solid product. Yield: 170 mg, 76 %. ^1H NMR (C_6D_6) δ -12.67 ppm (quint, Mn-H, $^2J_{PH}$ = 29 Hz), 1.39 (s, PMe_2, PCH_2). $^{31}P\{^1H\}$ (120 MHz, C_6D_6) 82.7 ppm (s).

Dehydrogenation of NH_3BH_3 using $MnH(H_2)(dmpe)_2$, 4-5 (generation of $Mn(\kappa^2$-$BH_4)(dmpe)_2$, 4-6. To a solution of 20 mg (0.06 mmol) of $MnH_3(dmpe)_2$ in 3 mL of DME was added 35 mg (1.1 mmol) of ammonia-borane and the solution was stirred for 24 h in a vial with

stir bar in the glove box at 50 °C. The reaction mixture changed from yellow to dark purple overnight. After full transformation was confirmed by $^{31}P\{^{1}H\}$ and ^{1}H NMR (in Mn-H region) spectroscopy, the solution was dried and extracted with 3 mL of hexane. Removal of the hexane and drying in vacuo obtained 50 mg of **4-6** contaminated with dmpe bis(borane). $^{31}P\{^{1}H\}$ (121 MHz, C_6D_6) 88.4 (s, 2P, Mn–P), 72.2 (s, 2P, Mn-P-H), 7.1 ppm (br mult, P-B). ^{1}H (300 MHz, C_6D_6) δ -16.41 ppm (br d, 4H, $^{2}J_{BH}$ = 70 Hz, Mn–H_2BH_2). ^{11}B (300 MHz, C_6D_6) δ 25.6 ppm (br 2t, $^{2}J_{BH}$ = 48 Hz, Mn-BH_4), -40 ppm (br qq, P-B). $^{11}B\{^{1}H\}$, (300 MHz, C_6D_6) δ 25.6 ppm (s, Mn-BH_4), -40 ppm (s, P-B).

Dehydrogenation of $MeNH_2BH_3$ using $MnH(H_2)(dmpe)_2$, 4-5. To 7 mg (0.02 mmol) of $MnH(H_2)(dmpe)_2$ in 3 mL of DME was added 18 mg (0.39 mmol) of methylamine-borane and the solution stirred for 24 h in a vial with stir bar in the glove box at 50 °C. The reaction changed from yellow to light purple overnight. Although incomplete conversion was confirmed by $^{31}P\{^{1}H\}$ and ^{1}H NMR (in Mn-H region) spectroscopy, the solution was dried and extracted with 3 mL of hexane. Removal of the hexane and drying in vacuo obtained **4-6**. Yield: 13 mg, 52 %. NMR $^{31}P\{^{1}H\}$ (121 MHz, C_6D_6) 88.4 ppm (s, 2P, Mn–P), 72.2 ppm (s, 2P, Mn-P-H), 6.7 ppm (br, P-B), 77.8 (SM), -48ppm (free dmpe). ^{1}H (300 MHz, C_6D_6) δ -16.41 ppm (br, 4H, $^{2}J_{BH}$ = 46 Hz, Mn–H_2BH_2), -13.4 ppm (br s, Mn-H). ^{11}B (96 MHz, C_6D_6) δ 25.6 ppm (br 2t, $^{2}J_{BH}$ = 48 Hz, Mn-BH_4), -40 ppm (br qq, P-B). $^{11}B\{^{1}H\}$, (96 MHz, C_6D_6) δ 25.6 ppm (s, Mn-BH_4), -40 ppm (s, P-B).

Dehydrogenation of Me_2NHBH_3 using $MnH(H_2)(dmpe)_2$, 4-5. To 20 mg (0.06 mmol) of $MnH_3(dmpe)_2$ in 3 mL of DME was added 66 mg (1.11 mmol) of dimethylamine-borane and stirred for 24 h in a vial with stir bar in the glove box at 50 °C. The reaction mixture changed from yellow to slight purple overnight. $^{31}P\{^{1}H\}$ (121 MHz, C_6D_6) 88.4 ppm (s, 2P, Mn–P), 72.2 ppm (s, 2P, Mn-P-H), 6.7 ppm (br, P-B), 77.8 (**4-5**), -48 ppm (free dmpe). ^{1}H (300 MHz, C_6D_6) δ -16.41

ppm (br, 4H, $^{2}J_{BH}$ = 46 Hz, Mn–H_2BH_2), -13.4 ppm (br s, Mn-H). ^{11}B (96 MHz, C_6D_6) δ 25.6 ppm (br 2t, $^{2}J_{BH}$ = 48 Hz, Mn-BH_4), -40 ppm (br qq, P-B). $^{11}B\{^{1}H\}$, (96 MHz, C_6D_6) δ 25.6 ppm (s, Mn-BH_4), -40 ppm (s, P-B).

4.5 **References**

1) Stephens, F. H.; Pons, V.; Baker, R. T. *Dalton Trans.* **2007**, *25*, 2613-2626.
2) Peng, B.; Cheng, J. *Energy Environ. Sci.* **2008**, *1*, 479-483.
3) Hamilton, C. H.; Baker, R. T.; Staubitz, A.; Manners, I. *Chem. Soc. Rev.* **2009**, *38*, 279-293.
4) Smythe, N. C.; Gordon, J. C. *Eur. J. Inorg. Chem.* **2010**, 509-521.
5) Staubitz, A.; Robertson, A. P. M.; Manners, I. *Chem. Rev.* **2010**, *110*, 4079-4124.
6) Li, H.; Yang, Q.; Chen, X.; Shore, S. G. *J. Organomet. Chem.* **2014**, *751*, 60-66.
7) Stowe, A. C.; Shaw, W. J.; Linehan, J. C.; Schmid, B.; Autrey, T. *PhysChemChemPhys* **2007**, *9*, 1831-1836.
8) Nguyen, V. S.; Matus, M. H.; Nguyen, M. T.; Dixon, D. A. *J. Phys. Chem. A* **2008**, *112*, 9946-9954.
9) Wang, P. *Dalton Trans.* **2012**, *41*, 4296-4302.
10) Keaton, R. J.; Blacquiere, J. M.; Baker, R. T. *J. Am. Chem. Soc.* **2007**, *129*, 1844−1845.
11) Staubitz, A.; Robertson, A. P. M.; Sloan, M. E.; Manners, I. *Chem. Rev.* **2010**, *110*, 4023-78.
12) Buss, J. A.; Edouard, G. A.; Cheng, C.; Shi, J.; Agapie, T. *J. Am. Chem. Soc.* **2014**, *136*, 11272−11275.
13) Bhattacharya, P.; Krause, J. A.; Guan, H. *J. Am. Chem. Soc.* **2014**, *136*, 11153−11161.
14) Johnson, H. C.; Hooper, T. N.; Weller, A. S. *Top. Organomet. Chem.* **2015**, *49*, 153- 220.
15) Zhan, W.-W.; Zhu, Q.-L.; Xu Q. *ACS Catal.* **2016**, *6*, 6892-6905.
16) Zhang, X.; Kam L.; Trerise, R.; Williams, T. J. *Acc. Chem. Res.* **2017**, *50*, 86–95.
17) Sutton, A. D.; Burrell, A. K.; Dixon, D. A.; Garner, E. B. III; Gordon, J. C.; Nakagawa, T.; Ott, K. C.; Robinson, J. P.; Vasiliu, M. *Science* **2011**, *331*, 1426−1429.
18) Denney, M. C.; Pons, V.; Hebden, T. J.; Heinekey, M.; Goldberg, K. I. *J. Am. Chem. Soc.* **2006**, *128*, 12048−12049.

19) Blaquiere, N.; Diallo-Garcia, S.; Gorelsky, S. I.; Black, D. A.; Fagnou, K. *J. Am. Chem. Soc.* **2008**, *130*, 14034−14035.

20) Kaβ, M.; Friedrich, A.; Drees, M.; Schneider, S. *Angew. Chem., Int. Ed.* **2009**, *48*, 905−907.

21) Staubitz, A.; Sloan, M. E.; Robertson, A. P. M.; Friedrich, A.; Schneider, S.; Gates, P. J.; auf der Gunne, J. S.; Manners, I. *J. Am. Chem. Soc.* **2010**, *132*, 13332−13345.

22) Baker, R. T.; Gordon, J. C.; Hamilton, C. W.; Henson, N. J.; Lin, P. H.; Maguire, S.; Murugesu, M.; Scott, B. L.; Smythe, N. C. *J. Am. Chem. Soc.* **2012**, *134*, 5598−5609.

23) Glüer, A.; Förster, M.; Celinski, V. R.; auf der Gunne, J. S.; Holthausen, M. C.; Schneider, S. *ACS Catal.* **2015**, *5*, 7214-7217.

24) Kim, D.-P.; Moon, K.-T.; Kho, J.-G.; Economy, J.; Gervais, C.; Babonneau, F. *Polym. Adv. Technol.* **1999**, *10*, 702-712.

25) Pons, V.; Baker, R. T.; Szymczak, N. K.; Heldebrant, D. J.; Linehan, J. C.; Matus, M. H.; Grant, D. J.; Dixon, D. A., *Chem. Commun.* **2008**, 6597-6599.

26) Alig, L.; Fritz, M.; Schneider, S. *Chem. Rev.* **2019**, *119*, 2681-2751.

27) (a) Bhunya, S.; Malakar, T.; Paul, A. *Chem. Commun.* **2014**, *50*, 5919-5922. (b) Bhunya, S.; Zimmerman, P. M.; Paul, A. *ACS Catal.* **2015**, *5*, 3478-3493.

28) Todisco, S.; Luconi, L.; Giambastini, G.; Rossin, A.; Peruzzini, M.; Golub, I. E.; Filippov, O. A.; Belkova, N. V.; Shubina, E. S. *Inorg. Chem.* **2017**, *56*, 4296-4307.

29) Coles, N. T.; Webster, R. L. *Isr. J. Chem.* **2017**, *57*, 1070.

30) (a) Girolami, G. S.; Howard, C. G.; Wilkinson, G.; Dawes, H. M.; Thornton-Pett, M.; Motevalli, M.; Hursthouse, M. B. *J. Chem. Soc., Dalton Trans.* **1985**, 921-929. (b) Girolami, G. S.; Wilkinson, G.; Thornton-Pett, M.; Hursthouse, M. B. *J. Am. Chem. Soc.* **1983**, *105*, 6752-6753. (c) Perthuisot, C.; Fan, M.; Jones, W. D. *Organometallics* **1992**, *11*, 3622-3629.

31) Anke, F.; Boye, S.; Spannenberg, A.; Lederer, A.; Heller, D.; Beweries, T. *Chem. Eur. J.* **2020**, *26*, 7889.

32) (a) Xu, P.; Xu, X. *Organometallics* **2019**, *38* (16), 3212-3217. (b) Bénac-Lestrille, G.; Helmstedt, U.; Vendier, L.; Alcaraz, G.; Clot, E.; Sabo-Etienne, S. *Inorg. Chem.* **2011**, *50* (21), 11039-11045.

33) Du, Y.; Cao, N.; Yang, L.; Luo, W.; Cheng, G. *New J. Chem.* **2013**, *37*, 3035.

Chapter 5: Conclusions and Future Outlook

5.1 Summary of Results in Context of the State of the Art

Despite the significant importance of organofluorine compounds in daily life, their synthesis still relies on older synthetic methods using toxic reagents such as anhydrous HF. Fluoroalkenes (FAs) have been identified as promising underutilized precursors to a wide range of organic products with applications in a variety of industries.[1] Fluorometallacycles can be important primary intermediates in these transformations, allowing for a host of functionalization reactions as summarized in **Chapter 1**.[2-6] Over the past 30 years, reactivity studies of metal fluorocarbenes have also expanded our knowledge,[7-14] but applications in catalysis are just starting to be realized.[15-17] The Baker, Vicic and Ogoshi groups have spent the last decade improving d^8 fluorometallacycle synthesis and expanding their reactivity profiles.[18-20] In contrast, reactivity studies of d^6 fluorometallacycles have been confined to a single publication on Fe[5] and an MSc thesis on Co.[21] In the latter work, treatment of Co hydride carbonyl complexes with TFE afforded novel Co hydride perfluoro-metallacyclopentanes but the reaction was hampered by a competing reaction that gave hydrogenated TFE and zerovalent Co-Co bonded dimer. Moreover, photolysis of the cobaltacycles did not give rise to expected reductive elimination and β-F elimination reactions that could form the basis of a catalyzed hydrodefluorodimerization process for conversion of C_2 to C_4 FAs. These observations provided the motivation for our efforts to prepare analogous d^4 fluorometallacycles that may show enhanced reactivity.

In **Chapter 2** our efforts to prepare Mn bromide fluorometallacycles met with mixed success. First, we showed that 1e- reduction of Mn dibromide bis(phosphine) complexes afforded paramagnetic products. Nonetheless, the DPPE and $P(O^iPr)_3$ derivatives reacted with TFE to afford diamagnetic products with ^{19}F NMR spectra that suggested formation of perfluorometalla-

cyclopentanes. However, further characterization was hampered by the fact that solvent removal reversed the reaction, suggesting that the displaced ligands can participate in a reversible reaction with the Mn center. In **Chapter 3**, we employed Mn bromide carbonyl complexes and several substituted derivatives with a view to also converting them to the Mn-H complexes. However, only in the case of the TFE reaction with $MnBr(CO)_3$ + 3 equiv. of dppe did we actually identify a Mn bromide fluorometallacycle, the first example of a d^4 metallacycle (**3-20)**. Instead, we found that photolysis of the manganese bromide complexes with fluoroalkenes in THF solution generated the Mn-H *in situ*, giving rise to insertion products (**3-8, 3-13** through **3-16)** that bear close resemblance to their d^6 Co analogue (for TFE). Evidence that the hydrogen source was the THF solvent was provided by characterization of the fluoroalkylated THF derivatives. Moreover, for all three fluoroalkenes tested, reaction conditions were identified that did not yield significant amounts of either the insertion product or hydrogenated fluoroalkene.

In **Chapter 4**, our efforts built on previous work using iron hydride dmpe complexes as ammonia-borane dehydrogenation catalysts. Our results demonstrated first that the *trans*-$MnH(H_2)(dmpe)_2$ catalyst (**4-5**) is significantly less active than its Fe analogues *cis*-$FeH_2(dmpe)_2$ (**4-1**) or [*trans*-$FeH(H_2)(dmpe)_2]^+$ (**4-3**). Moreover, in contrast to its cationic Fe analogue (**4-3**) that affords mostly cyclic products, catalyst **4-5** at 5 mol% loading afforded mostly insoluble poly(aminoborane). Although we did not get a chance to test the Mn catalyst resting state, Mn(κ^2-BH_4)$(dmpe)_2$ (**4-6**) in the presence of triethylamine (which can abstract BH_3 to reform the Mn-H), we were able to show that the dehydrogenation rate falls significantly for the methyl-substituted amine-boranes MAB and DMAB. Most importantly, we observed significant formation of dmpe bis(borane), confirming that the Mn catalyst is more prone to catalyst decomposition (*vs* the Fe analogues) under the reducing environment associated with amine-borane dehydrogenation.

5.2 Future Prospects

Although we have identified the first example of d^4 fluorometallacycle, we have been as yet unable to confirm their solid-state structures by X-ray diffraction. This is particularly important in light of the large $^3J_{FH}$ and $^4J_{FH}$ coupling constants observed by NMR spectroscopy. Monitoring the thermolysis of these Mn hydride fluorometallacyles by NMR, with a view to observing reductive elimination, would also be informative. A great deal of additional work is needed in order to obtain a sufficient number of d^4 fluorometallacycles for insightful reactivity studies. An extensive solvent study may help identify reaction conditions for the exclusive synthesis of ligand-substituted manganese bromide fluorometallacycles and the easily prepared Mn methyl carbonyl complexes should also be tried.

From our amine-borane-dehydrogenation studies, it is apparent that not even the strong electron-donor bis(phosphine) dmpe can stabilize the Mn center under these strongly reducing conditions. It would be interesting to see if pincer-ligated Mn hydride complexes such as **1-1-1-3** typically employed at elevated temperatures,[22] would give rise to more active and stable catalysts for this application.

5.3 References

1) Sicard, A. J.; Baker, R. T. *Chem. Rev.* **2020**, *120* (17), 9164-9303.
2) Daniels, A. L.; Da Gama, J. G.; Edjoc, R.; Gabidullin, B. M.; Baker, R. T. *Inorganics* **2019**, *7*, 3.
3) Harrison, D. J.; Daniels, A. L.; Guan, J.; Gabidullin, B. M.; Hall, M. B.; Baker, R. T. *Angew. Chem. Int. Ed* **2018**, *57*, 5772-5776.
4) Trnka, T. M.; Day, M. W.; Grubbs, R. H. *Angew. Chem. Int. Ed.* **2001**, *40*, 3441-3444.
5) Ghostine, K.; Gabidullin, B.M.; Baker, R. T. *Polyhedron* **2020**, *185*, 114587-114592.
6) Andrella, N. O.; Sicard, A. J.; Gorelsky, S. I.; Korobkov, I.; Baker, R. T. *Chem. Sci.* **2015**, *6*, 6392-6397.

7) Harrison, D. J.; Gorelsky, S. I.; Lee, G. M.; Korobkov, I.; Baker, R. T. *Organometallics* **2013**, *32*, 12-15.
8) Harrison, D. J.; Lee, G. M.; Leclerc, M. C.; Korobkov, I.; Baker, R. T. *J. Am. Chem. Soc.* **2013**, *135*, 18296-18299.
9) Lee, G. M.; Harrison, D. J.; Korobkov, I.; Baker, R. T. *Chem. Commun.* **2014**, *50*, 1128-1130.
10) Fuller, J. T.; Harrison, D. J.; Leclerc, M. C.; Baker, R. T.; Ess, D. H.; Hughes, R. P. *Organometallics* **2015**, *34*, 5210-5213.
11) Harrison, D. J.; Daniels, A. L.; Korobkov, I.; Baker, R. T. *Organometallics* **2015**, *34*, 5683-55686.
12) Leclerc, M. C.; Bayne, J. M.; Lee, G. M.; Gorelsky, S. I.; Vasiliu, M.; Korobkov, I.; Harrison, D. J.; Dixon, D. A.; Baker, R. T. *J. Am. Chem. Soc.* **2015**, *137*, 16064-16073.
13) Lee, G. M.; Leung, A. S. C.; Harrison, D. J.; Korobkov, I.; Hughes, R. P.; Baker, R. T. *Organometallics* **2017**, *36*, 5683-5686.
14) Rochon, A.; Elsby, M. R.; Baker, R. T. *Can. J. Chem.* **2020**. https://doi.org/10.1139/cjc-2020-0372.
15) Fu, X.-P.; Xue, X.-S.; Zhang, X.-Y.; Xiao, Y.-L., Zhang, S.; Guo, Y.-L.; Leng, X.; Houk, K. N.; Zhang, X. *Nature Chem.* **2019**, *11*, 948-956.
16) Peng, L.; Wang, H.; Guo, C. *J. Am. Chem. Soc.* **2021**, *143* (17), 6376-6381.
17) Liu, X.; Sheng, H.; Zhou, Y.; Song, Q. *Org. Lett.* **2021**, *23* (7), 2543-2547.
18) Giffin, K. A.; Pua, L. A.; Piotrkowski, S.; Gabidulin, B. M.; Korobkov, I.; Hughes, R. P.; Baker, R. T. *J. Am. Chem. Soc.* **2017**, *139*, 4075.
19) Kaplan, P. T.; Xu, L.; Chen, B.; McGarry, K. R.; Yu, S.; Wang, H.; Vicic, D. A. *Organometallics* **2013**, *32*, 7552–7558.
20) Ohashi, M.; Shibata, M.; Saijo, H.; Kambara, T.; Ogoshi, S. *Organometallics* **2013**, *32* (13), 3631–3639.
21) Ghostine, K., University of Ottawa MSc thesis, **2018**.
22) (a) Chakraborty, S.; Daw, P.; Ben David, Y.; Milstein, D. *ACS Catal.* **2018**, *8* (11), 10300-10305. (b) Mukherjee, A.; Nerush, A.; Leitus, G.; Shimon, L. J. W.; Ben-David, Y.; Espinosa Jalapa, N. A.; Milstein, D. *J. Am. Chem. Soc.* **2016**, *138*, 4298−4301. (c)

Mastalir, M.; Glatz, M.; Gorgas, N.; Stöger, B.; Pittenauer, E.; Allmaier, G.; Veiros, L. F.; Kirchner, K. *Chem. Eur. J.* **2016**, *22*, 12316−12320.

Appendices

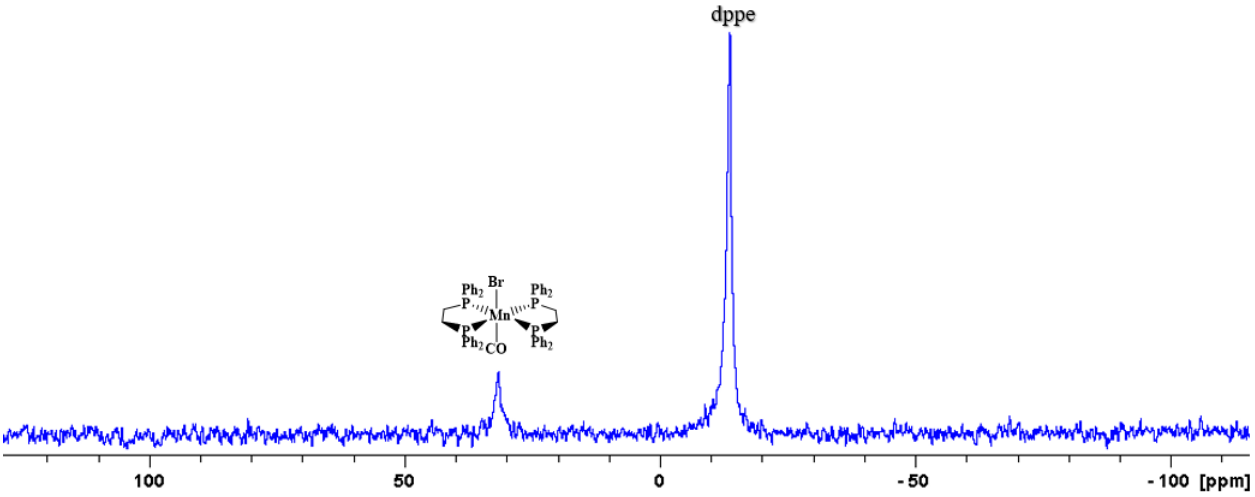

Figure A.1. $^{31}P\{^{1}H\}$ NMR (121 MHz, C_6D_6) spectrum for complex $MnBr(DPPE)_2(CO)$, **2-2A.**

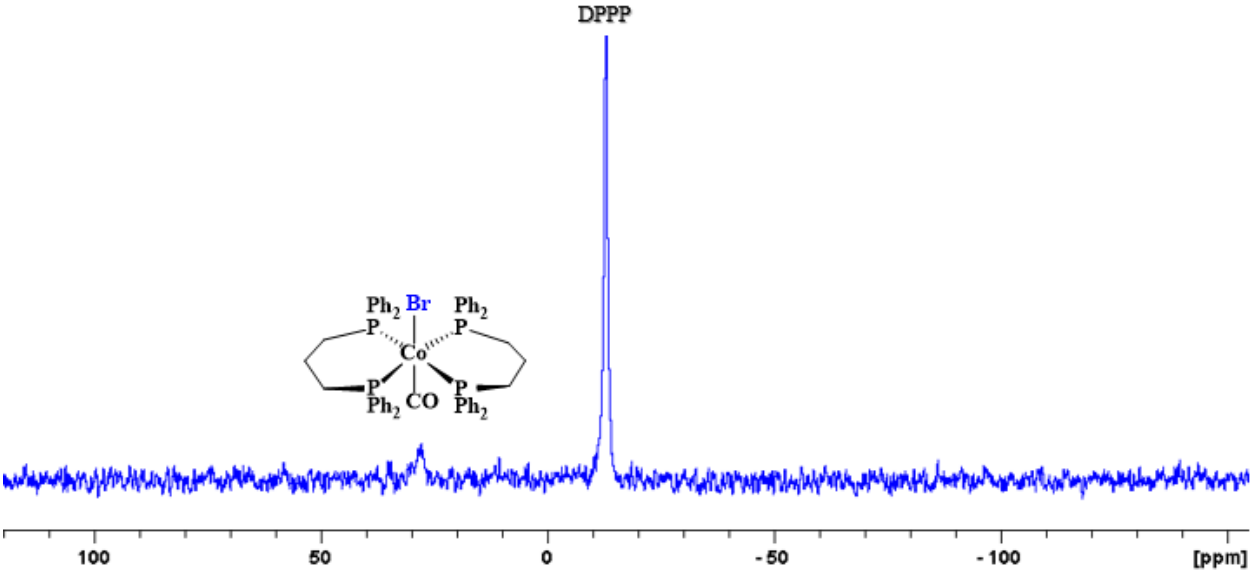

Figure A.2. $^{31}P\{^{1}H\}$ NMR (121 MHz, C_6D_6) spectrum for complex $MnBr(DPPP)_2(CO)$, **2-2B.**

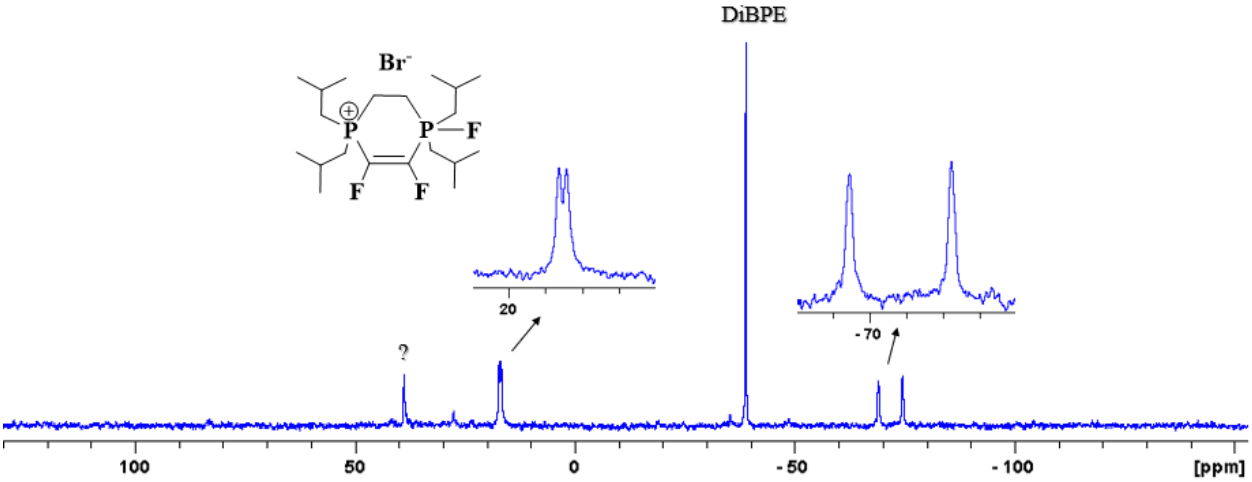

Figure A.3. $^{31}P\{^{1}H\}$ NMR (121 MHz, C_6D_6) spectrum for complex $[(i\text{-}Bu)_2P(\mu\text{-}CH_2CH_2)(\mu\text{-}CF{=}CF)PF(i\text{-}Bu)_2]Br$, **2-3.**

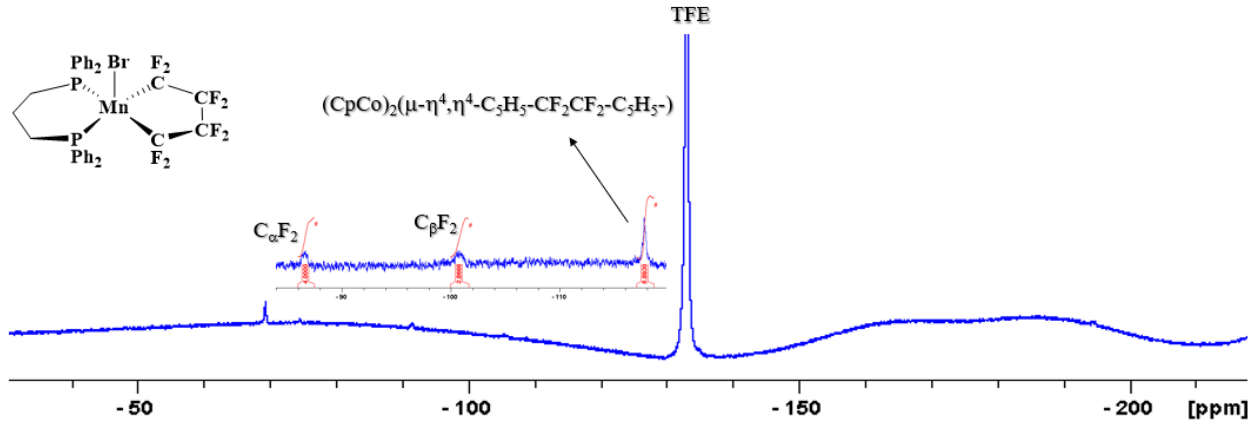

Figure A.4. $^{19}F\{^{1}H\}$ NMR (282 MHz, THF) spectrum for complex $MnBr(1,4\text{-}C_4F_8)(dppp)$, **2-6.**

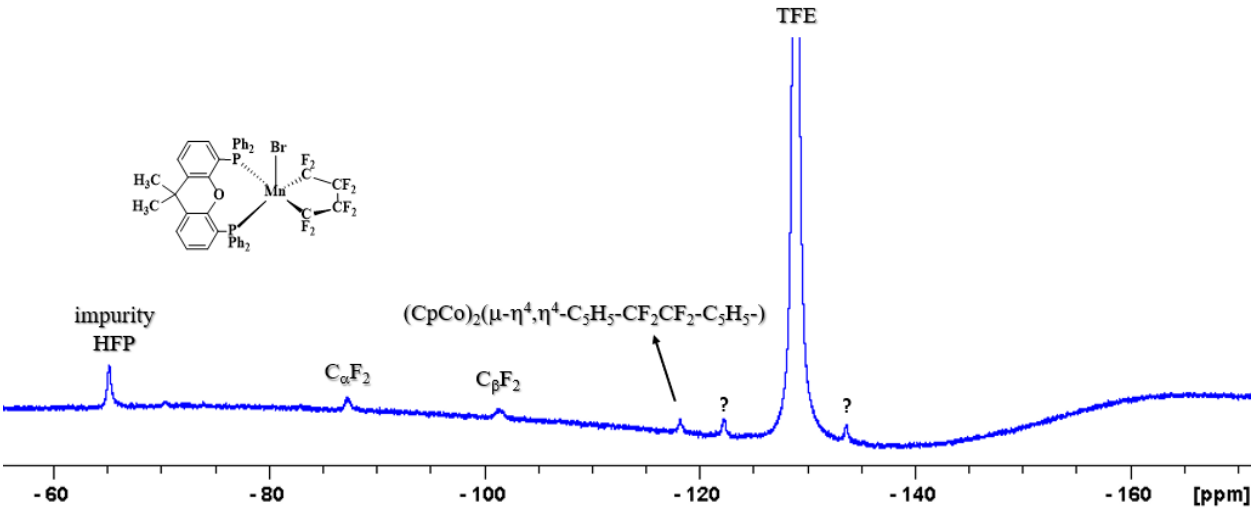

Figure A.5. $^{19}F\{^1H\}$ NMR (282 MHz, THF) spectrum for complex MnBr(1,4-C_4F_8)(Xantphos), **2-7.**

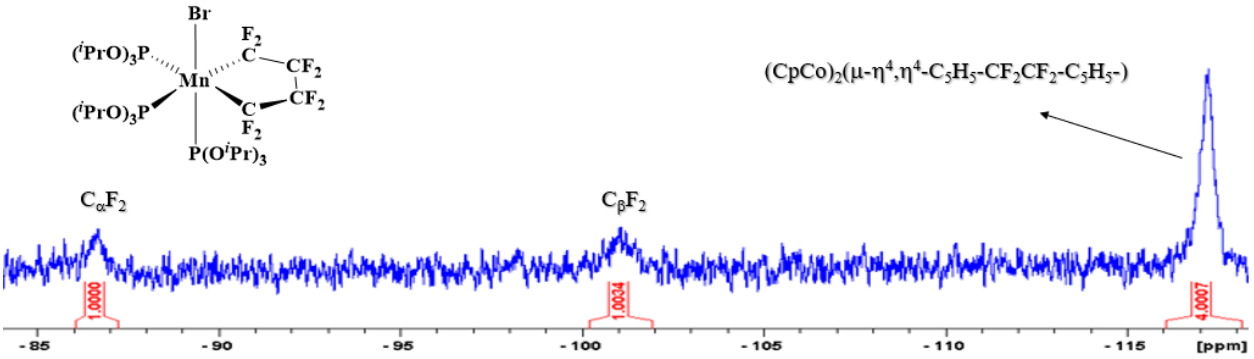

Figure A.6. $^{19}F\{^1H\}$ NMR (282 MHz, THF) spectrum for complex MnBr(1,4-C_4F_8)[$P(O^iPr)_3$]$_3$, **2-8.**

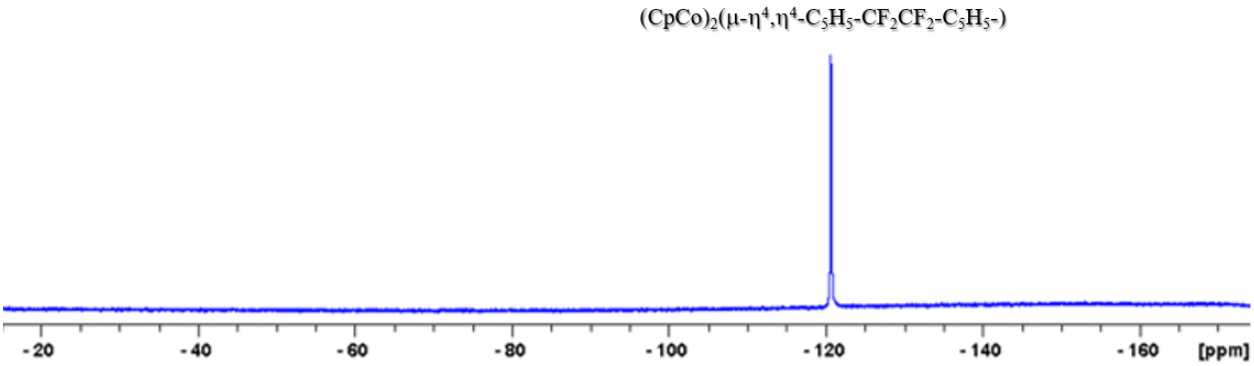

Figure A.7. $^{19}F\{^1H\}$ NMR (282 MHz, C_6D_6) spectrum for complex $(CpCo)_2(\mu\text{-}\eta^4,\eta^4\text{-}C_5H_5\text{-}CF_2CF_2\text{-}C_5H_5\text{-})$, **2-4** after removal of solvent and dissolution in C_6D_6.

	2-3
Empirical formula	$C_{20}H_{40}BrF_3P_2$
Formula weight, g/mol	479.38
Crystal system	monoclinic
Space group	$C\,2/c$
a, Å	28.240(8)
b, Å	11.005(3)
c, Å	16.218(4)
α, °	90
β, °	90.752(9)
γ, °	90
V, Å^3	5040(2)
Z	8
T, K	200(2)
ρ_{calc}, g/cm^3	2.035
μ, mm^{-1}	4.415
$2\theta_{max}$, °	41.624
Total/unique reflections	9642/2543
Reflections $[I_o \geq 2\sigma(I_o)]$	1464
R_1, wR_2 $[I_o \geq 2\sigma(I_o)]$	0.1577, 0.3818
Goodness of fit	2.349

Table A.1. X-ray diffraction data collection and structure refinement details for complex **2-3.**

	2-4
Empirical formula	$C_{22}H_{20}Co_2F_4$
Formula weight, g/mol	478.24
Crystal system	orthorhombic
Space group	*P b c* a
a, Å	9.6373(10)
b, Å	9.2597(8)
c, Å	20.752(2)
α, °	90
β, °	90
γ, °	90
V, Å^3	1851.9(3)
Z	4
T, K	200(2)
ρ_{calc}, g/cm^3	1.715
μ, mm^{-1}	1.834
$2\theta_{max}$, °	53.49
Total/unique reflections	13248/1892
Reflections $[I_o \geq 2\sigma(I_o)]$	1117
R_1, wR_2 $[I_o \geq 2\sigma(I_o)]$	0.0541, 0.1143
Goodness of fit	1.041

Table A.2. X-ray diffraction data collection and structure refinement details for complex **2-4.**

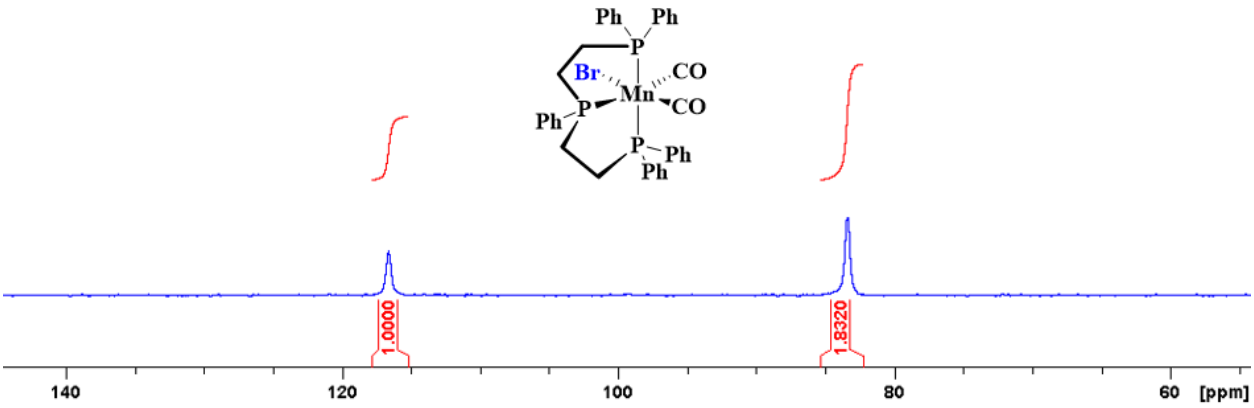

Figure A.8. $^{31}P\{^1H\}$ NMR spectrum (121 MHz, C_6D_6) of *cis*, *mer*-MnBr(triphos)$(CO)_2$, **3-4.**

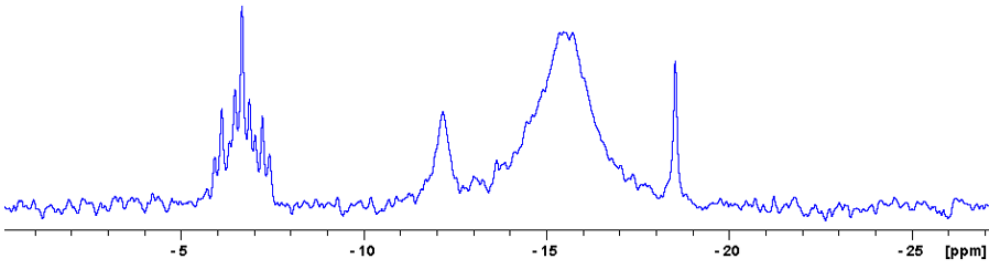

Figure A.9. $^{31}P\{^{1}H\}$ NMR spectrum (121 MHz, C_6D_6) of $Mn[CF_2CF_2H](dppe(CO)_3$, **3-8.**

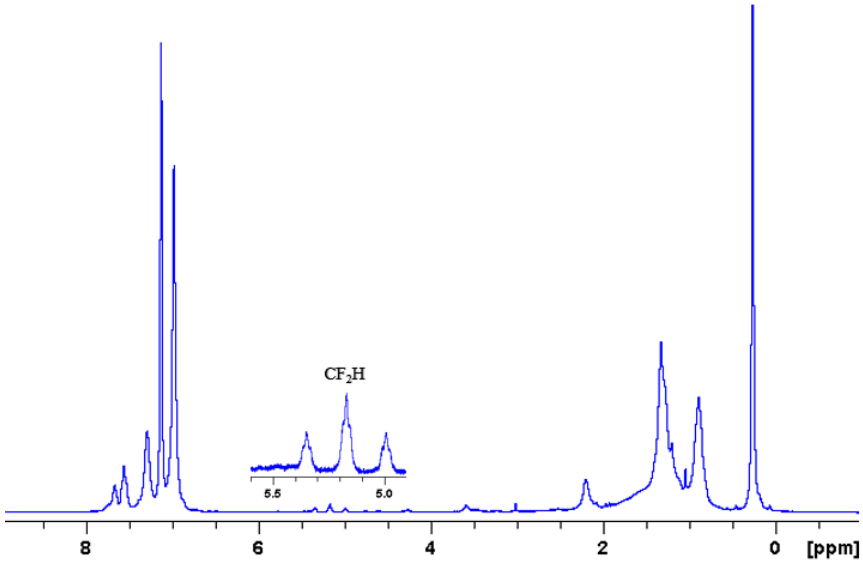

Figure A.10. ^{1}H NMR (300 MHz, C_6D_6) spectrum of $Mn[CF_2CF_2H](dppe)(CO)_3$, **3-8.**

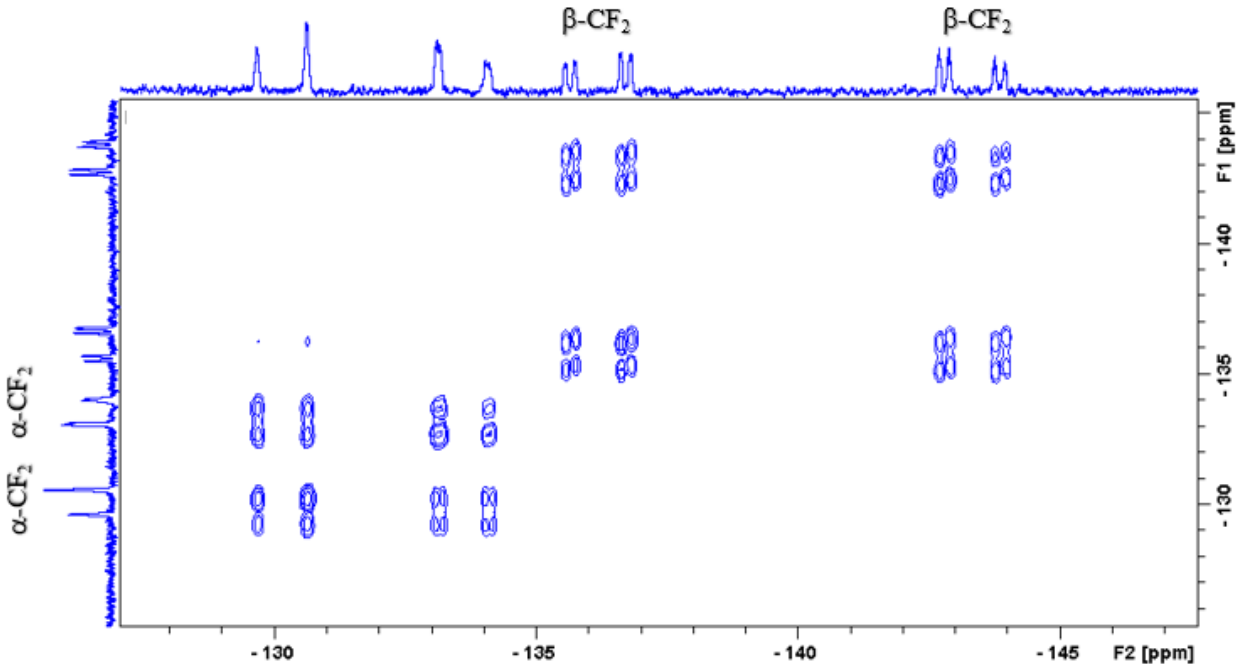

Figure A.11. ^{19}F-^{19}F COSY NMR (282 MHz, C_6D_6) spectrum of O[-$(CH_2)_3CH(CF_2CF_2H)$-], **3-9.**

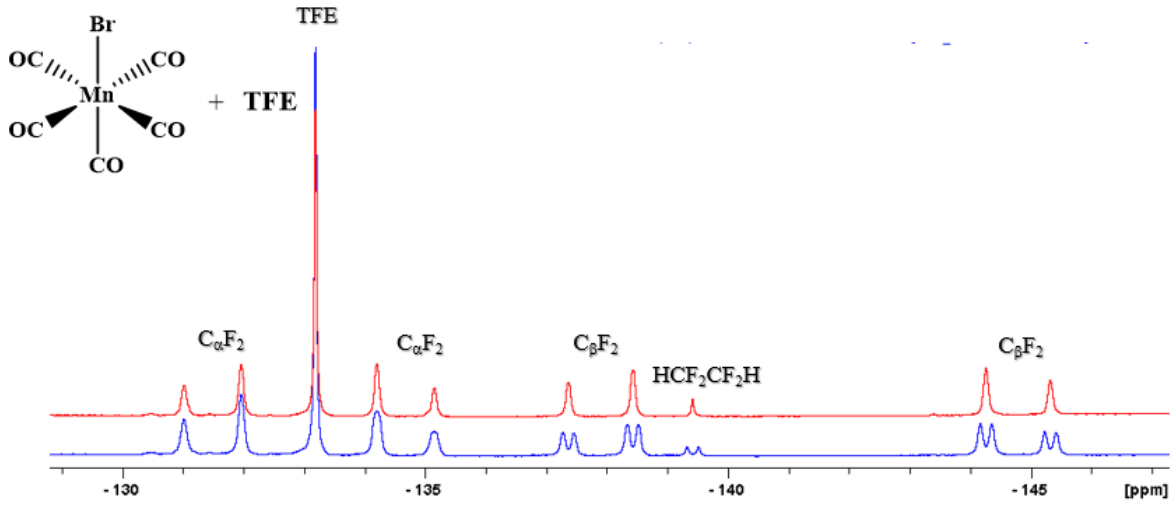

Figure A.12. ^{19}F and $^{19}F\{^1H\}$ NMR (282 MHz, THF) spectra of $MnBr(CO)_5$, **3-1** + TFE reaction after 24 h (top: $^{19}F\{^1H\}$; bottom: ^{19}F).

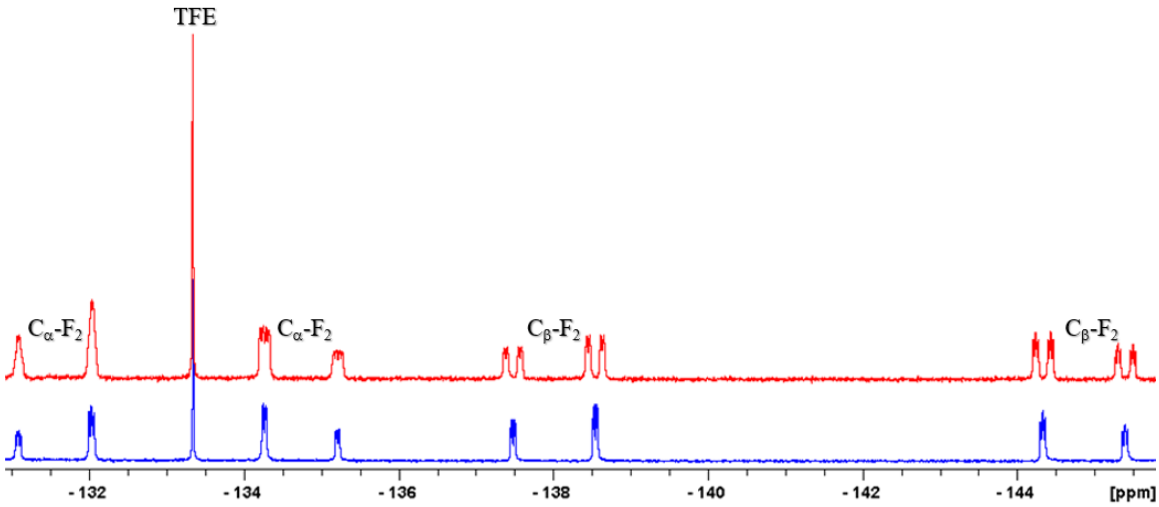

Figure A.13. ^{19}F and $^{19}F\{^1H\}$ NMR spectra of O[-$(CH_2)_3CH(CF_2CF_2H)$-], **3-9** derived from photolysis of $MnBr(triphos)(CO)_2$ (**3-4**) and TFE after 5 d (blue = proton decoupled).

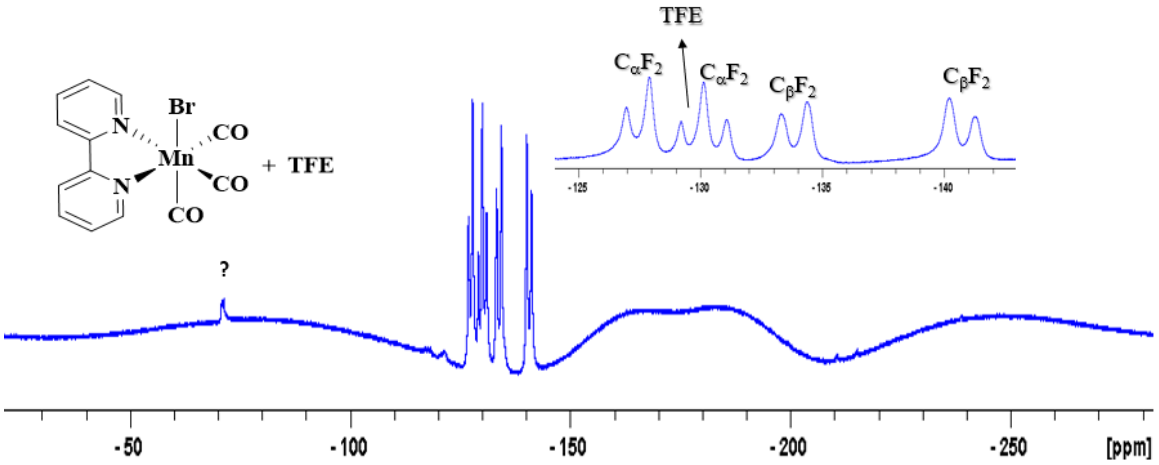

Figure A.14. ^{19}F NMR (282 MHz, THF) spectrum of reaction of $MnBr(Bipy)(CO)_3$, **3-5**, with TFE.

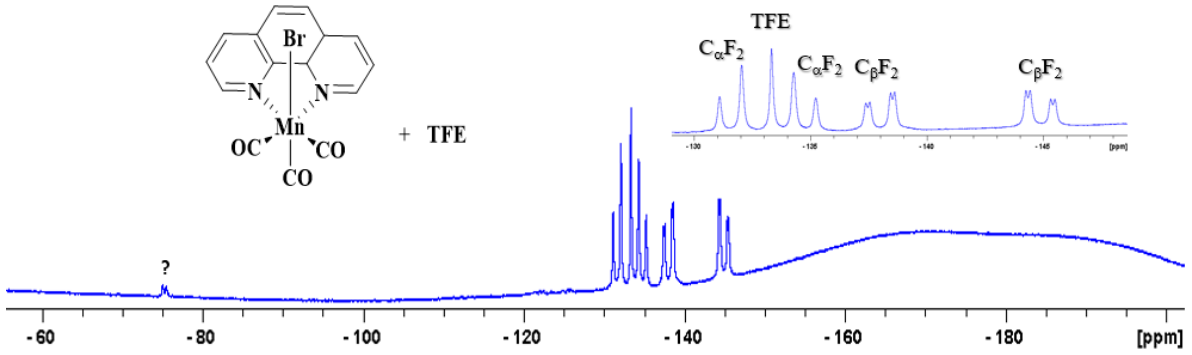

Figure A.15. ^{19}F NMR (282 MHz, THF) spectrum of reaction of $MnBr(Phen)(CO)_3$, **3-6**, with TFE.

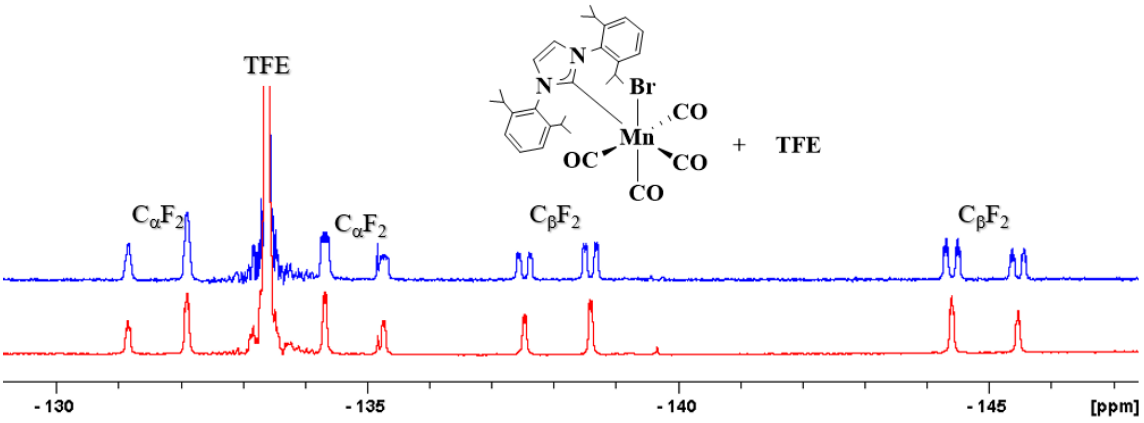

Figure A.16. ^{19}F NMR (282 MHz, THF) spectra of the reaction $MnBr(IPr)(CO)_4$, **3-7**, with TFE (top: $^{19}F\{^1H\}$; bottom: ^{19}F).

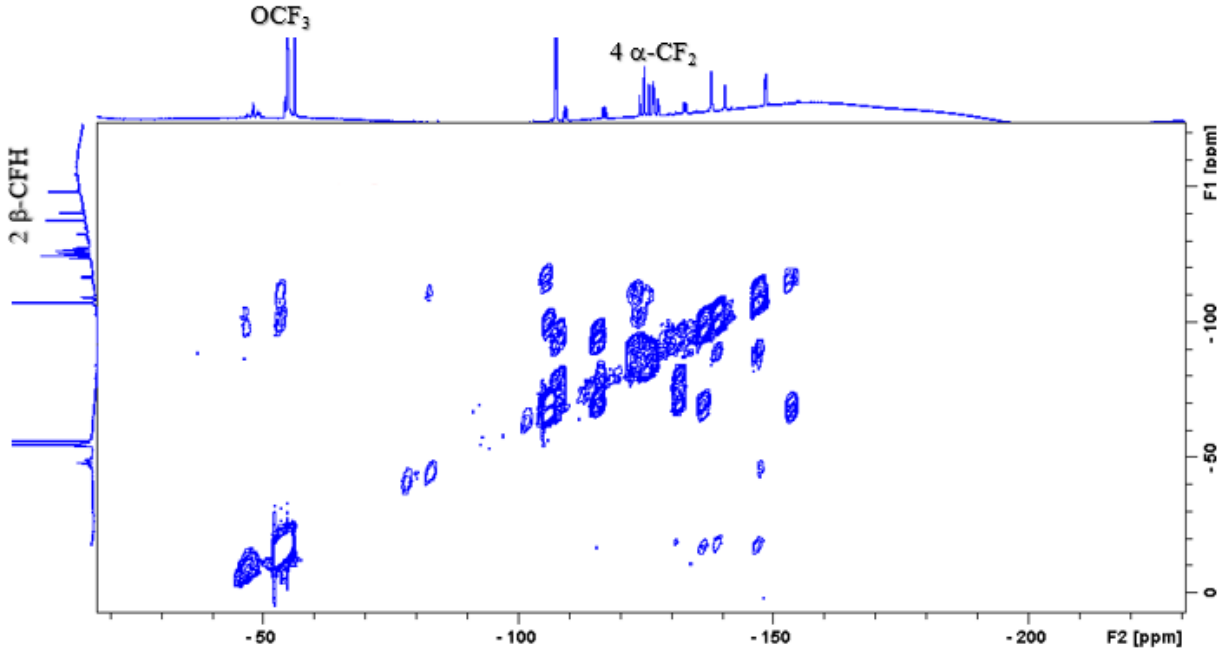

Figure A.17. ^{19}F-^{19}F COSY NMR (282 MHz, THF) spectrum of diastereomers $O\{-(CH_2)_3CH[CF_2CFH(OCF_3)]-\}$, **3-11** and **3-12.**

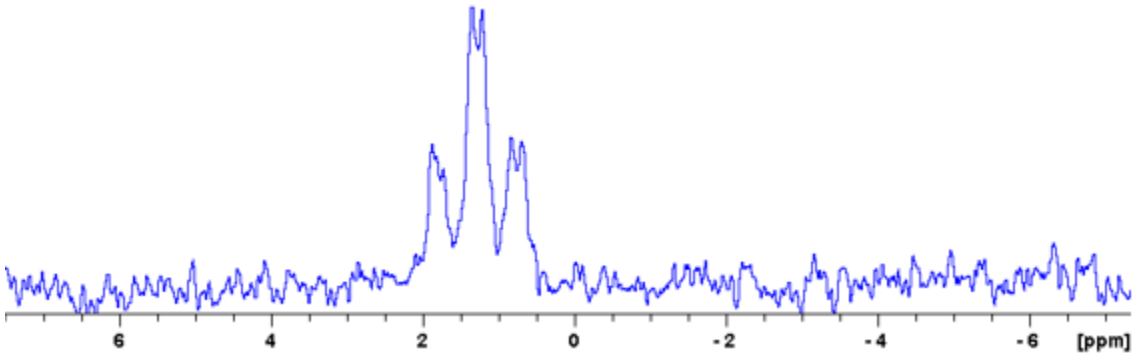

Figure A.18. $^{31}P\{^{1}H\}$ NMR (121 MHz, THF) spectrum of $Mn[CF_2CHF(OCF_3)](dppe)(CO)_3$, **3-13.**

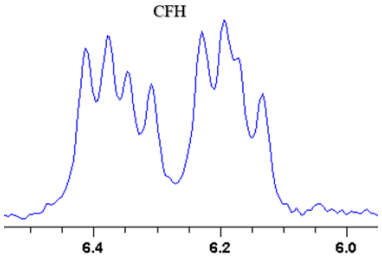

Figure A.19. ^{1}H NMR (300 MHz, C_6D_6) spectrum of $Mn[CF_2CFH(OCF_3)](dppe)(CO)_3$, **3-13.**

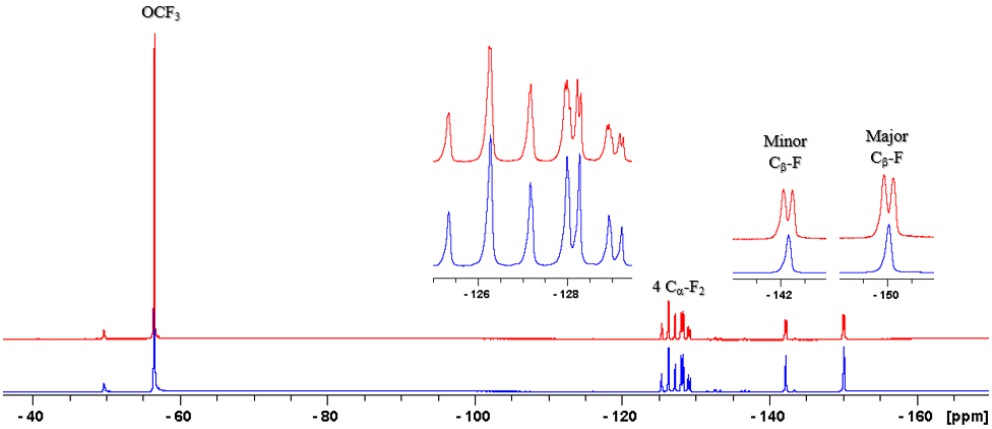

Figure A.20. ^{19}F NMR (282 MHz, THF) spectra of $MnBr(Bipy)(CO)_3$, **3-5** + PMVE reaction after 2 d (top: ^{19}F; bottom: $^{19}F\{^{1}H\}$).

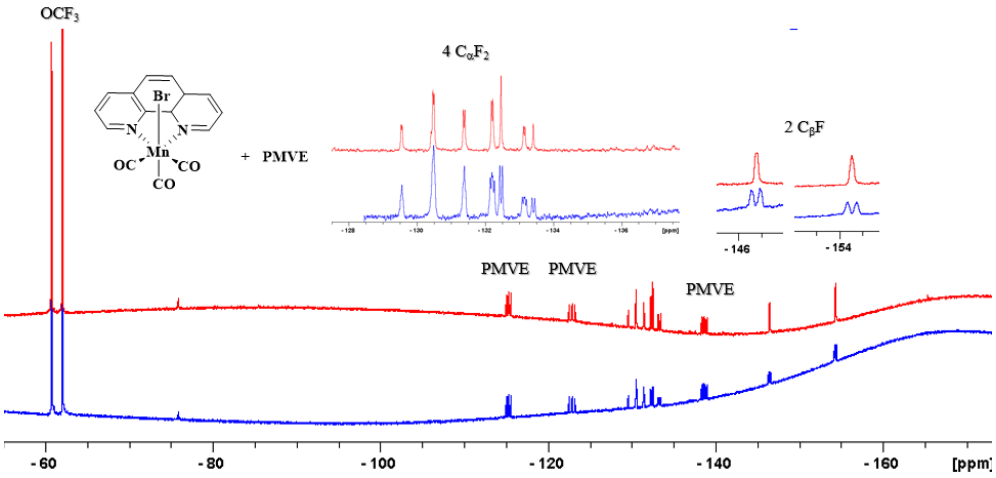

Figure A.21. ^{19}F NMR (282 MHz, THF) spectra of MnBr(Phen)$(CO)_3$, **3-6** + PMVE reaction after 2 d (top: $^{19}F\{^1H\}$; bottom: ^{19}F).

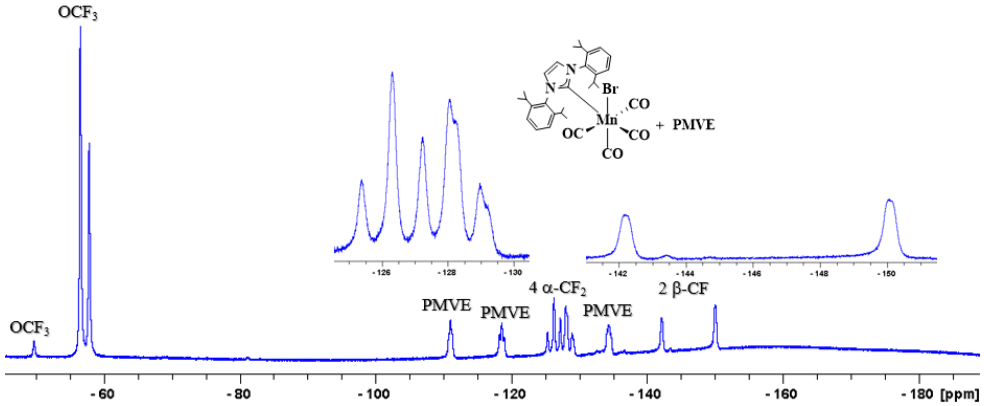

Figure A.22. ^{19}F NMR (282 MHz, THF) spectrum of MnBr(IPr)$(CO)_4$, **3-7** + PMVE reaction after 2 d.

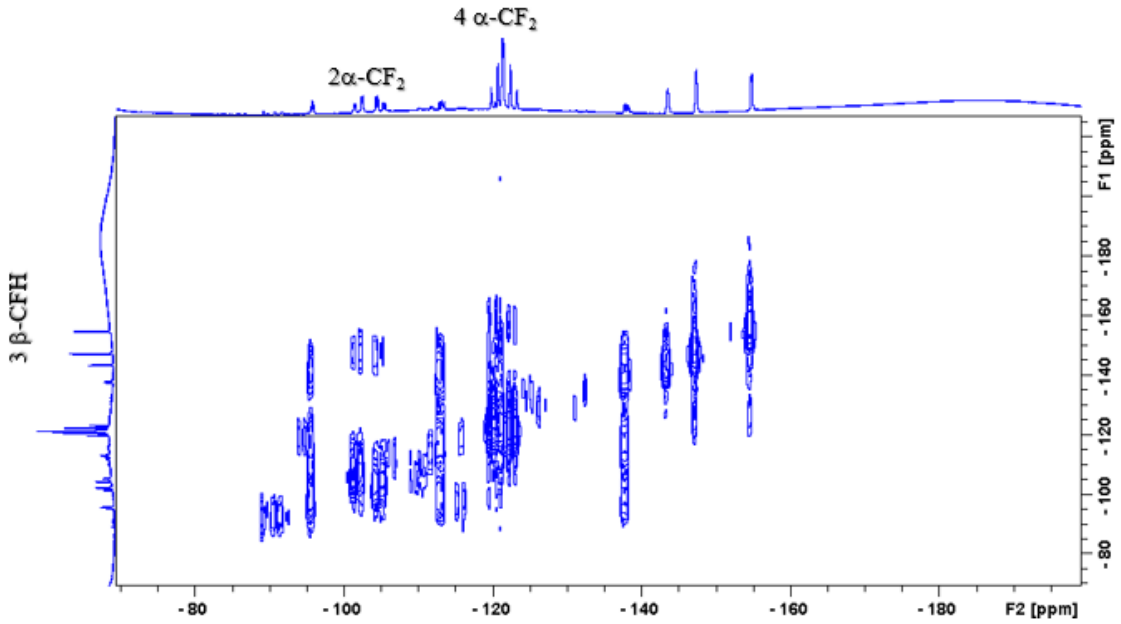

Figure A.23. ^{19}F-^{19}F COSY NMR (282 MHz, THF) spectrum of diastereomers O[-$(CH_2)_3CH(CF_2CFHCl)$-], **3-14** and **3-15.**

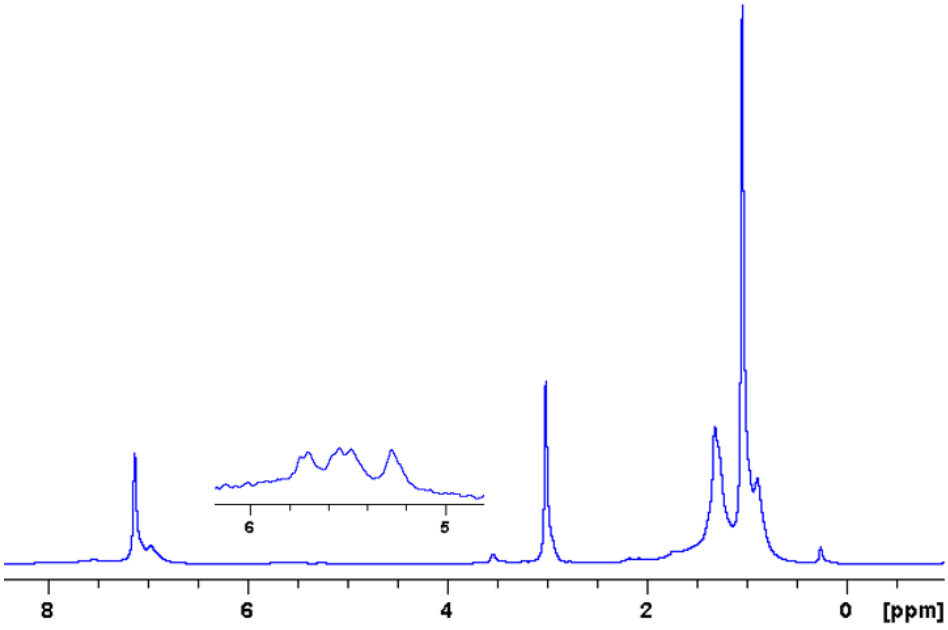

Figure A.24. ^{1}H NMR (300 MHz, THF) spectrum of $Mn[CF_2CHFCl](DPPE)(CO)_3$, **3-16.**

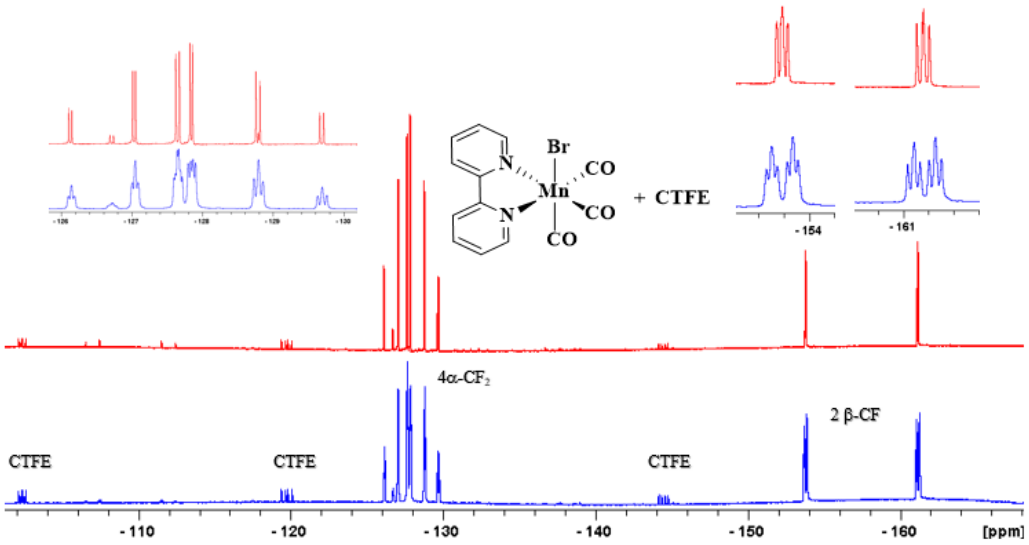

Figure A.25. ^{19}F NMR (282 MHz, THF) spectra of MnBr(Bipy)$(CO)_3$, **3-5** + CTFE reaction after 2 d (top: $^{19}F\{^1H\}$; bottom: ^{19}F).

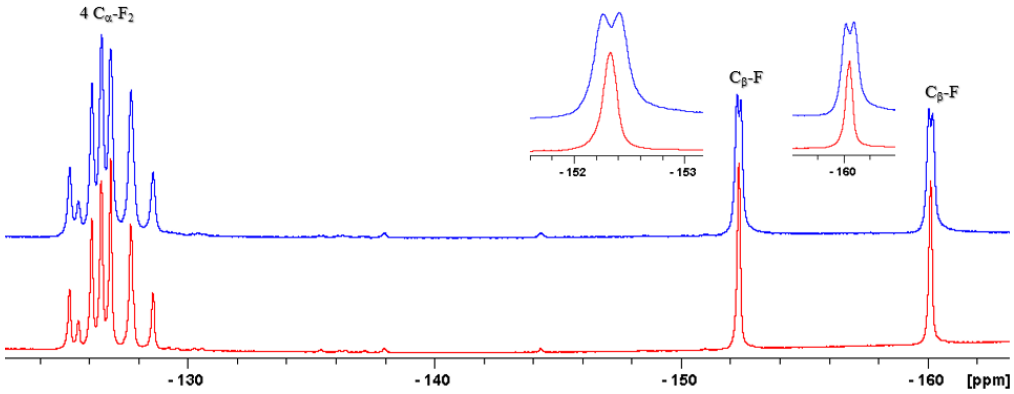

Figure A.26. ^{19}F NMR (282 MHz, THF) spectra of MnBr(Phen)$(CO)_3$, **3-6** + CTFE reaction after 2 d (top: ^{19}F; bottom: $^{19}F\{^1H\}$).

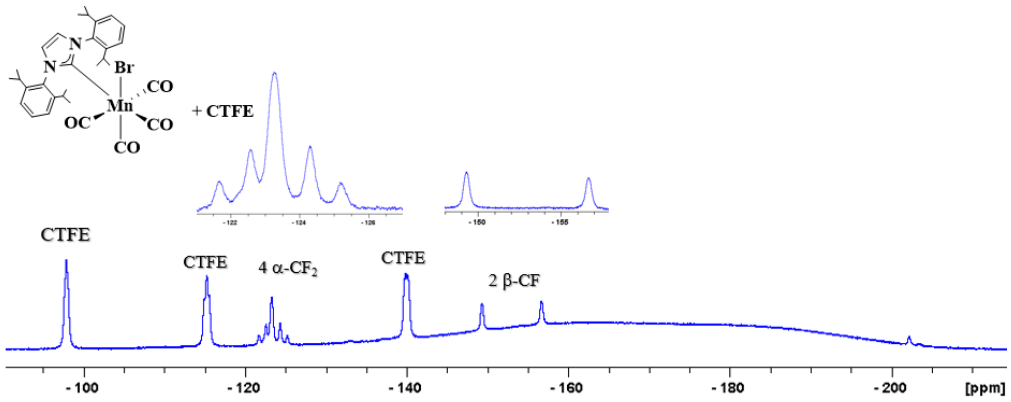

Figure A.27. ^{19}F NMR (282 MHz, THF) spectrum of MnBr(IPr)$(CO)_4$, **3-7** + CTFE reaction after 2 d.

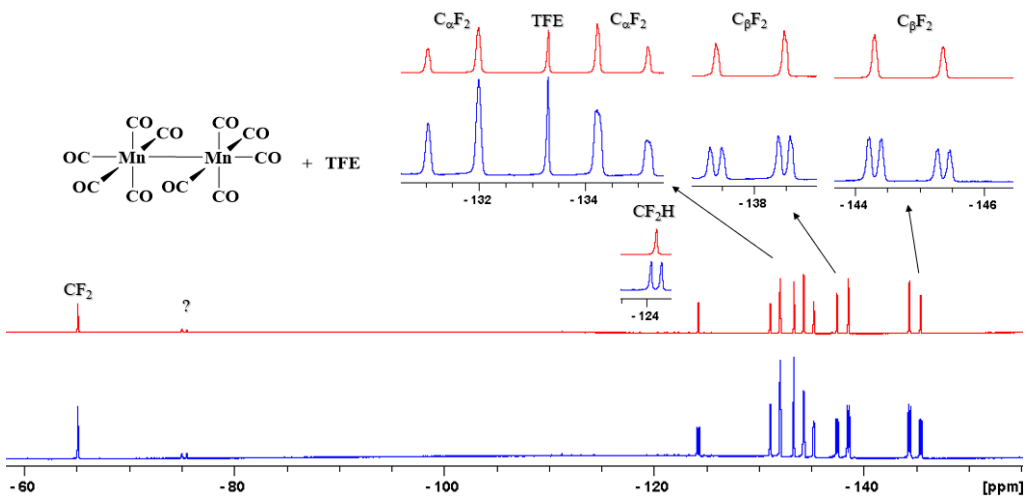

Figure A.28. ^{19}F NMR (282 MHz, THF) spectra after heating $Mn_2(CO)_{10}$ + TFE at 65 °C in THF for 3 d (top: $^{19}F\{^1H\}$; bottom: ^{19}F).

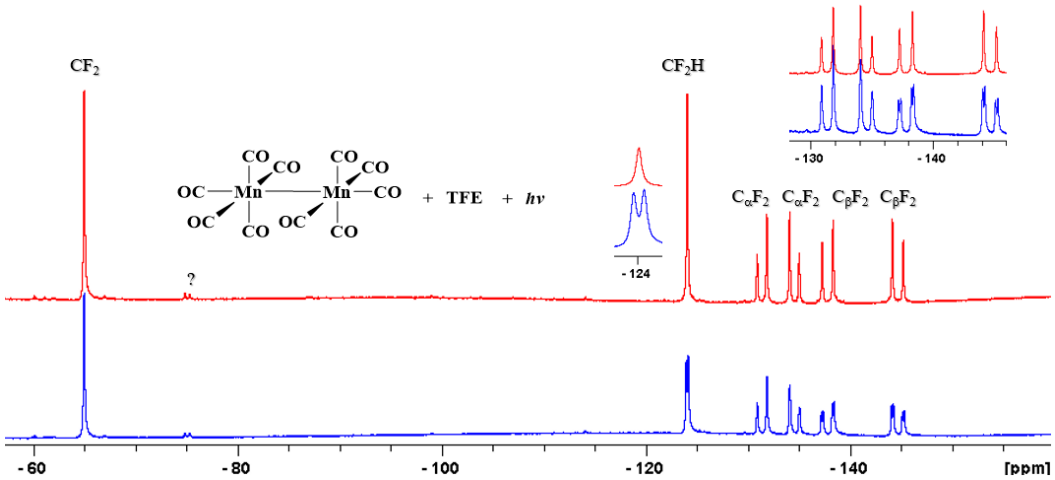

Figure A.29. ^{19}F NMR (282 MHz, THF) spectra after photolysis of $Mn_2(CO)_{10}$ + TFE in THF for 3 d (top: $^{19}F\{^1H\}$; bottom: ^{19}F).

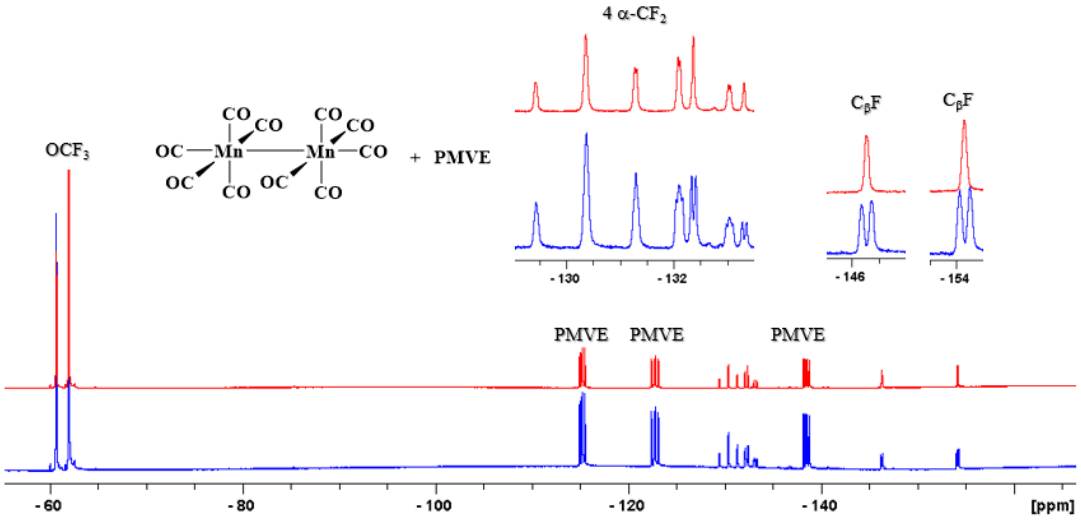

Figure A.30. ^{19}F NMR (282 MHz, THF) spectra after heating $Mn_2(CO)_{10}$ + PMVE at 65 °C in THF for 3 d (top: $^{19}F\{^1H\}$; bottom: ^{19}F).

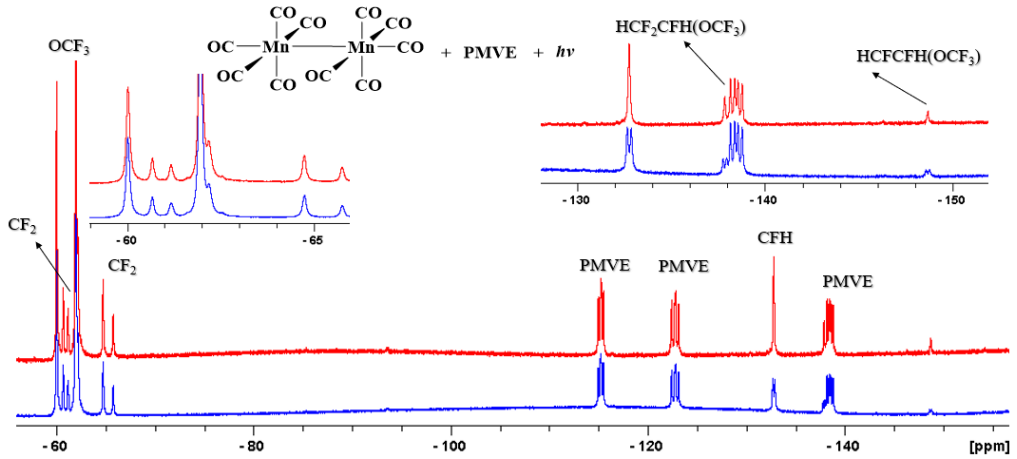

Figure A.31. ^{19}F NMR (282 MHz, THF) spectra after photolysis of $Mn_2(CO)_{10}$ + PMVE in THF for 3 d (top: $^{19}F\{^1H\}$; bottom: ^{19}F).

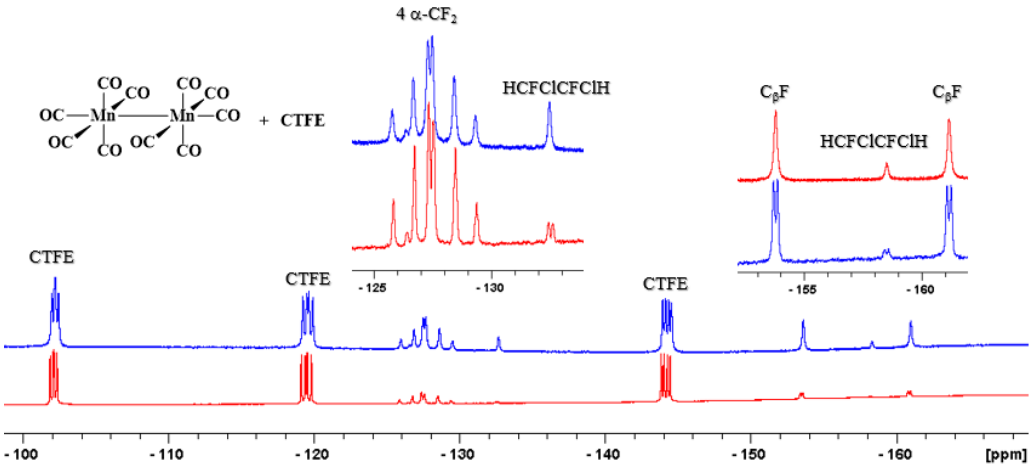

Figure A.32. ^{19}F NMR (282 MHz, THF) spectra after heating $Mn_2(CO)_{10}$ + CTFE at 65 °C in THF for 3 d (top: $^{19}F\{^1H\}$; bottom: ^{19}F).

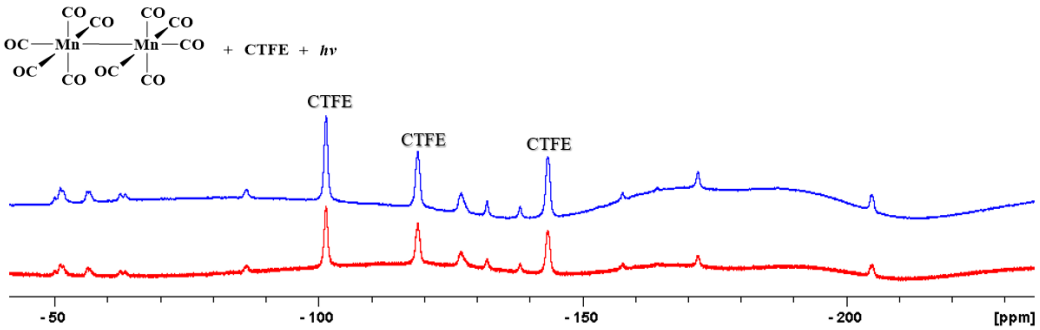

Figure A.33. ^{19}F NMR (282 MHz, THF) spectra after photolysis of $Mn_2(CO)_{10}$ + CTFE in THF for 3 d (top: $^{19}F\{^1H\}$; bottom: ^{19}F).

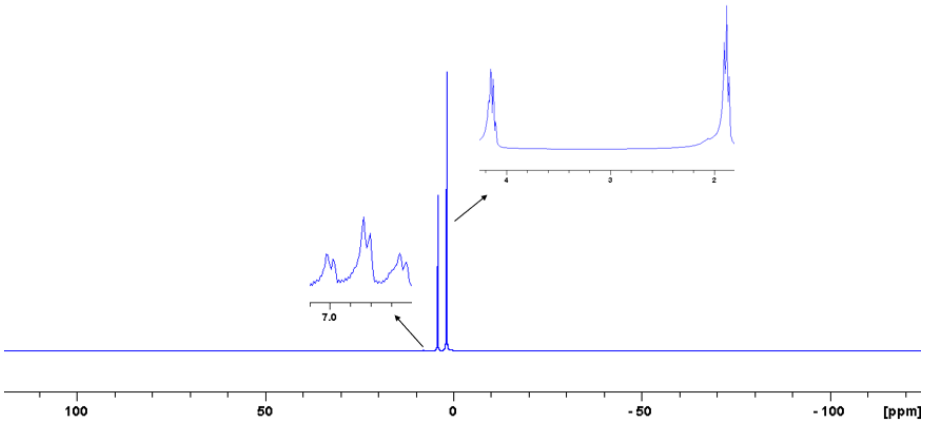

Figure A.34. ^1H NMR (300 MHz, Et_2O) spectrum of reaction of $MnBr(DPPE)_2(CO)$, **3-3** with TFE in diethyl ether.

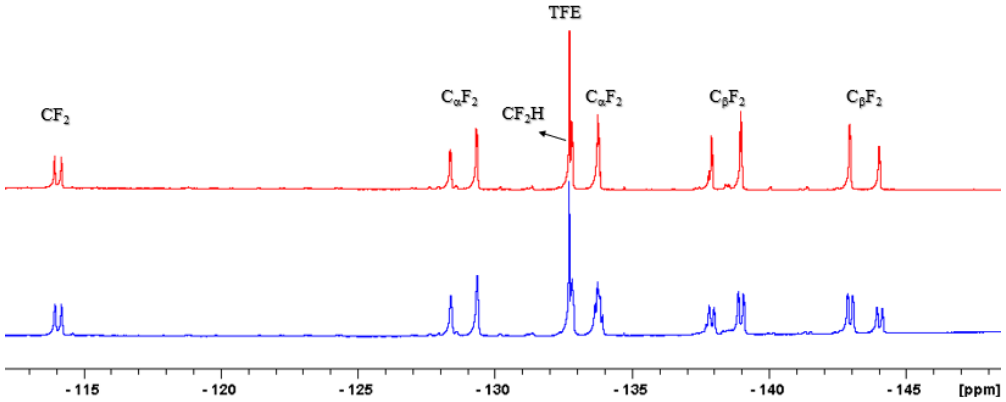

Figure A.35. ^{19}F and $^{19}F\{^{1}H\}$ NMR (282 MHz, Et_2O) spectrum of reaction of $MnBr(DPPE)_2(CO)$, **3-3** with TFE in diethyl ether after 1 d (top: $^{19}F\{^{1}H\}$; bottom: ^{19}F).

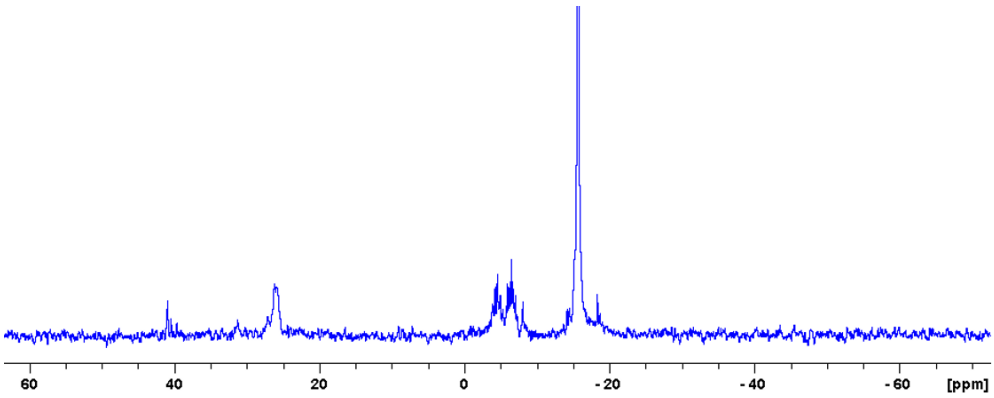

Figure A.36. $^{31}P\{^{1}H\}$ NMR spectrum (121 MHz, C_6D_6) of $Mn(CF_2CF_2H)(DPPE)(CO)_3$ (**3-8**) and possibly $MnBr[-CF_2)_4-](DPPE)(CO)$ (**3-20**).

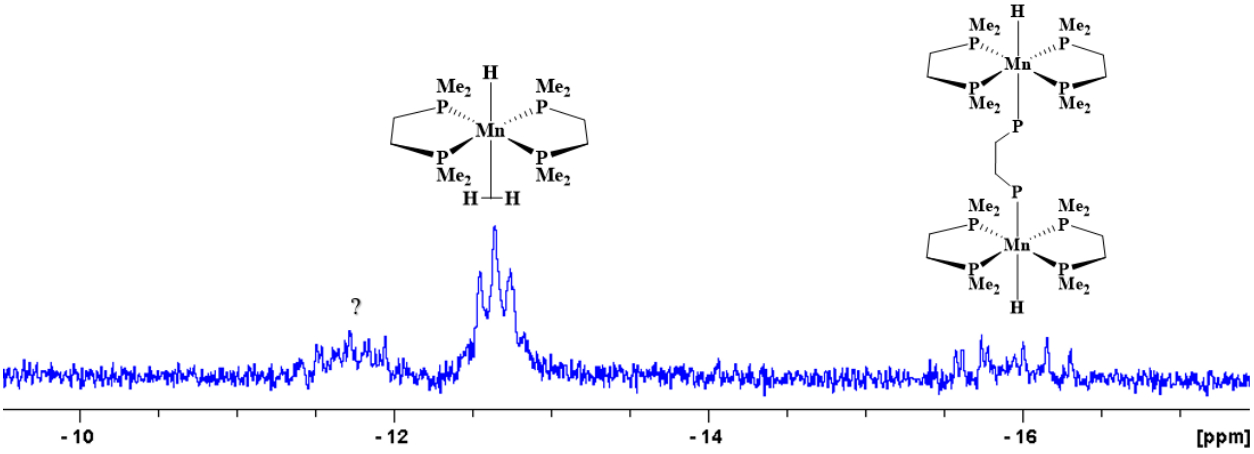

Figure A.37. Portion of ^{1}H NMR (300 MHz, C_6D_6) spectrum of $MnH(H_2)(dmpe)_2$, **4-5.**

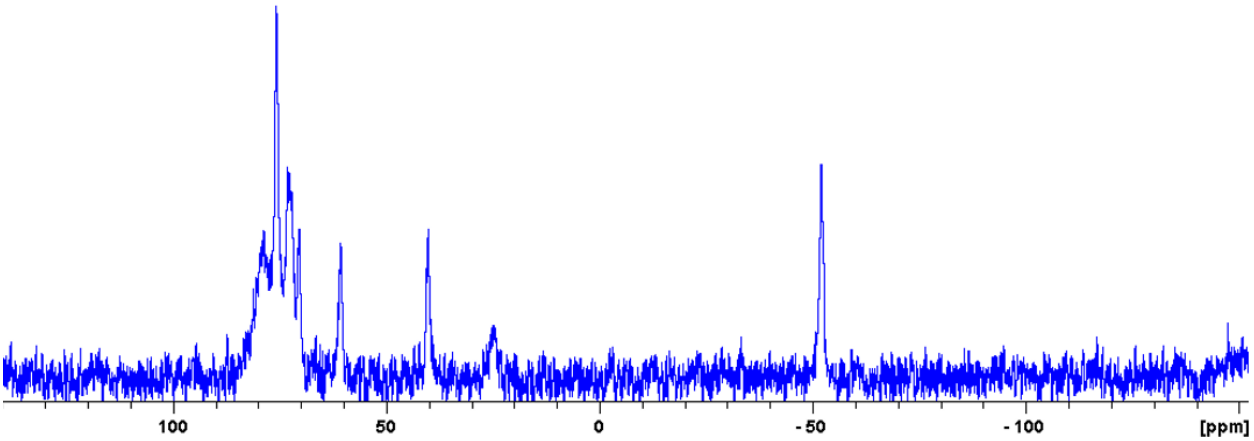

Figure A.38. $^{31}P\{^{1}H\}$ NMR (121 MHz, C_6D_6) spectrum of $MnH(H_2)(dmpe)_2$, **4-5.**

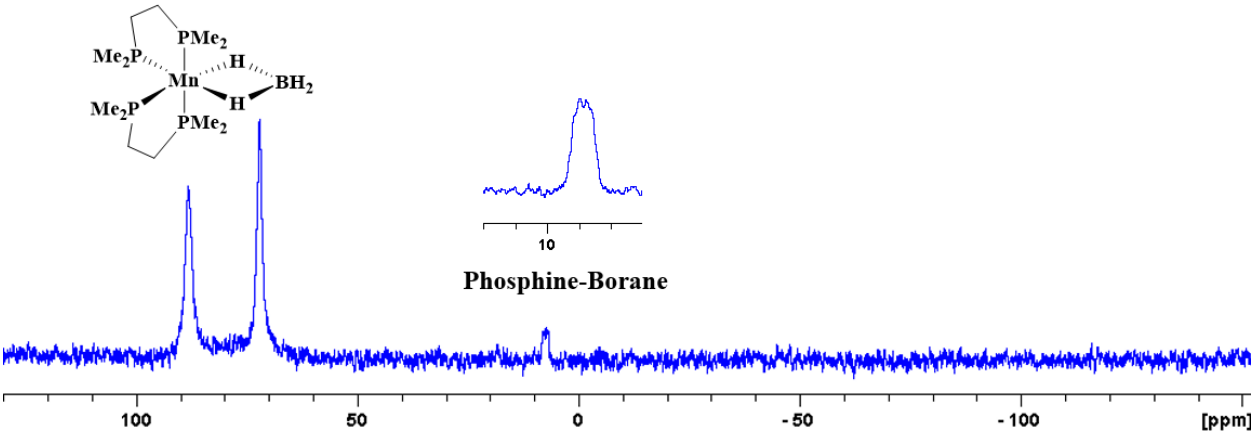

Figure A.39. $^{31}P\{^{1}H\}$ NMR (121 MHz, C_6D_6) spectrum after AB dehydrogenation catalyzed by $MnH(H_2)(dmpe)_2$, **4-5**; generation of $Mn(BH_4)(dmpe)_2$, **4-6.**

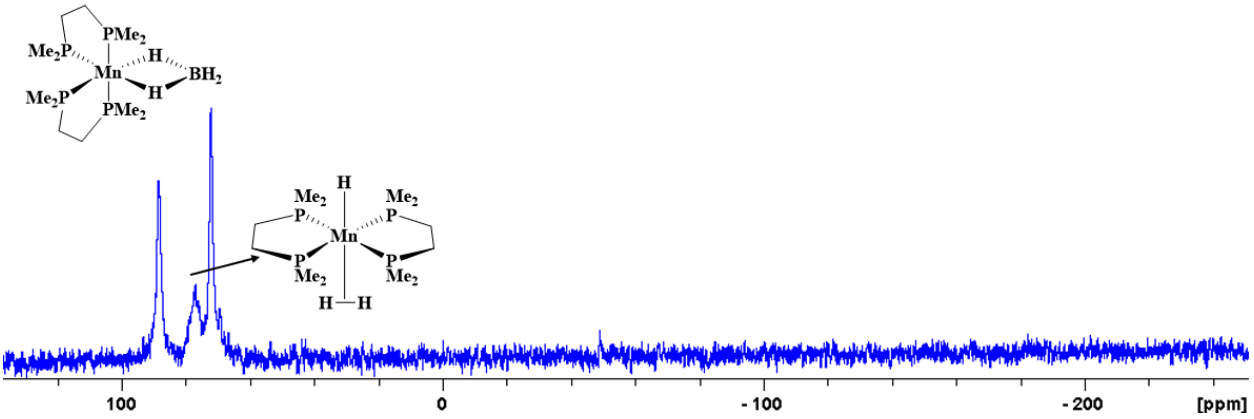

Figure A.40. $^{31}P\{^{1}H\}$ NMR (121 MHz, C_6D_6) spectrum after MeAB dehydrogenation catalyzed by $MnH(H_2)(dmpe)_2$, **4-5.**

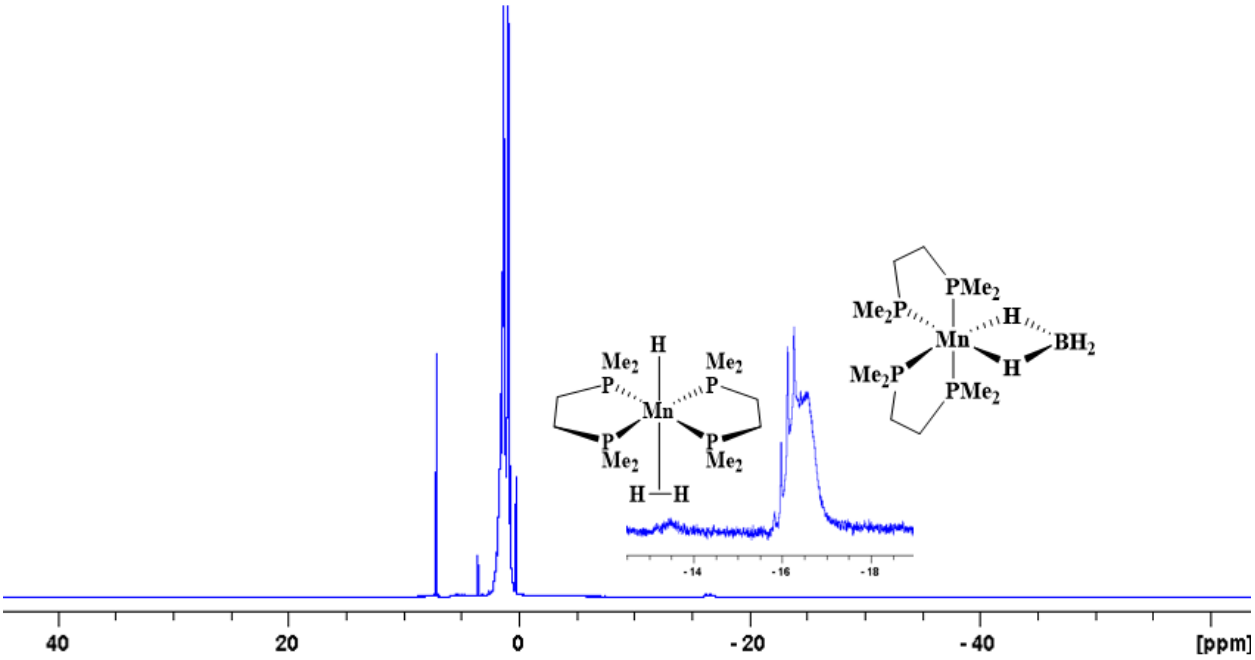

Figure A.41. ^{1}H NMR (300 MHz, C_6D_6) spectrum after MeAB dehydrogenation catalyzed by $MnH(H_2)(dmpe)_2$, **4-5.**

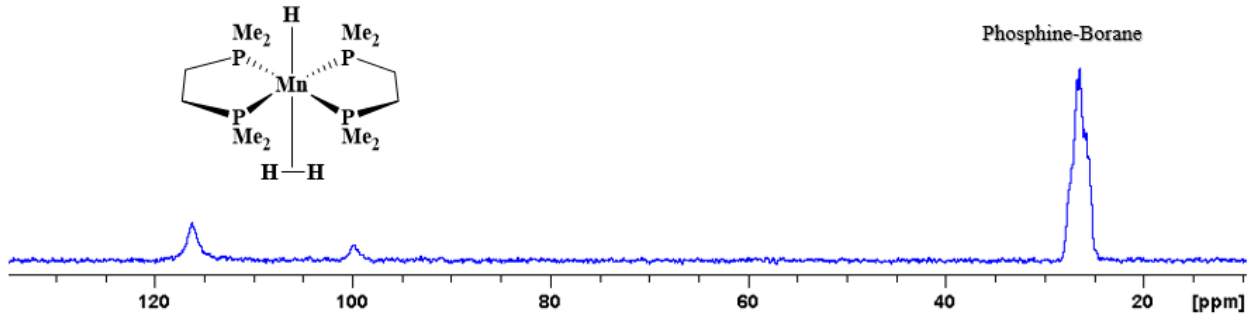

Figure A.42. $^{31}P\{^{1}H\}$ NMR (121 MHz, C_6D_6) spectrum after DMAB dehydrogenation catalyzed by $MnH(H_2)(dmpe)_2$, **4-5.**

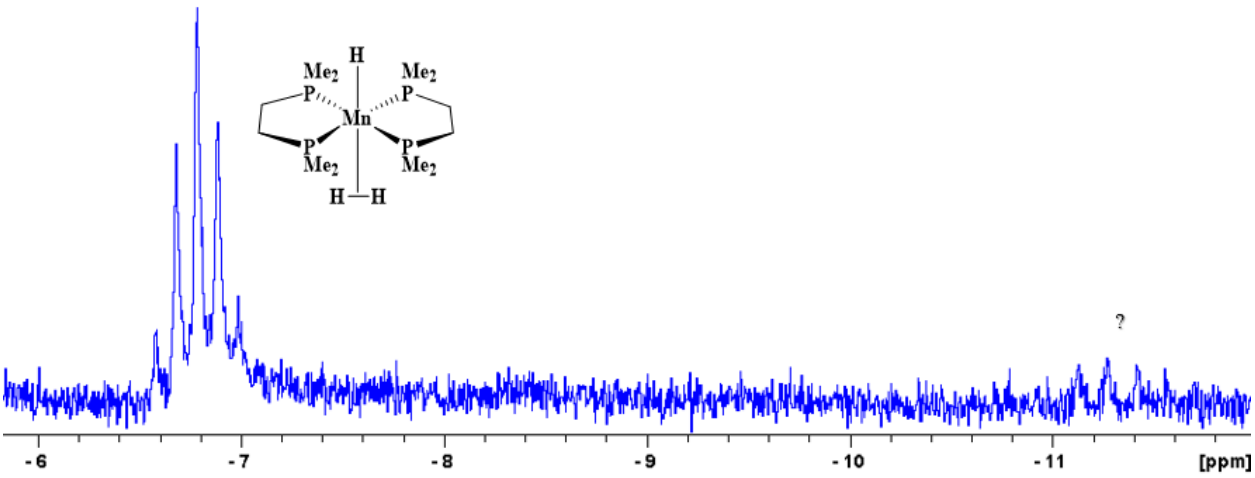

Figure A.43. Portion of ^{1}H NMR (300 MHz, C_6D_6) spectrum safter DMAB dehydrogenation catalyzed by $MnH(H_2)(dmpe)_2$, **4-5.**

Figure Permissions

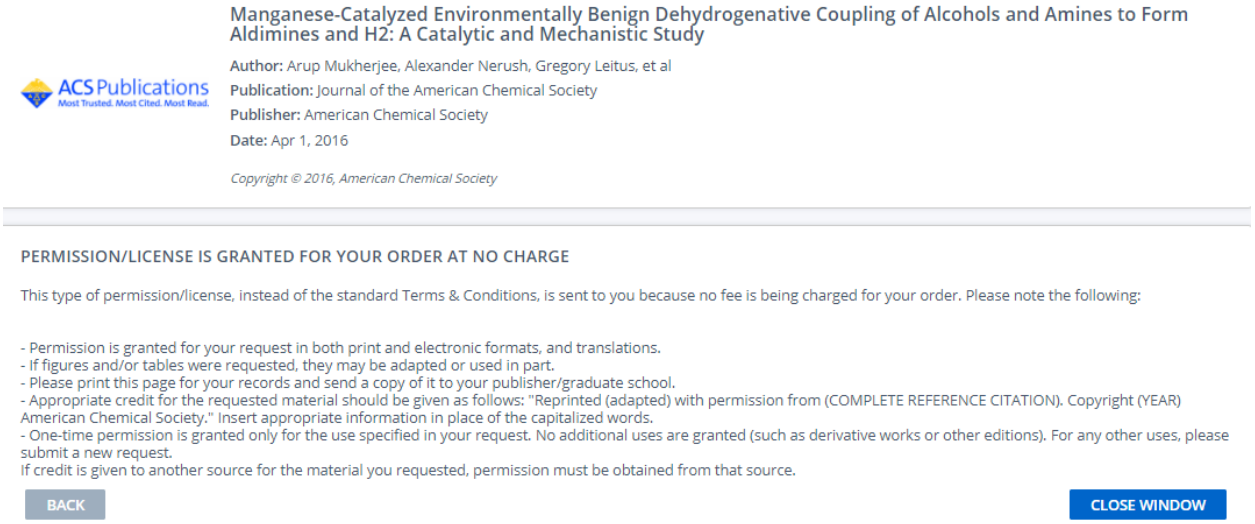

Manganese-Catalyzed Environmentally Benign Dehydrogenative Coupling of Alcohols and Amines to Form Aldimines and H2: A Catalytic and Mechanistic Study

Author: Arup Mukherjee, Alexander Nerush, Gregory Leitus, et al
Publication: Journal of the American Chemical Society
Publisher: American Chemical Society
Date: Apr 1, 2016

Copyright © 2016, American Chemical Society

PERMISSION/LICENSE IS GRANTED FOR YOUR ORDER AT NO CHARGE

This type of permission/license, instead of the standard Terms & Conditions, is sent to you because no fee is being charged for your order. Please note the following:

- Permission is granted for your request in both print and electronic formats, and translations.
- If figures and/or tables were requested, they may be adapted or used in part.
- Please print this page for your records and send a copy of it to your publisher/graduate school.
- Appropriate credit for the requested material should be given as follows: "Reprinted (adapted) with permission from (COMPLETE REFERENCE CITATION). Copyright (YEAR) American Chemical Society." Insert appropriate information in place of the capitalized words.
- One-time permission is granted only for the use specified in your request. No additional uses are granted (such as derivative works or other editions). For any other uses, please submit a new request.

If credit is given to another source for the material you requested, permission must be obtained from that source.

BACK CLOSE WINDOW

Figure P.1. Scheme **1.1** catalytic synthesis of imines by dehydrogenative coupling (**1-1**).

This Agreement between University of Ottawa -- Bakr Barnawi ("You") and John Wiley and Sons ("John Wiley and Sons") consists of your license details and the terms and conditions provided by John Wiley and Sons and Copyright Clearance Center.

License Number	5074310462785
License date	May 22, 2021
Licensed Content Publisher	John Wiley and Sons
Licensed Content Publication	Chemistry - A European Journal
Licensed Content Title	Divergent Coupling of Alcohols and Amines Catalyzed by Isoelectronic Hydride MnI and FeII PNP Pincer Complexes
Licensed Content Author	Matthias Mastalir, Mathias Glatz, Nikolaus Gorgas, et al
Licensed Content Date	Jul 27, 2016
Licensed Content Volume	22

Figure P.2. Scheme **1.1** catalytic synthesis of imines by dehydrogenative coupling (**1-2**).

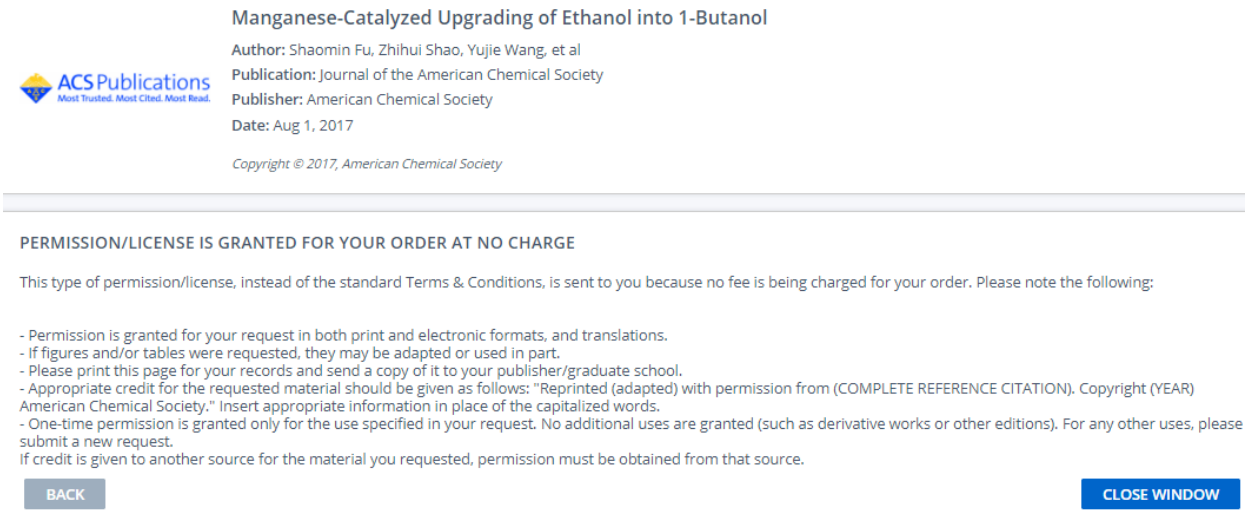

Figure P.3. Scheme **1.2** manganese-catalyzed Guerbet reaction (**1-3**).

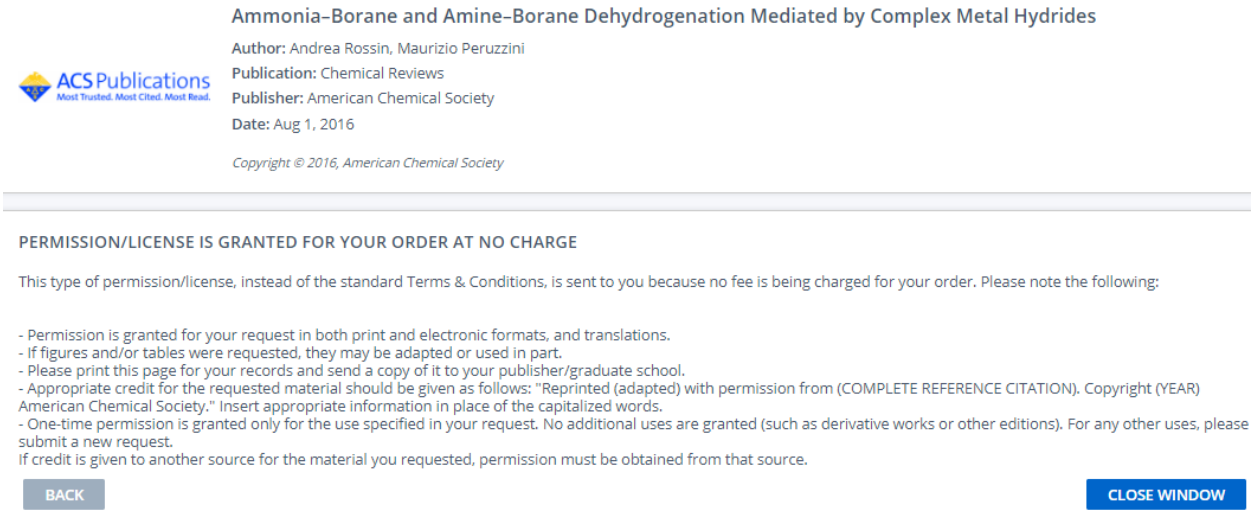

Figure P.4. Scheme **1.3** general scheme for AB dehydrogenation using **Type I** (**A**) or **Type II** catalysts (**B**).

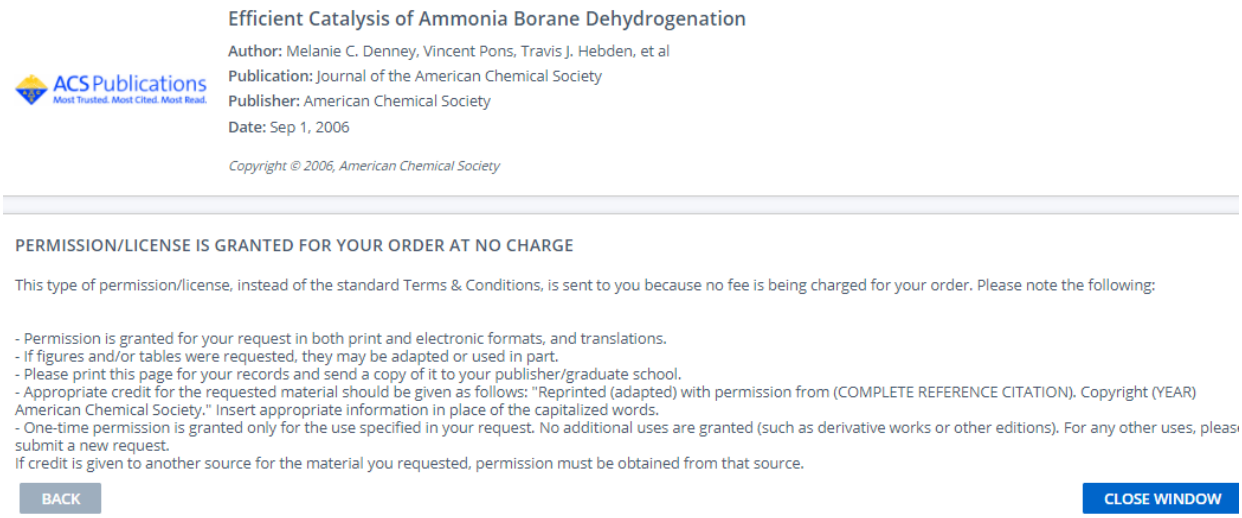

Figure P.5. Figure **1.1** typical **type I** (**1-4**) AB dehydrogenation catalysts.

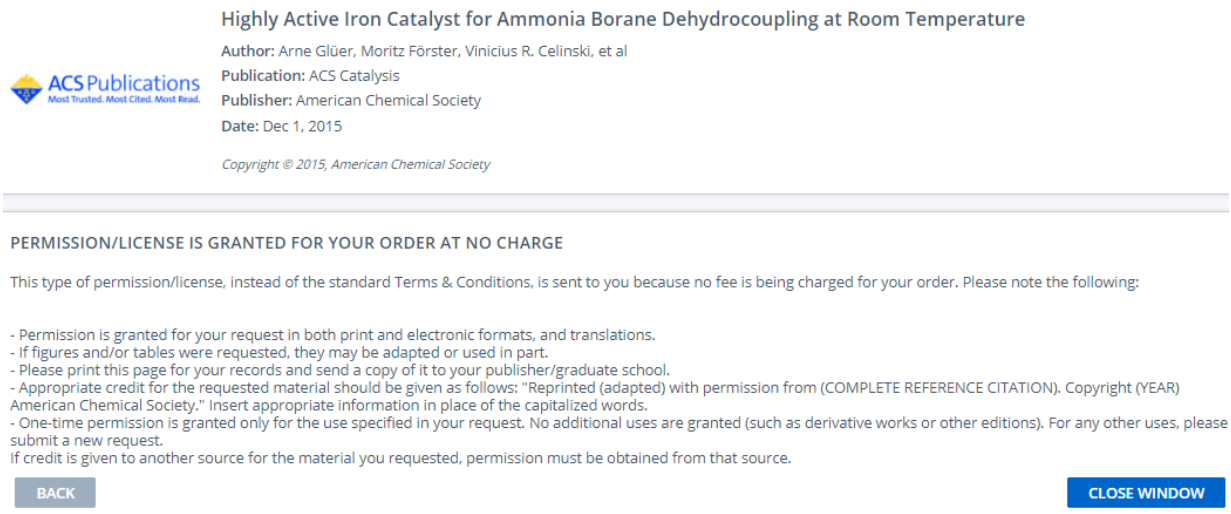

Figure P.6. Figure **1.1** typical **type I** (**1-5**) AB dehydrogenation catalysts.

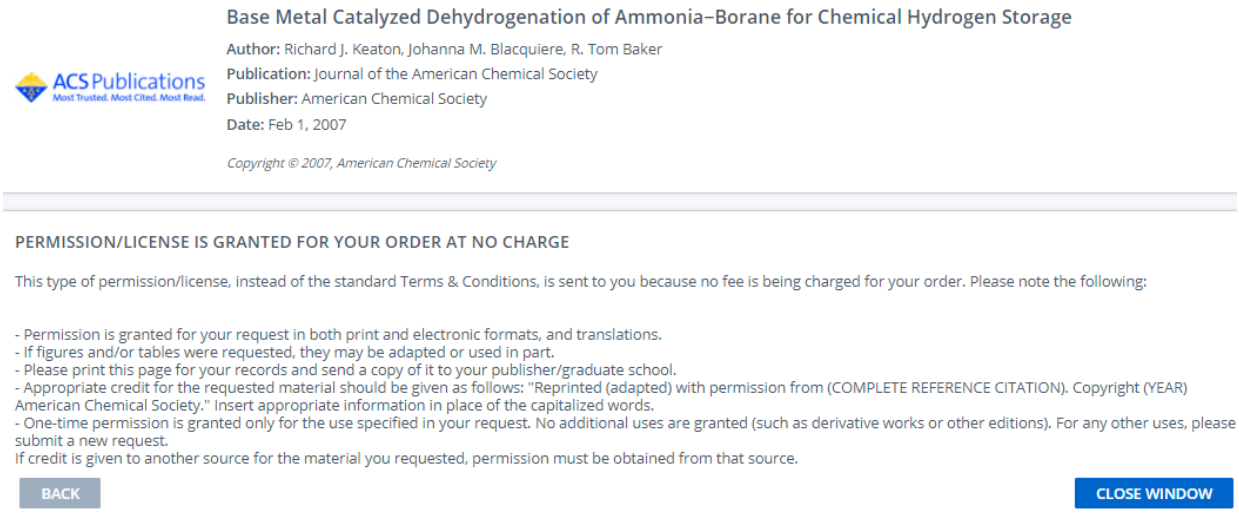

Figure P.7. Figure **1.1** typical **type II** (**1-6**) AB dehydrogenation catalysts.

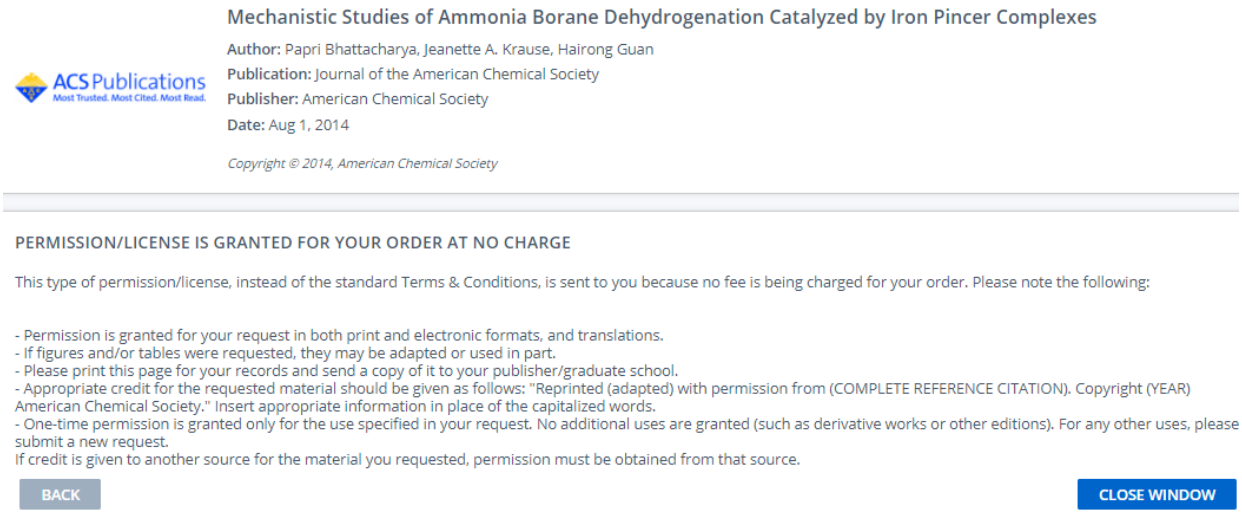

Figure P.8. Figure **1.1** typical **type II** (**1-7**) AB dehydrogenation catalysts.

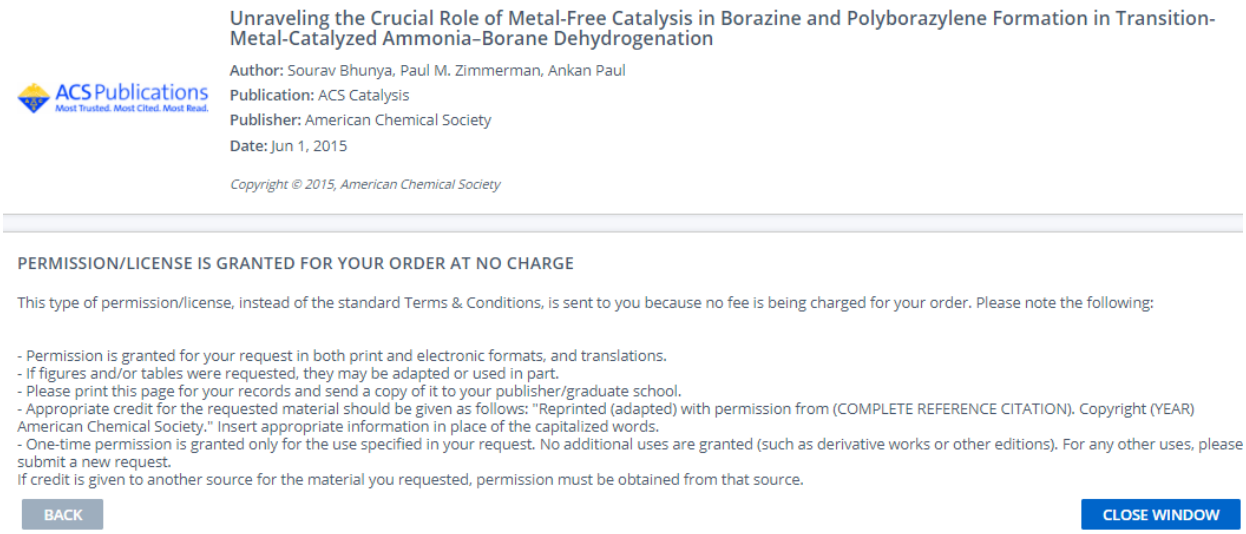

Unraveling the Crucial Role of Metal-Free Catalysis in Borazine and Polyborazylene Formation in Transition-Metal-Catalyzed Ammonia–Borane Dehydrogenation

Author: Sourav Bhunya, Paul M. Zimmerman, Ankan Paul
Publication: ACS Catalysis
Publisher: American Chemical Society
Date: Jun 1, 2015

Copyright © 2015, American Chemical Society

PERMISSION/LICENSE IS GRANTED FOR YOUR ORDER AT NO CHARGE

This type of permission/license, instead of the standard Terms & Conditions, is sent to you because no fee is being charged for your order. Please note the following:

- Permission is granted for your request in both print and electronic formats, and translations.
- If figures and/or tables were requested, they may be adapted or used in part.
- Please print this page for your records and send a copy of it to your publisher/graduate school.
- Appropriate credit for the requested material should be given as follows: "Reprinted (adapted) with permission from (COMPLETE REFERENCE CITATION). Copyright (YEAR) American Chemical Society." Insert appropriate information in place of the capitalized words.
- One-time permission is granted only for the use specified in your request. No additional uses are granted (such as derivative works or other editions). For any other uses, please submit a new request.

If credit is given to another source for the material you requested, permission must be obtained from that source.

BACK CLOSE WINDOW

Figure P.9. Scheme **1.4** proposed catalytic cycle for AB dehydrogenation using **type I** catalysts.

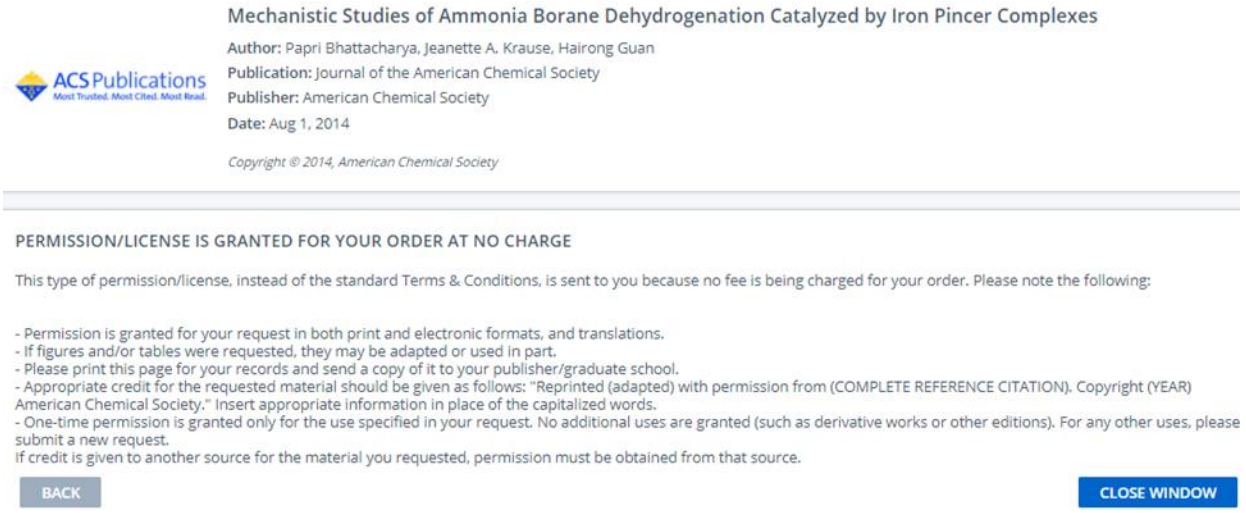

Mechanistic Studies of Ammonia Borane Dehydrogenation Catalyzed by Iron Pincer Complexes

Author: Papri Bhattacharya, Jeanette A. Krause, Hairong Guan
Publication: Journal of the American Chemical Society
Publisher: American Chemical Society
Date: Aug 1, 2014

Copyright © 2014, American Chemical Society

PERMISSION/LICENSE IS GRANTED FOR YOUR ORDER AT NO CHARGE

This type of permission/license, instead of the standard Terms & Conditions, is sent to you because no fee is being charged for your order. Please note the following:

- Permission is granted for your request in both print and electronic formats, and translations.
- If figures and/or tables were requested, they may be adapted or used in part.
- Please print this page for your records and send a copy of it to your publisher/graduate school.
- Appropriate credit for the requested material should be given as follows: "Reprinted (adapted) with permission from (COMPLETE REFERENCE CITATION). Copyright (YEAR) American Chemical Society." Insert appropriate information in place of the capitalized words.
- One-time permission is granted only for the use specified in your request. No additional uses are granted (such as derivative works or other editions). For any other uses, please submit a new request.

If credit is given to another source for the material you requested, permission must be obtained from that source.

BACK CLOSE WINDOW

Figure P.10. Scheme **1.5** proposed cycle for Fe-catalytic dehydrogenation of AB.

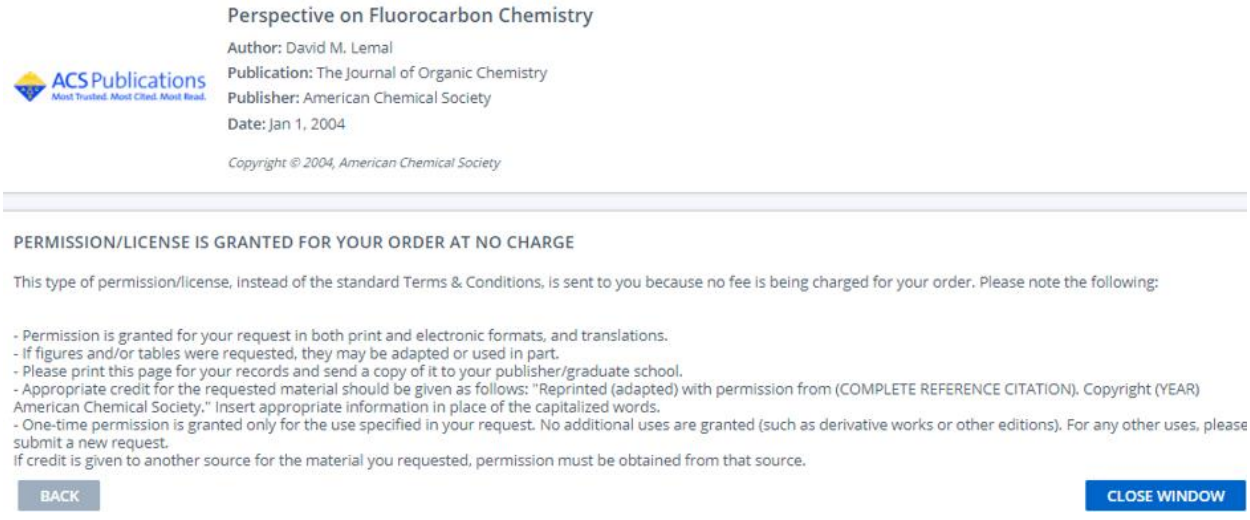

Perspective on Fluorocarbon Chemistry

Author: David M. Lemal
Publication: The Journal of Organic Chemistry
Publisher: American Chemical Society
Date: Jan 1, 2004

Copyright © 2004, American Chemical Society

PERMISSION/LICENSE IS GRANTED FOR YOUR ORDER AT NO CHARGE

This type of permission/license, instead of the standard Terms & Conditions, is sent to you because no fee is being charged for your order. Please note the following:

- Permission is granted for your request in both print and electronic formats, and translations.
- If figures and/or tables were requested, they may be adapted or used in part.
- Please print this page for your records and send a copy of it to your publisher/graduate school.
- Appropriate credit for the requested material should be given as follows: "Reprinted (adapted) with permission from (COMPLETE REFERENCE CITATION). Copyright (YEAR) American Chemical Society." Insert appropriate information in place of the capitalized words.
- One-time permission is granted only for the use specified in your request. No additional uses are granted (such as derivative works or other editions). For any other uses, please submit a new request.

If credit is given to another source for the material you requested, permission must be obtained from that source.

BACK CLOSE WINDOW

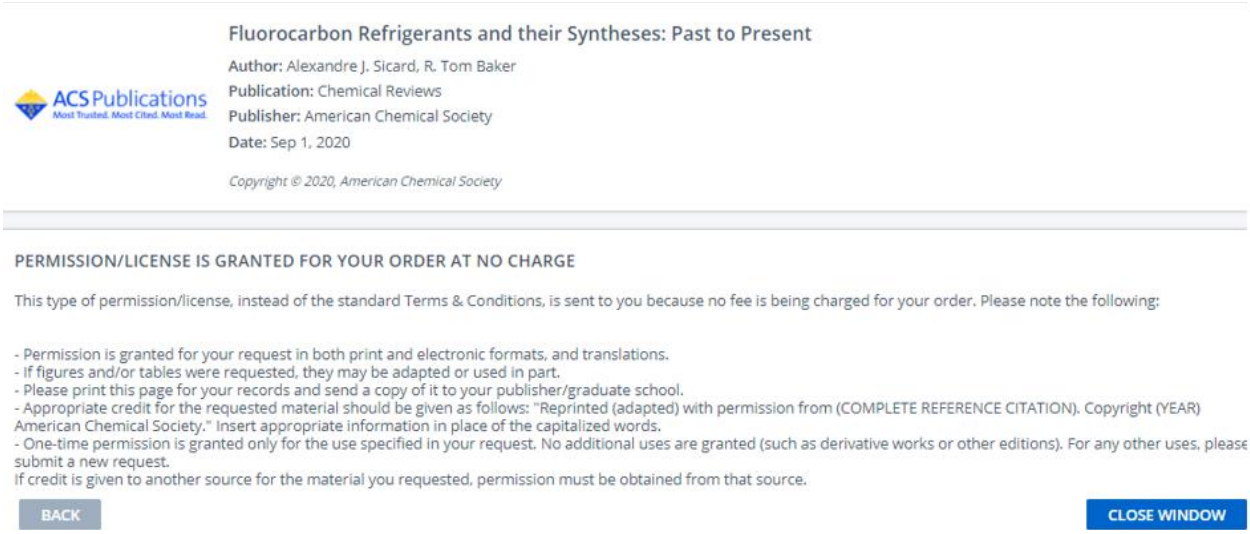

Figure P.11. Figure **1.2** selection of important CFCs, HCFCs, HFCs, HFOs and HCFOs.

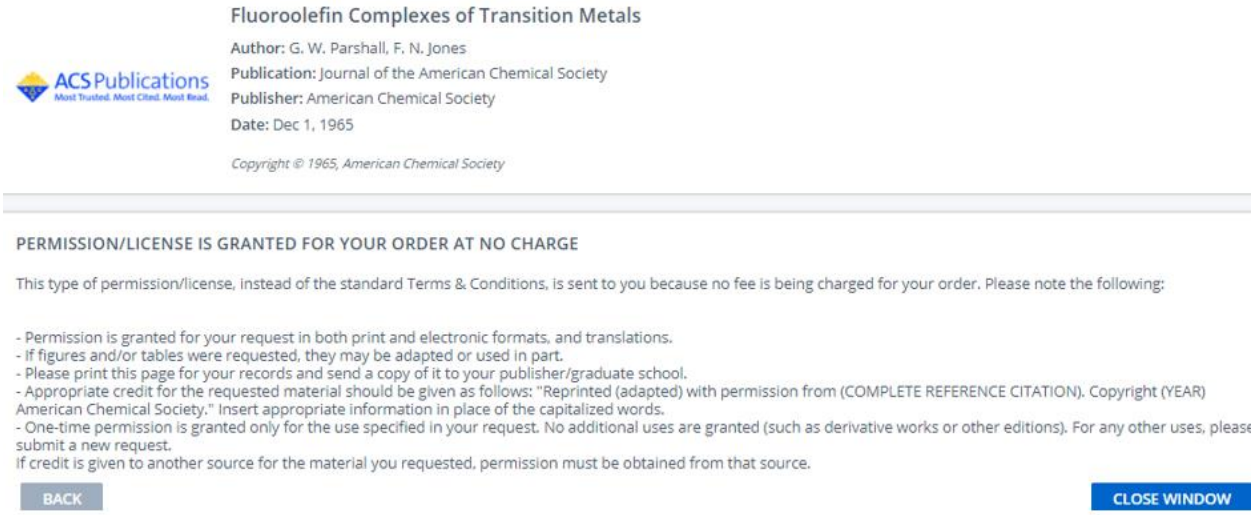

Figure P.12. Figure **1.3** example of important fluoroolefin complexes for Rh.

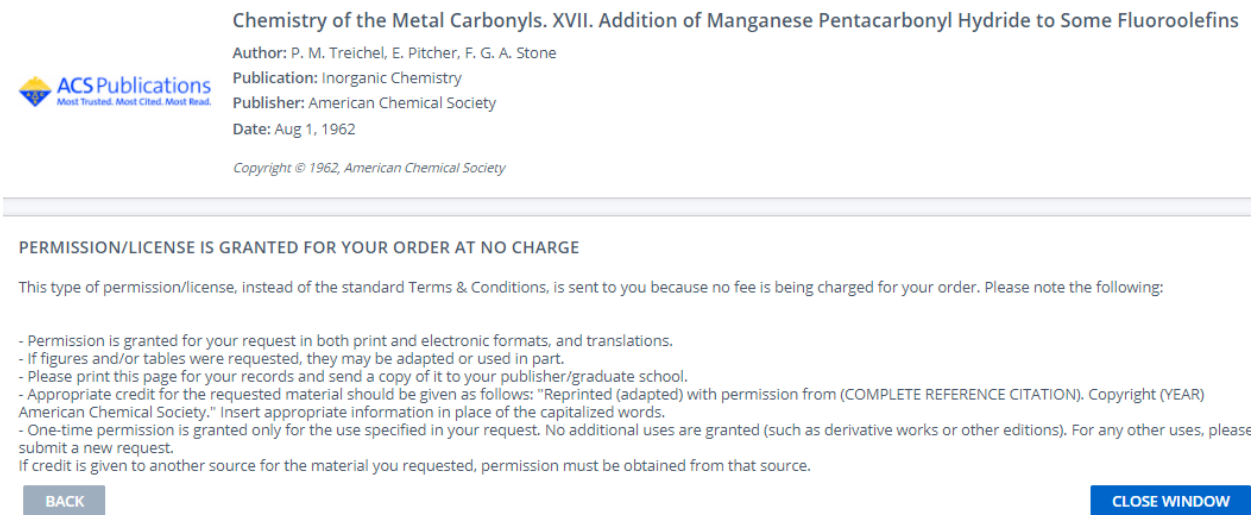

Chemistry of the Metal Carbonyls. XVII. Addition of Manganese Pentacarbonyl Hydride to Some Fluoroolefins

Author: P. M. Treichel, E. Pitcher, F. G. A. Stone
Publication: Inorganic Chemistry
Publisher: American Chemical Society
Date: Aug 1, 1962

Copyright © 1962, American Chemical Society

PERMISSION/LICENSE IS GRANTED FOR YOUR ORDER AT NO CHARGE

This type of permission/license, instead of the standard Terms & Conditions, is sent to you because no fee is being charged for your order. Please note the following:

- Permission is granted for your request in both print and electronic formats, and translations.
- If figures and/or tables were requested, they may be adapted or used in part.
- Please print this page for your records and send a copy of it to your publisher/graduate school.
- Appropriate credit for the requested material should be given as follows: "Reprinted (adapted) with permission from (COMPLETE REFERENCE CITATION). Copyright (YEAR) American Chemical Society." Insert appropriate information in place of the capitalized words.
- One-time permission is granted only for the use specified in your request. No additional uses are granted (such as derivative works or other editions). For any other uses, please submit a new request.

If credit is given to another source for the material you requested, permission must be obtained from that source.

BACK CLOSE WINDOW

Figure P.13. Scheme **1.6** insertion into metals hydrides to form insertion product, $MnH(CO)_5$.

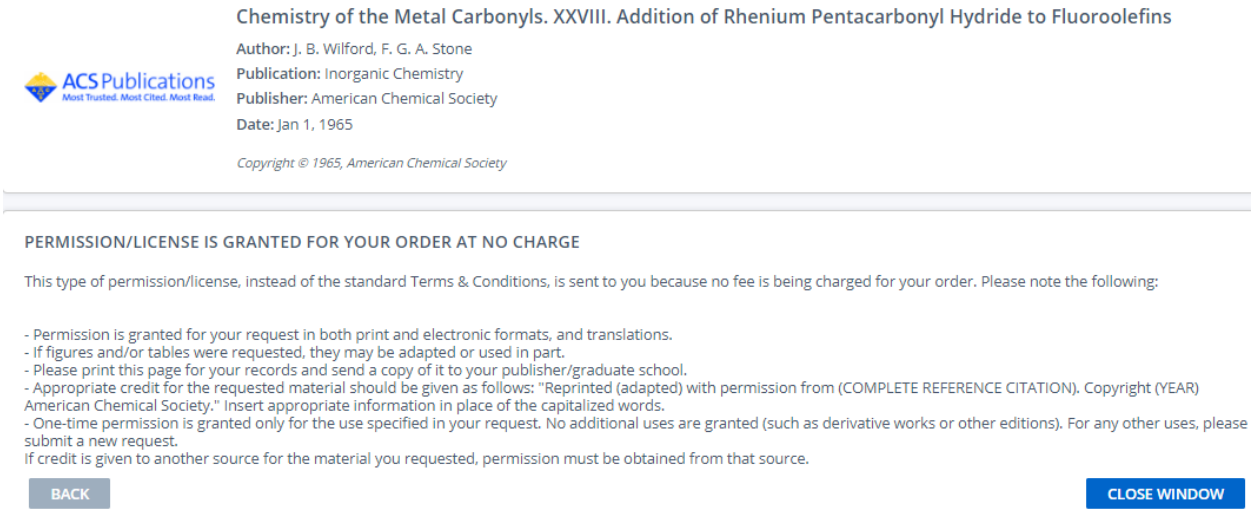

Chemistry of the Metal Carbonyls. XXVIII. Addition of Rhenium Pentacarbonyl Hydride to Fluoroolefins

Author: J. B. Wilford, F. G. A. Stone
Publication: Inorganic Chemistry
Publisher: American Chemical Society
Date: Jan 1, 1965

Copyright © 1965, American Chemical Society

PERMISSION/LICENSE IS GRANTED FOR YOUR ORDER AT NO CHARGE

This type of permission/license, instead of the standard Terms & Conditions, is sent to you because no fee is being charged for your order. Please note the following:

- Permission is granted for your request in both print and electronic formats, and translations.
- If figures and/or tables were requested, they may be adapted or used in part.
- Please print this page for your records and send a copy of it to your publisher/graduate school.
- Appropriate credit for the requested material should be given as follows: "Reprinted (adapted) with permission from (COMPLETE REFERENCE CITATION). Copyright (YEAR) American Chemical Society." Insert appropriate information in place of the capitalized words.
- One-time permission is granted only for the use specified in your request. No additional uses are granted (such as derivative works or other editions). For any other uses, please submit a new request.

If credit is given to another source for the material you requested, permission must be obtained from that source.

BACK CLOSE WINDOW

Figure P.14. Scheme **1.6** insertion into metals hydrides to form insertion product, $ReH(CO)_5$.

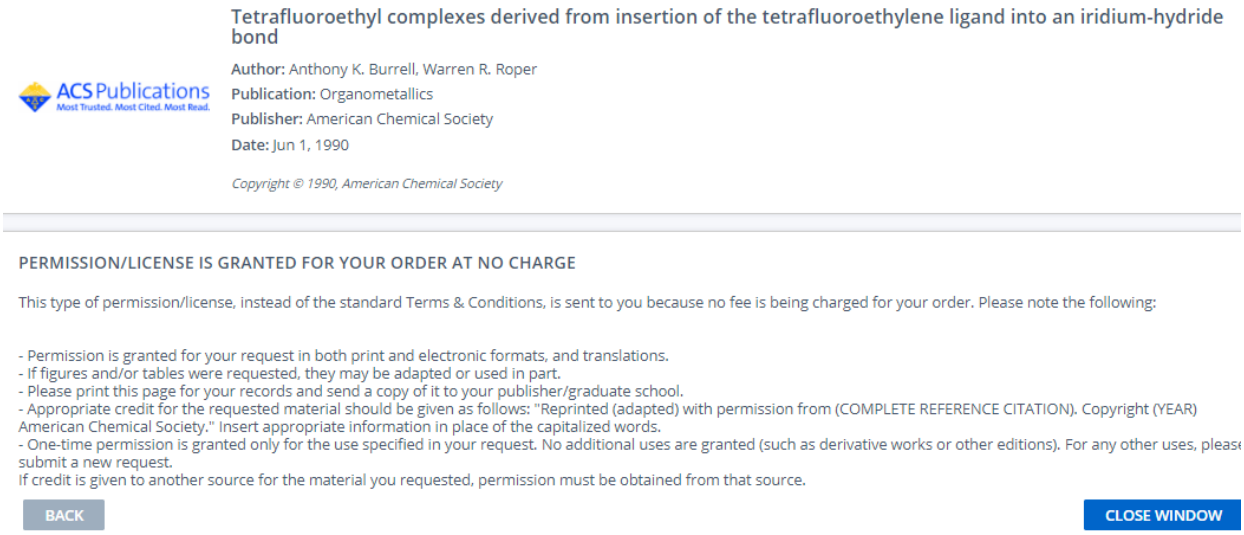

Tetrafluoroethyl complexes derived from insertion of the tetrafluoroethylene ligand into an iridium-hydride bond

Author: Anthony K. Burrell, Warren R. Roper
Publication: Organometallics
Publisher: American Chemical Society
Date: Jun 1, 1990

Copyright © 1990, American Chemical Society

PERMISSION/LICENSE IS GRANTED FOR YOUR ORDER AT NO CHARGE

This type of permission/license, instead of the standard Terms & Conditions, is sent to you because no fee is being charged for your order. Please note the following:

- Permission is granted for your request in both print and electronic formats, and translations.
- If figures and/or tables were requested, they may be adapted or used in part.
- Please print this page for your records and send a copy of it to your publisher/graduate school.
- Appropriate credit for the requested material should be given as follows: "Reprinted (adapted) with permission from (COMPLETE REFERENCE CITATION). Copyright (YEAR) American Chemical Society." Insert appropriate information in place of the capitalized words.
- One-time permission is granted only for the use specified in your request. No additional uses are granted (such as derivative works or other editions). For any other uses, please submit a new request.

If credit is given to another source for the material you requested, permission must be obtained from that source.

BACK CLOSE WINDOW

Figure P.15. Scheme **1.7** insertion of TFE into Ir-H bond and coordination of a second TFE.

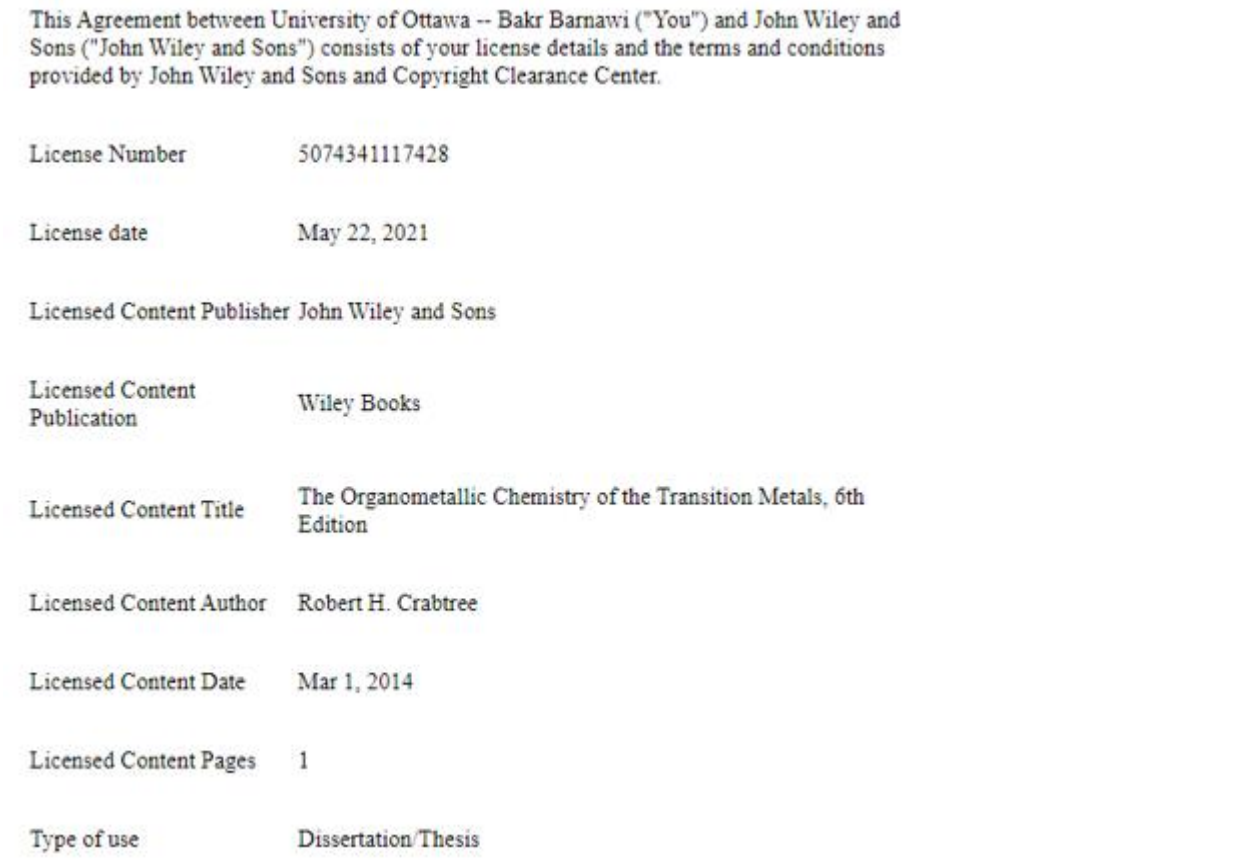

This Agreement between University of Ottawa -- Bakr Barnawi ("You") and John Wiley and Sons ("John Wiley and Sons") consists of your license details and the terms and conditions provided by John Wiley and Sons and Copyright Clearance Center.

License Number	5074341117428
License date	May 22, 2021
Licensed Content Publisher	John Wiley and Sons
Licensed Content Publication	Wiley Books
Licensed Content Title	The Organometallic Chemistry of the Transition Metals, 6th Edition
Licensed Content Author	Robert H. Crabtree
Licensed Content Date	Mar 1, 2014
Licensed Content Pages	1
Type of use	Dissertation/Thesis

Figure P.16. Scheme **1.8** oxidative coupling to form a perfluorometallacyclopentane.

This Agreement between University of Ottawa -- Bakr Barnawi ("You") and Elsevier ("Elsevier") consists of your license details and the terms and conditions provided by Elsevier and Copyright Clearance Center.

License Number	5076280670773
License date	May 25, 2021
Licensed Content Publisher	Elsevier
Licensed Content Publication	Journal of Inorganic and Nuclear Chemistry
Licensed Content Title	A novel heterocyclic cobalt compound
Licensed Content Author	T.D. Coyle,R.B. Kings,E. Pitcher,S.L. Stafford,P. Teichel,F.G.A. Stone
Licensed Content Date	Nov 1, 1961
Licensed Content Volume	20
Licensed Content Issue	1-2
Licensed Content Pages	2
Start Page	172
End Page	173
Type of Use	reuse in a thesis/dissertation
Portion	figures/tables/illustrations
Number of figures/tables/illustrations	1

Figure P.17. Figure **1.4** first reported perfluorometallacyle for d^6 cobaltacyclopentane.

ACS Publications
Most Trusted. Most Cited. Most Read.

Carbon–Fluorine Bond Activation of Tetrafluoroethylene on Palladium(0) and Nickel(0): Heat or Lewis Acidic Additive Promoted Oxidative Addition

Author: Masato Ohashi, Mitsutoshi Shibata, Hiroki Saijo, et al
Publication: Organometallics
Publisher: American Chemical Society
Date: Jul 1, 2013

Copyright © 2013, American Chemical Society

PERMISSION/LICENSE IS GRANTED FOR YOUR ORDER AT NO CHARGE

This type of permission/license, instead of the standard Terms & Conditions, is sent to you because no fee is being charged for your order. Please note the following:

- Permission is granted for your request in both print and electronic formats, and translations.
- If figures and/or tables were requested, they may be adapted or used in part.
- Please print this page for your records and send a copy of it to your publisher/graduate school.
- Appropriate credit for the requested material should be given as follows: "Reprinted (adapted) with permission from (COMPLETE REFERENCE CITATION). Copyright (YEAR) American Chemical Society." Insert appropriate information in place of the capitalized words.
- One-time permission is granted only for the use specified in your request. No additional uses are granted (such as derivative works or other editions). For any other uses, please submit a new request.

If credit is given to another source for the material you requested, permission must be obtained from that source.

BACK CLOSE WINDOW

Figure P.18. Scheme **1.9** ligand effects on perfluoronickelacycle formation.

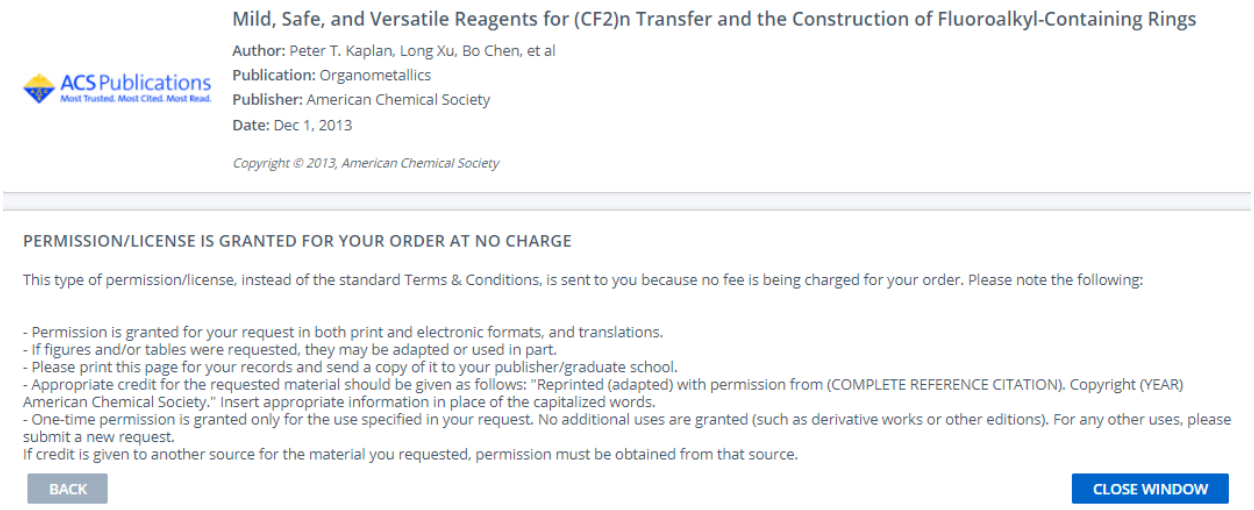

Figure P.19. Scheme **1.10** synthesis of perfluoronickelacycles via a transmetallation reaction.

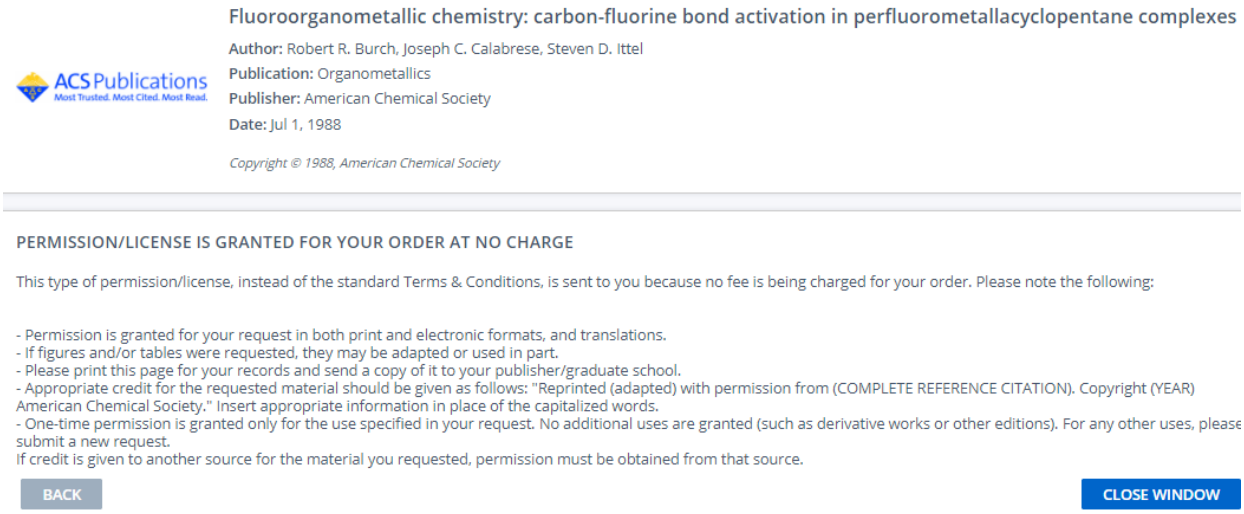

Figure P.20. Scheme **1.14** Cα-F abstraction from a bis(phosphine) nickel perfluorocyclopentane.

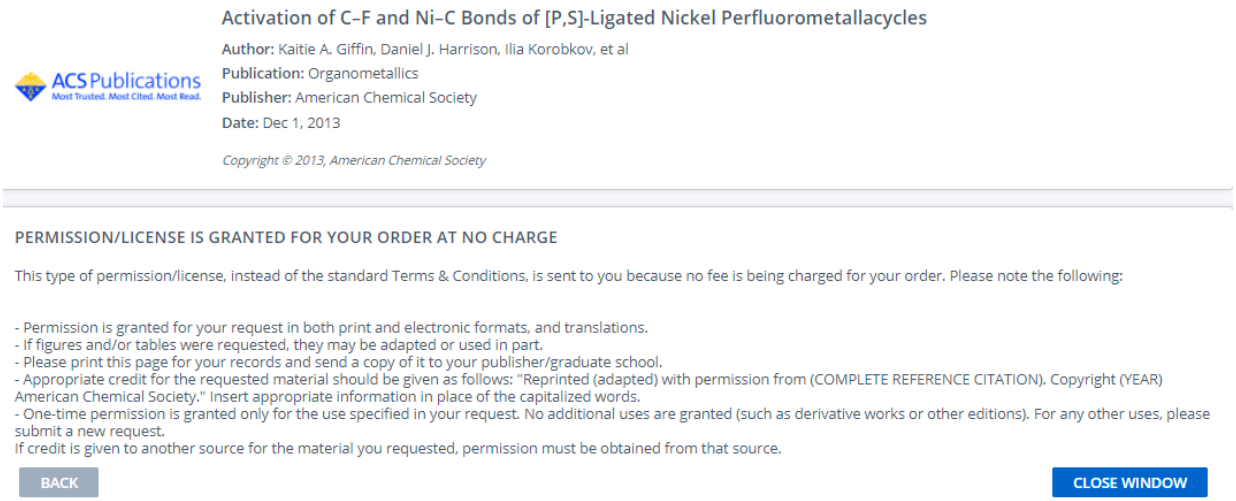

Figure P.21. Scheme **1.15** Cα-F activation from a [P,SIpr]-ligated metal perfluorocyclopentane by TMS-OTf.

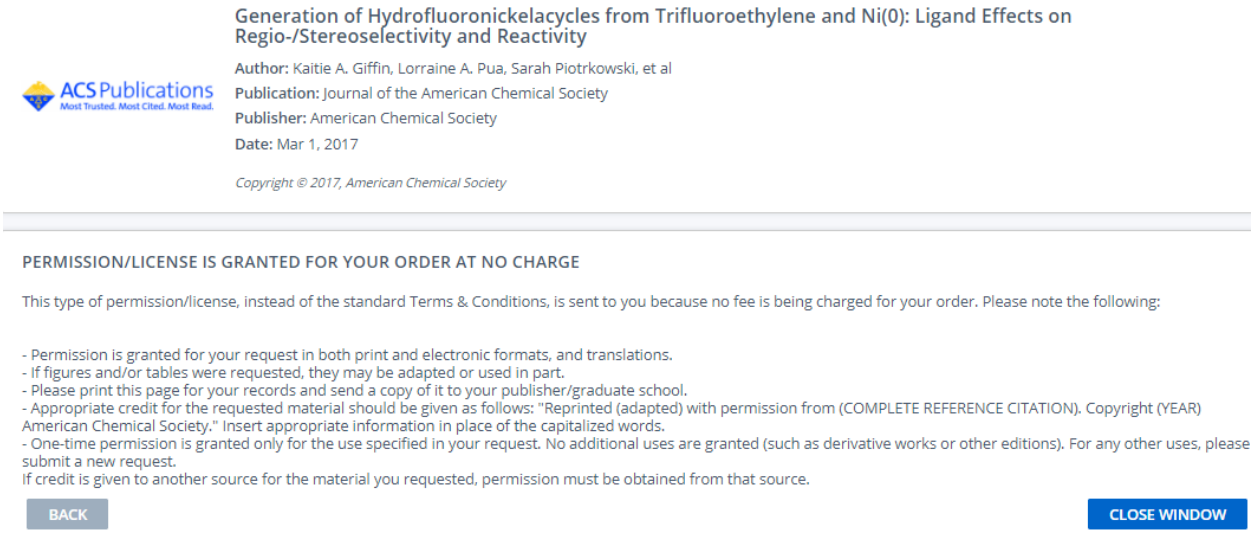

Figure P.22. Scheme **1.16** reactivity of phosphonium-functionalized nickelacyclopentane.

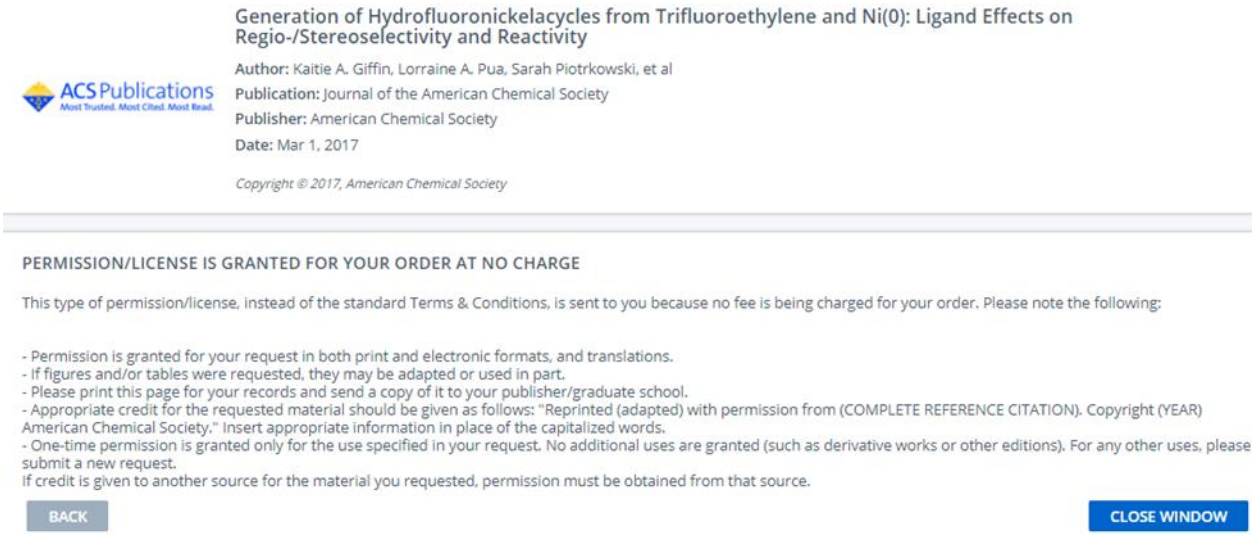

Generation of Hydrofluoronickelacycles from Trifluoroethylene and Ni(0): Ligand Effects on Regio-/Stereoselectivity and Reactivity

Author: Kaitie A. Giffin, Lorraine A. Pua, Sarah Piotrkowski, et al
Publication: Journal of the American Chemical Society
Publisher: American Chemical Society
Date: Mar 1, 2017

Copyright © 2017, American Chemical Society

PERMISSION/LICENSE IS GRANTED FOR YOUR ORDER AT NO CHARGE

This type of permission/license, instead of the standard Terms & Conditions, is sent to you because no fee is being charged for your order. Please note the following:

- Permission is granted for your request in both print and electronic formats, and translations.
- If figures and/or tables were requested, they may be adapted or used in part.
- Please print this page for your records and send a copy of it to your publisher/graduate school.
- Appropriate credit for the requested material should be given as follows: "Reprinted (adapted) with permission from (COMPLETE REFERENCE CITATION). Copyright (YEAR) American Chemical Society." Insert appropriate information in place of the capitalized words.
- One-time permission is granted only for the use specified in your request. No additional uses are granted (such as derivative works or other editions). For any other uses, please submit a new request.

If credit is given to another source for the material you requested, permission must be obtained from that source.

BACK CLOSE WINDOW

Figure P.23. Scheme **1.19** reactivity of nickelacyclopentane derived from trifluoroethylene.

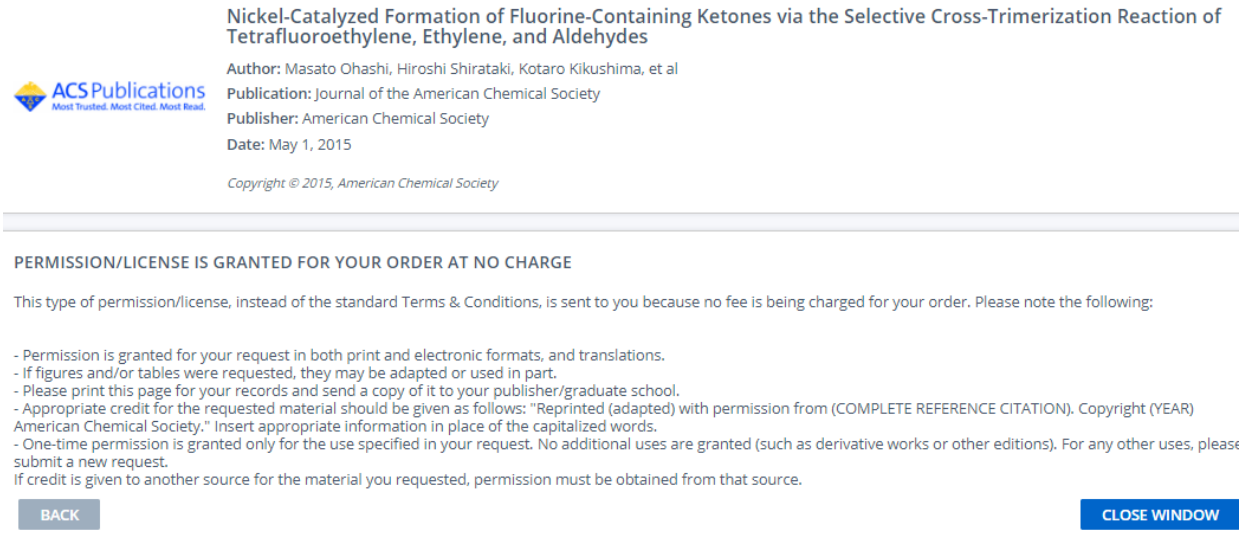

Nickel-Catalyzed Formation of Fluorine-Containing Ketones via the Selective Cross-Trimerization Reaction of Tetrafluoroethylene, Ethylene, and Aldehydes

Author: Masato Ohashi, Hiroshi Shirataki, Kotaro Kikushima, et al
Publication: Journal of the American Chemical Society
Publisher: American Chemical Society
Date: May 1, 2015

Copyright © 2015, American Chemical Society

PERMISSION/LICENSE IS GRANTED FOR YOUR ORDER AT NO CHARGE

This type of permission/license, instead of the standard Terms & Conditions, is sent to you because no fee is being charged for your order. Please note the following:

- Permission is granted for your request in both print and electronic formats, and translations.
- If figures and/or tables were requested, they may be adapted or used in part.
- Please print this page for your records and send a copy of it to your publisher/graduate school.
- Appropriate credit for the requested material should be given as follows: "Reprinted (adapted) with permission from (COMPLETE REFERENCE CITATION). Copyright (YEAR) American Chemical Society." Insert appropriate information in place of the capitalized words.
- One-time permission is granted only for the use specified in your request. No additional uses are granted (such as derivative works or other editions). For any other uses, please submit a new request.

If credit is given to another source for the material you requested, permission must be obtained from that source.

BACK CLOSE WINDOW

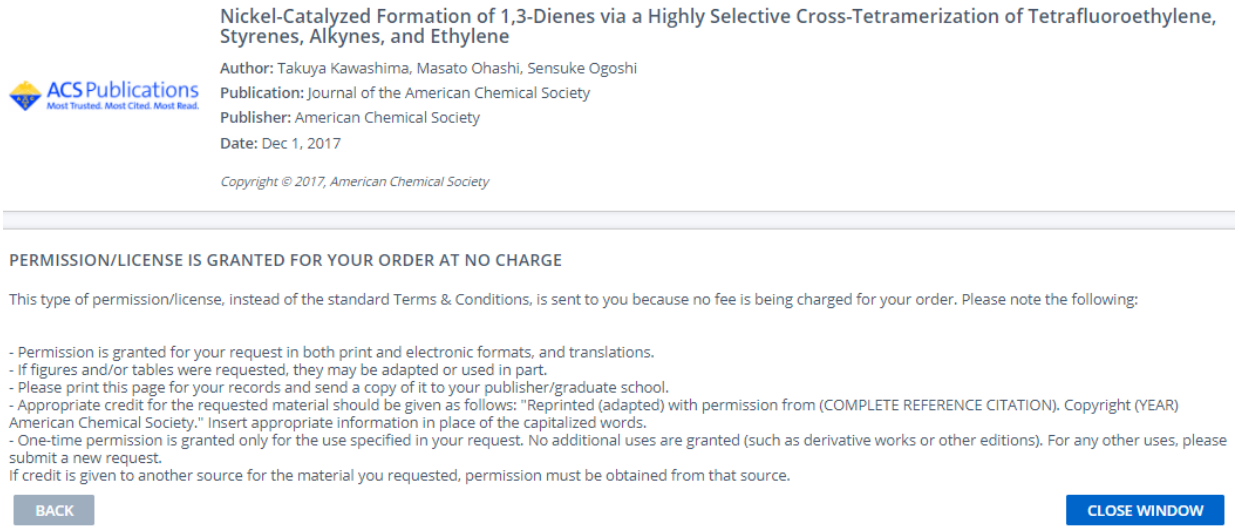

Figure P.24. Scheme **1.22** Ni-catalyzed selective cross trimerization reactions **a**,**b**.

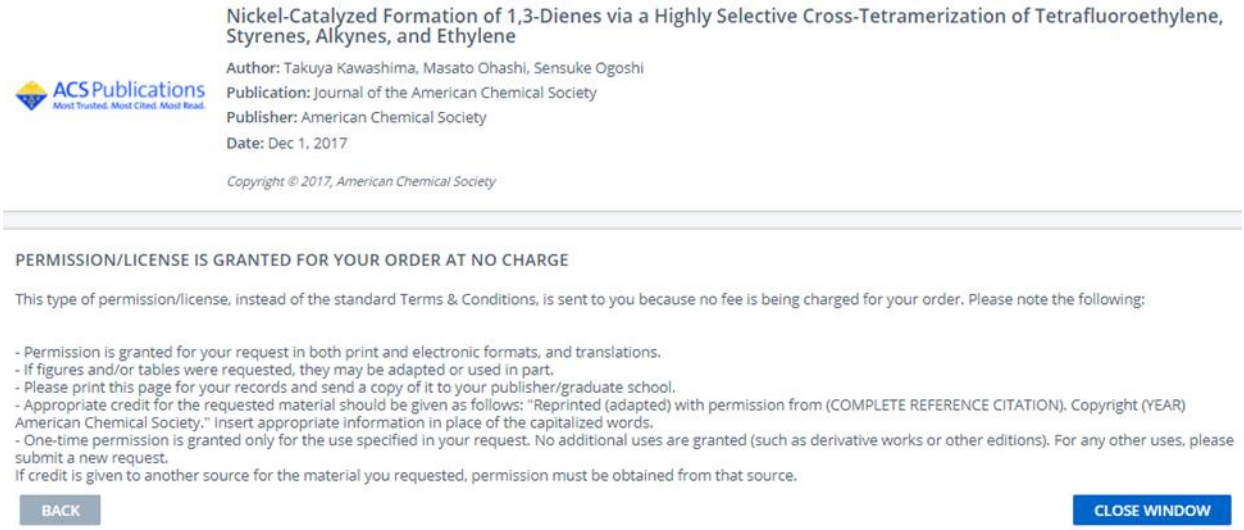

Figure P.25. Scheme **1.23** Ni-catalyzed selective cross tetramerization reaction.

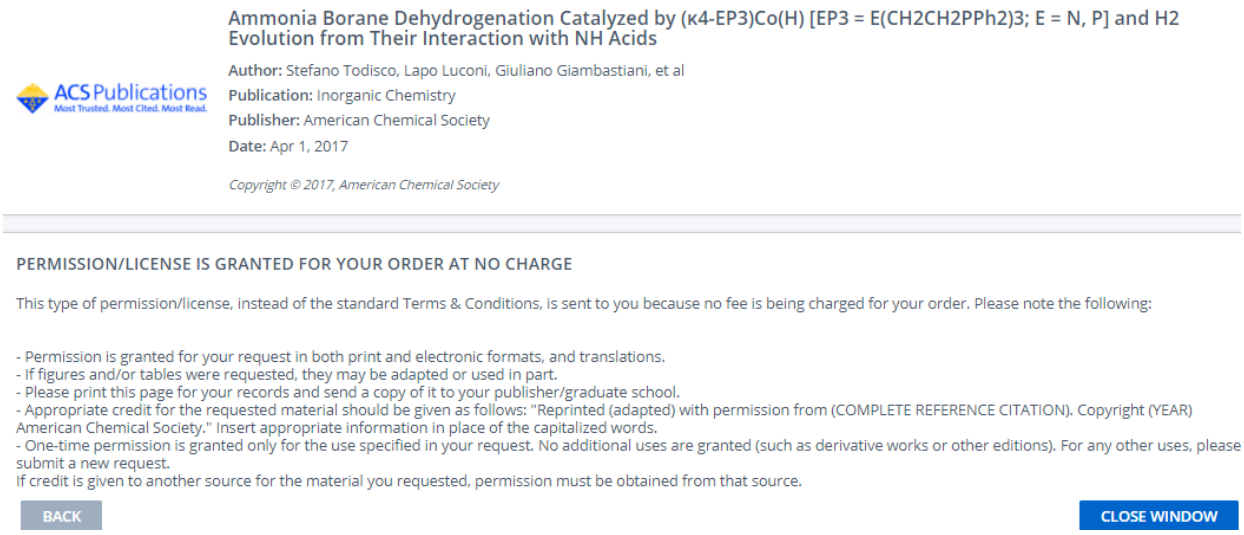

Figure P.26. Scheme **4.2**18e- Co hydride AB dehydrogenation catalysts.

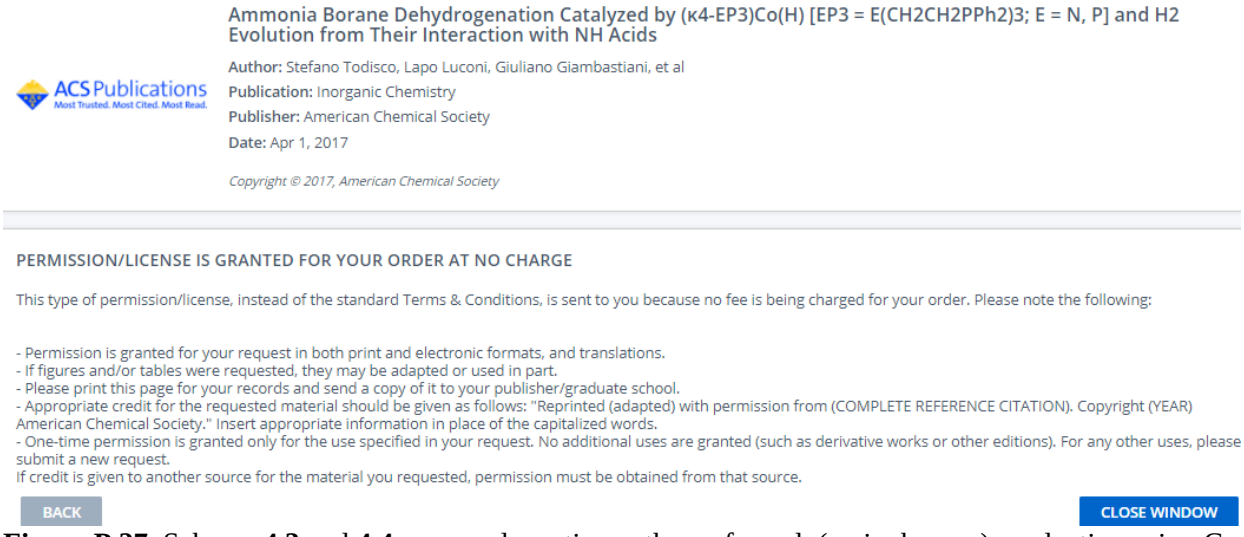

Figure P.27. Scheme **4.3** and **4.4** proposed reaction pathway for poly(aminoborane) production using Co-H catalyst **1** and **2**.